Lamp

CR-134172

HEAT PIPE RADIATOR

FINAL REPORT

GRUMMAN

HEAT PIPE RADIATOR
FINAL REPORT

Prepared for

National Aeronautics and Space Administration
Johnson Space Center
Houston, Texas 77058

Contract NAS 9-12848

By

Grumman Aerospace Corporation
Bethpage, New York 11714

Prepared by: B. Swerdling
J. Alario

Approved by: R. Haslett

I

HPR-14

October 1973

FOREWORD

This report was prepared by Grumman Aerospace Corporation for the Johnson Space Center of the National Aeronautics and Space Administration. The work was done under Contract NAS 9-12848, with Mr. B. French serving as Technical Monitor.

The work was performed from June 1972 to September 1973 under the direction of Mr. R. Haslett as program manager and Mr. B. Swerdling and Mr. J. Alario as project engineers. A major contribution was made by Mr. R. Hembach in thermal analysis and bench testing. Contributions were also made by Mr. J. Valentine in structural design and by Mr. W. Combs in fabrication. A special tribute is paid to Dr. J. Sellers, Jr. of Tuskeegee University for his help with the system test data analysis.

CONTENTS

ILLUSTRATIONS

ILLUSTRATIONS (Cont.)

TABLES

GLOSSARY

Symbols

A	area
C_p	specific heat
D	diameter
D_h	hydraulic diameter
G	mass flow per unit area
g	gravitational acceleration
g_c	gravitational constant
h	convective film coefficient
M	mass flow rate
N_2	nitrogen gas
NH_3	ammonia
P	pressure
ΔP	pressure drop
Q	heat flux
T	temperature
U	overall heat transfer coefficient
V	volume
W	mass flow rate
ϵ	surface emittance
λ	latent heat
μ	absolute viscosity
ρ	density
σ	surface tension; Stefan-Boltzmann Constant
η	effectiveness

Subscripts

a	absorbed
c	condenser; core
e	evaporator
f	fin
g	inert gas
H	header
i	inside surface
M	mean
R	reservoir
REJ	rejected
V	vapor
X	heat exchanger

Section 1

SUMMARY

A 15,000 watt spacecraft waste heat rejection system utilizing heat pipe radiator panels has been investigated. Of the several concepts initially identified, a series system was selected for more in-depth analysis. As a demonstration of system feasibility, a nominal 500 watt radiator panel has been designed, built and tested. The panel, which is a module of the 15,000 watt system, consists of a variable conductance heat pipe (VCHP) header, and six isothermalizer heat pipes attached to a radiating fin. The thermal load to the VCHP is supplied by a Freon-21 liquid loop via an integral heat exchanger.

This report describes the results of the system studies, details the radiator design, and presents the test results for both the heat pipe components and the assembled radiator panel. These results support the feasibility of using heat pipes in a spacecraft waste heat rejection system.

Section 2

INTRODUCTION

The heat pipe is an extremely efficient thermal control device that can transfer heat with very little temperature drop. This is accomplished by the evaporation, vapor transport, condensation and return by capillary action of a working fluid within a sealed container. In addition to superior thermal performance, heat pipes have no moving parts, require no electrical power, do not generate noise or vibration, and can be made self-regulating. These features make heat pipes attractive for the long-life, high reliability thermal control applications frequently needed for spacecraft.

Recent engineering applications of heat pipe technology have developed hardware that represents significant advances in the thermal control field (Ref. 1, 2, 3). Experiments have also been flown that demonstrate the ability of the heat pipe to operate predictably in space (Ref. 4, 5). The fact that the heat transport capacities of these devices have now been extended to the kilowatt range (Ref. 6) make their application to large scale thermal conditioning systems a real possibility. Recent studies that evaluated heat pipe applications for Space Station (Ref. 7), and Space Shuttle (Ref. 8) indicated that heat pipes as fin isothermalizers coupled to a variable conductance heat pipe (VCHP) as a temperature controller are viable candidates for spaceborne heat rejection systems.

When the heat pipe radiator and the conventional parallel-tube, fluid-loop radiator (Ref. 9, 10, 11), are compared for the same heat rejection capacity, it is found that the fluid radiator has a smaller area but the heat-pipe radiator requires no electrical power, has no parts that can wear out, and does not generate noise or vibration; these advantages become more important as mission time increases. Consequently, as a first step towards realizing the benefits of heat pipe technology in a large scale heat rejection system, a program was initiated by the Johnson Space Center to evaluate the feasibility of a self-regulating heat pipe space radiator.

The objective of the program was basically threefold, namely: (a) investigate a 15,000 watt spacecraft waste heat rejection system using heat pipes; (b) analytically design the heat-pipe radiator systems, and (c) fabricate and test a typical component module of the system.

Section 3

SYSTEM STUDY

The performance requirements used for the heat pipe radiator system tradeoff studies given in Table 3-1 are those of the Shuttle vehicle at the time this program was initiated. The basic heat pipe system was ground-ruled to be a modular system consisting of multiple 4 X 8 ft panels. Each panel, or module, has a variable conductance heat pipe (VCHP) header and six fixed conductance feeder heat pipes spaced on 8-in. centers. A fin effectiveness of .90 and a surface emittance of .90 are assumed. The thermal load is supplied by a Freon-21 liquid loop through a heat exhanger attached to the evaporator section of the VCHP header.

Table 3-1 - Radiator System Design Requirements

	Maximum	Minimum
Net heat rejection, watts	15,000 (51,225 Btu/hr)	300 (1020 Btu/hr)
Absorbed flux, watts/m^2	190 (60 Btu/hr-ft^2)	79 (25 Btu/hr-ft^2)
Freon-21 inlet temp., ^oK	338.7 (150^oF)	278.7 (42^oF)
Freon-21 outlet temp., ^oK	278.7 (42^oF)	277.5 (40^oF)
Flow rate, kg/S	.234 (1850 lb/hr)	.234 (1850 lb/hr)

The three types of systems that were investigated, series, parallel and series/parallel, are described below.

- Series - All of the required panels are sequentially arranged so that the coolant flows from the outlet of one heat exchanger to the inlet of the next. The major feature is that each successive panel operates at a lower temperature than the previous one. This results in a variation in the heat rejected by each panel; the panel nearest the inlet handles the most load and that nearest the outlet handles the least. See Figure 3-1.
- Parallel - The coolant enters all of the panels simultaneously, at the same temperature. The inlet temperature of each panel is the same and the outlet temperature of each panel is the same; the total system heat load is equally distributed between all panels. See Figure 3-2.

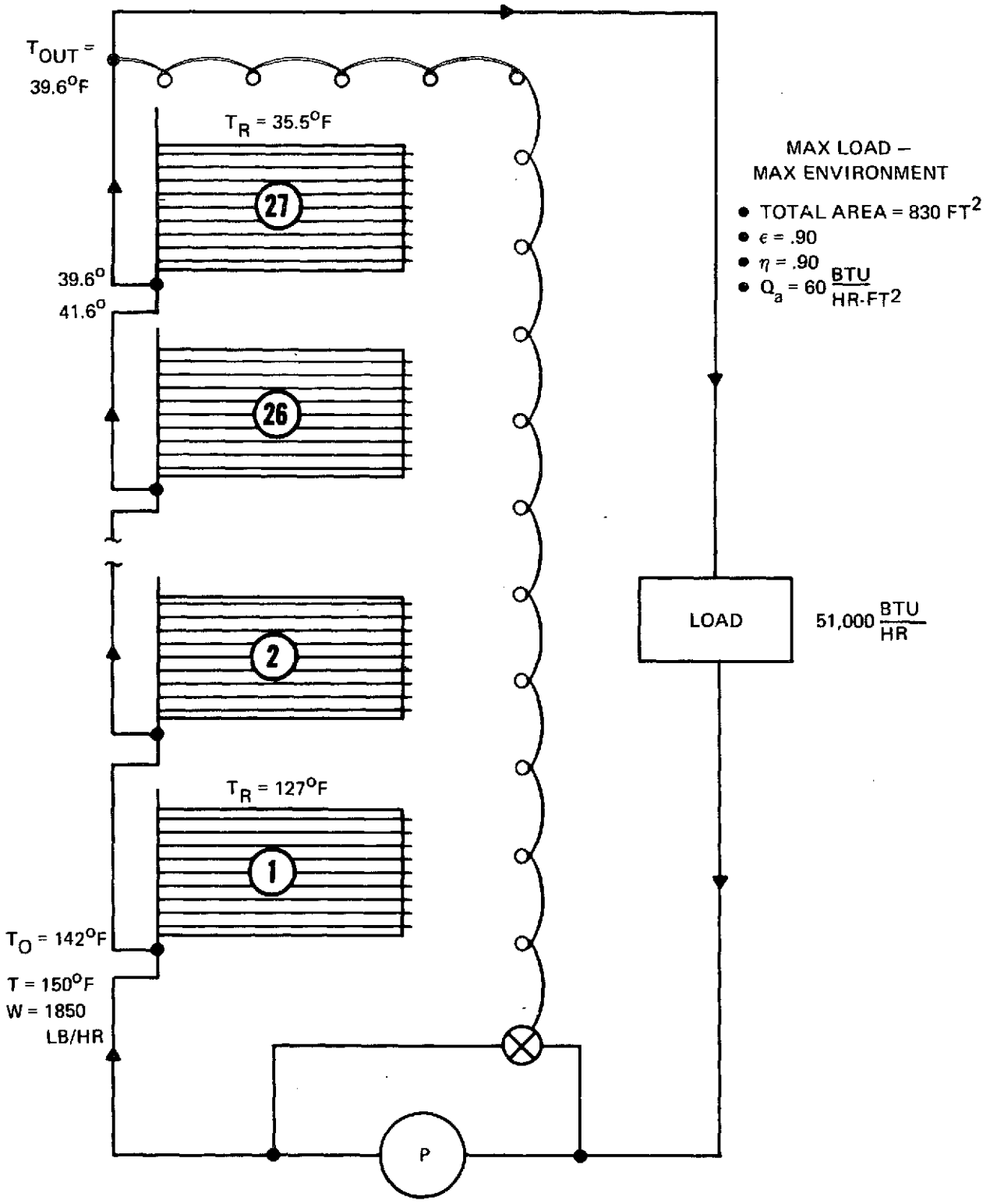

Figure 3-1 Series System

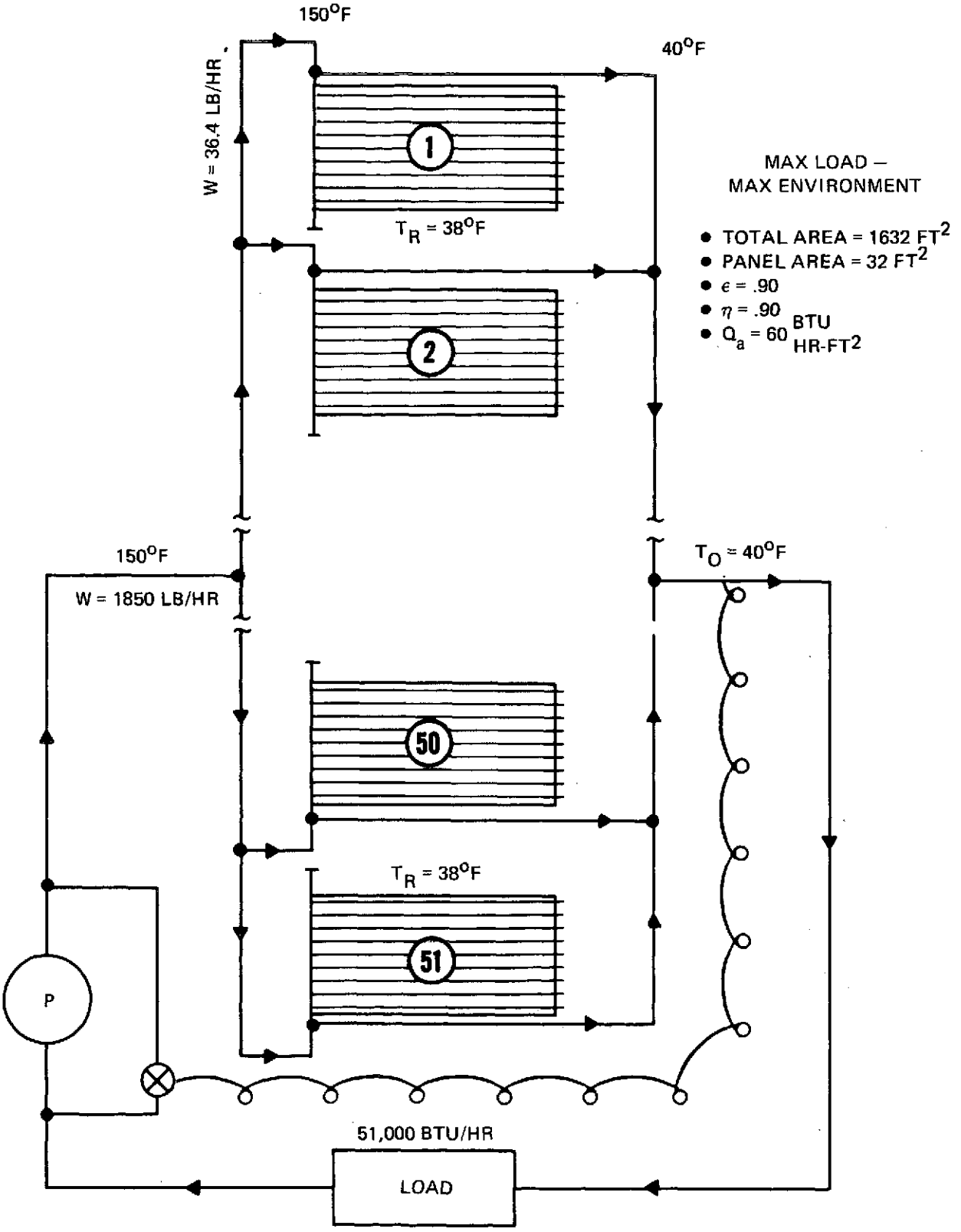

Figure 3-2 Parallel System

- Series/Parallel - A combination of the series and parallel systems where the required number of panels is divided into two or more parallel runs of series panels. See Figures 3-3 and 3-4.

System temperatures for the maximum design load condition are also indicated in Figures 3-1 through 3-4.

3.1 METHOD OF ANALYSIS

Each system was evaluated in an essentially identical manner using an existing computer program. The program assumes a flat radiator with an unrestricted view of space. (A segment of the model is shown in Figure 3-5.) Heat is transferred from the Freon loop via the integral heat exchanger, to the evaporator section of the VCHP header, and then through the condenser section of the header to the attached evaporators of the feeder heat pipes. Finally the condenser sections of the feeder pipes distribute the heat to the radiator fin. The following equations describe the analytical model for a single radiator panel.

Net Heat Rejection

$$Q_{REJ} = \eta \left[\epsilon A \sigma T_{Root}^4 - Q_a \right] \tag{3-1}$$

Heat Exchanger Outlet Temperature

$$T_{out} = T_{in} - \frac{Q_{REJ}}{WC_p} \tag{3-2}$$

Fluid Mean Temperature

$$T_M = T_V + \frac{T_{in} - T_{out}}{\ln \left(\frac{T_{in} - T_V}{T_{out} - T_V} \right)} \tag{3-3}$$

VCHP Header Vapor Temperature

$$T_V = T_M - \frac{Q_{REJ}}{COND1} \tag{3-4}$$

Panel Root Temperature

$$T_{Root} = T_V - \frac{Q_{REJ}}{COND2} \tag{3-5}$$

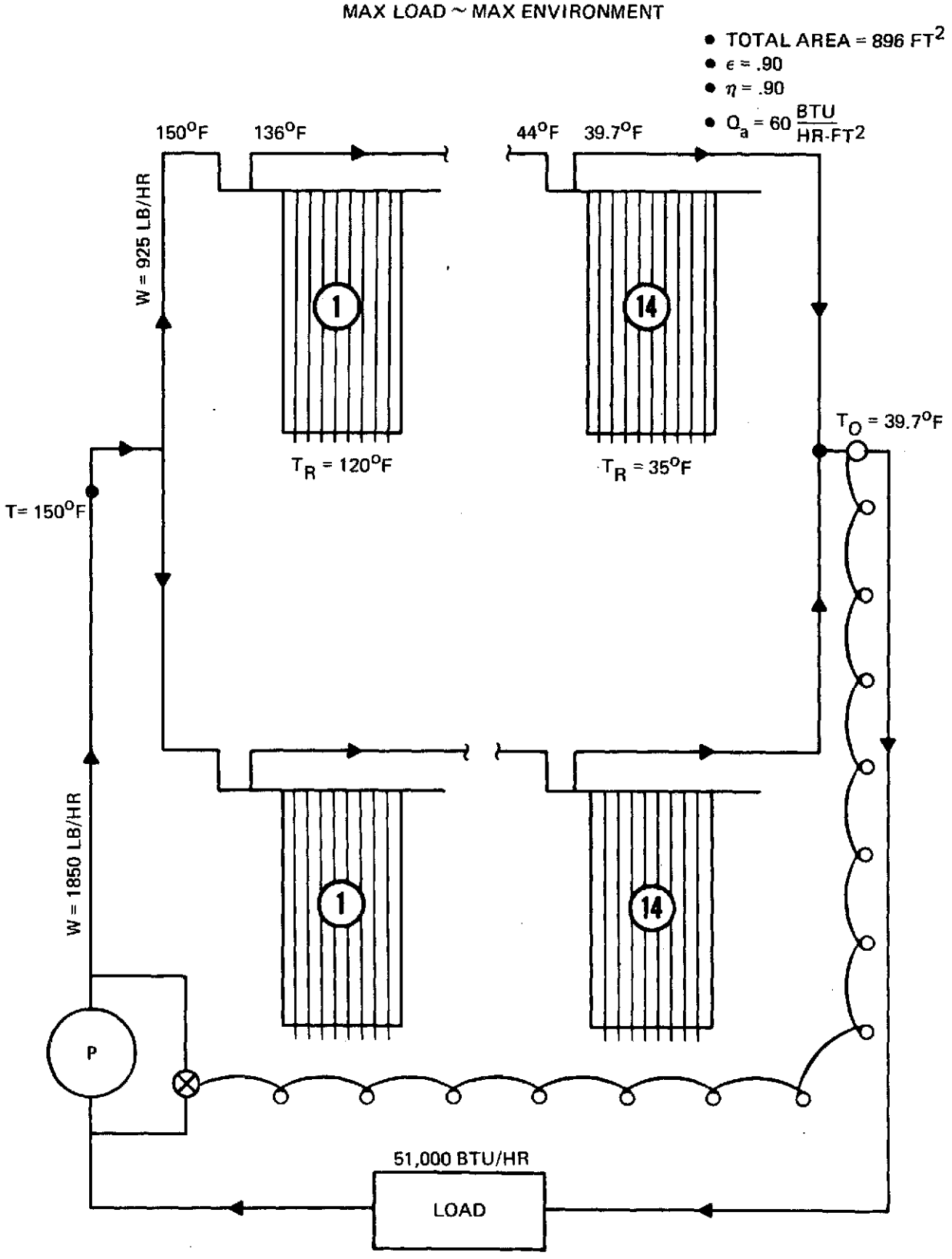

Figure 3-3 Two Series In Parallel

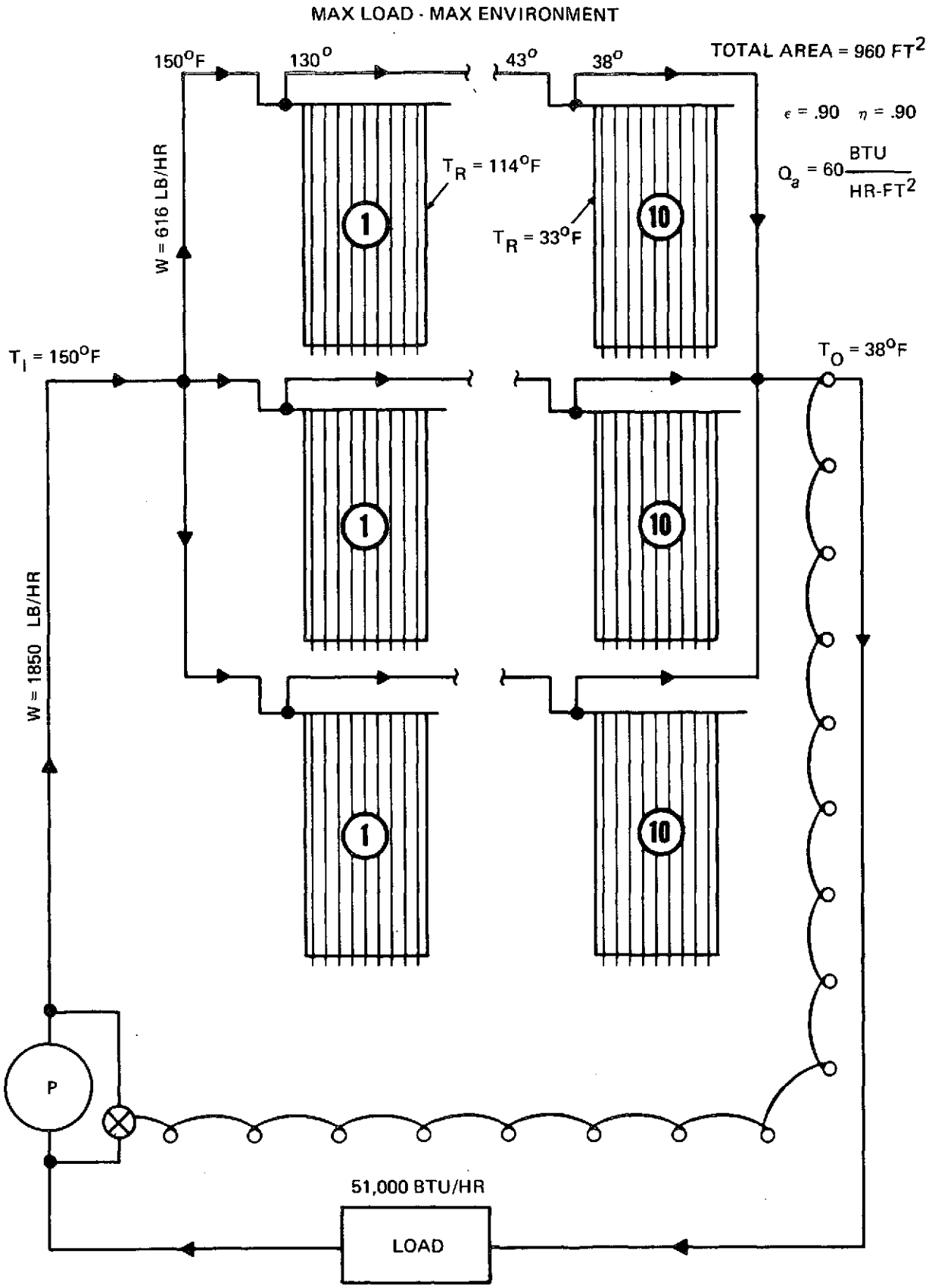

Figure 3-4 Three Series In Parallel

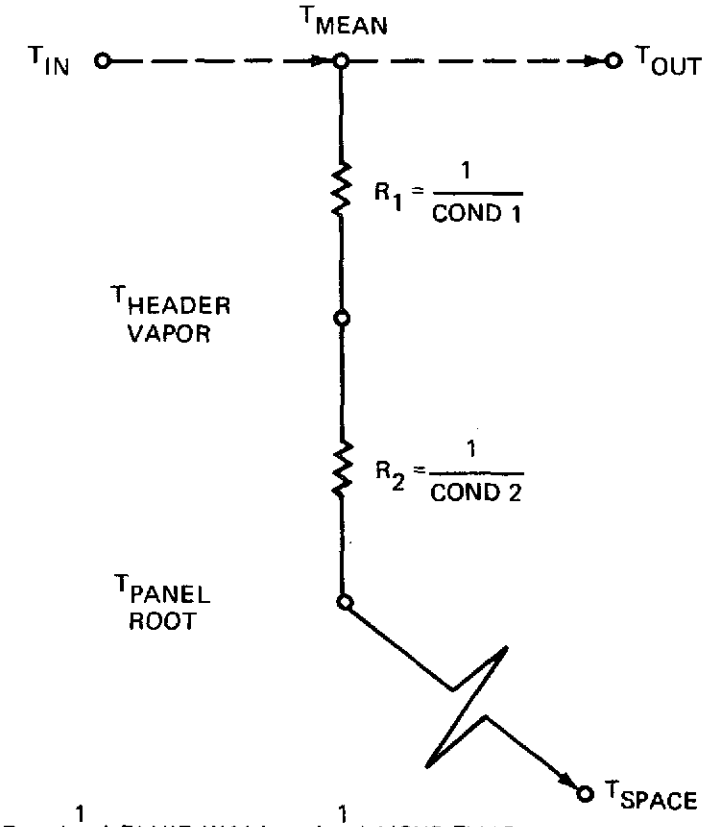

$R_1 = (\frac{1}{HA})$ FLUID-WALL + $(\frac{1}{HA})$ VCHP EVAP

$R_2 = (\frac{1}{HA})$ VCHP COND. + $(\frac{1}{HA})$ VCHP/FEEDER HP INTERFACE

+ $(\frac{1}{HA})$ FEEDER EVAP + $(\frac{1}{HA})$ FEEDER COND.

Figure 3-5 Radiator Module Thermal Model

Equations (3-1) through (3-5) can be combined after defining $R^1 = \left(\epsilon A\sigma T_{Root}^4 - Q_a\right)$ to give

$$T_{in} - T_{Root} + \left[\frac{\eta}{WC_p} \frac{e^{\frac{COND1}{WC_p}}}{\left(1 - e^{\frac{COND1}{WC_p}}\right)} - \frac{\eta}{COND2}\right] R^1 = 0 \qquad (3\text{-}6)$$

Since R^1 is a function of T_{Root}, equation (3-6) can be solved numerically for T_{Root}. Then, once T_{Root} is known, Q_{REJ} and T_{out} may be found. To analyze a radiator system containing a number of panels in series, T_{out} of the first panel would be T_{in} of the second panel, etc. Equation (3-6) was programmed and solved by Newton's method; the listing of the computer program is contained in Appendix A.

3.2 RESULTS

Using the above equations, the total radiator area and number of panels required for the maximum load, maximum environment condition was determined. The results are summarized in Table 3-2.

The parallel system requires 150 m^2 (1632 ft^2) of radiator area while the all series systems requires 77 m^2 (830 ft^2). The combined series/parallel approach requires areas between these two extremes. The smaller area for the series case is a direct result of the higher header vapor temperatures attainable as compared to the parallel case. Typically, the header vapor temperature of a panel is slightly lower than the heat exchanger outlet temperature. Thus, for the series case this allows a higher average radiating temperature resulting in greater thermal efficiency. For example, as shown in Table 3-2 the parallel panel maximum temperature is 275°K (38°F) vs the series maximum of 326°K (127°F). This effective radiating temperature phenomenon is characteristic of heat pipe systems and is summarized in Figure 3-6, which shows the header vapor temperature for each panel in each of the four systems shown in the table. The associated heat rejection for each panel is shown in the curves of Figure 3-7. These two figures emphasize that the first few panels in the series systems are very effective (by a factor of two or three) while the last panel is no worse than the best parallel panel.

3.3 VCHP RESERVOIR SIZING

With the radiator system configuration established, the VCHP reservoir can be defined. The reservoir size is a function of the desired control band established by the radiator requirement and the temperature of the reservoir. The size can be determined by calculating the gas inventory at the hot (full open) and cold case (full close) operating conditions.

Table 3-2 - Summary of System Results for Q_{REJ} = 15,000 W @ Q_a = 60 Btu/Hr-Ft^2

System	Branch Flow Rate, W		Total Area		Max T_{Root}		Header T_V		Panel Temp. Range	
	lb/hr	Kg/S	ft^2	m^2	^oF	^oK	^oF	^oK	^oF	^oK
Parallel	36.4	.0046	1632	150	37.9	276	39.9	277.5	38	276.5
Series	1850	.234	830	77	127	326	134.1	330	35-127	275-326
2 Series/Parallel	925	.117	896	81.3	119.6	322	126.1	325.5	35-120	275-322
3 Series/Parallel	616	.0075	960	87.3	113.8	319	120.0	322	33-114	274-319

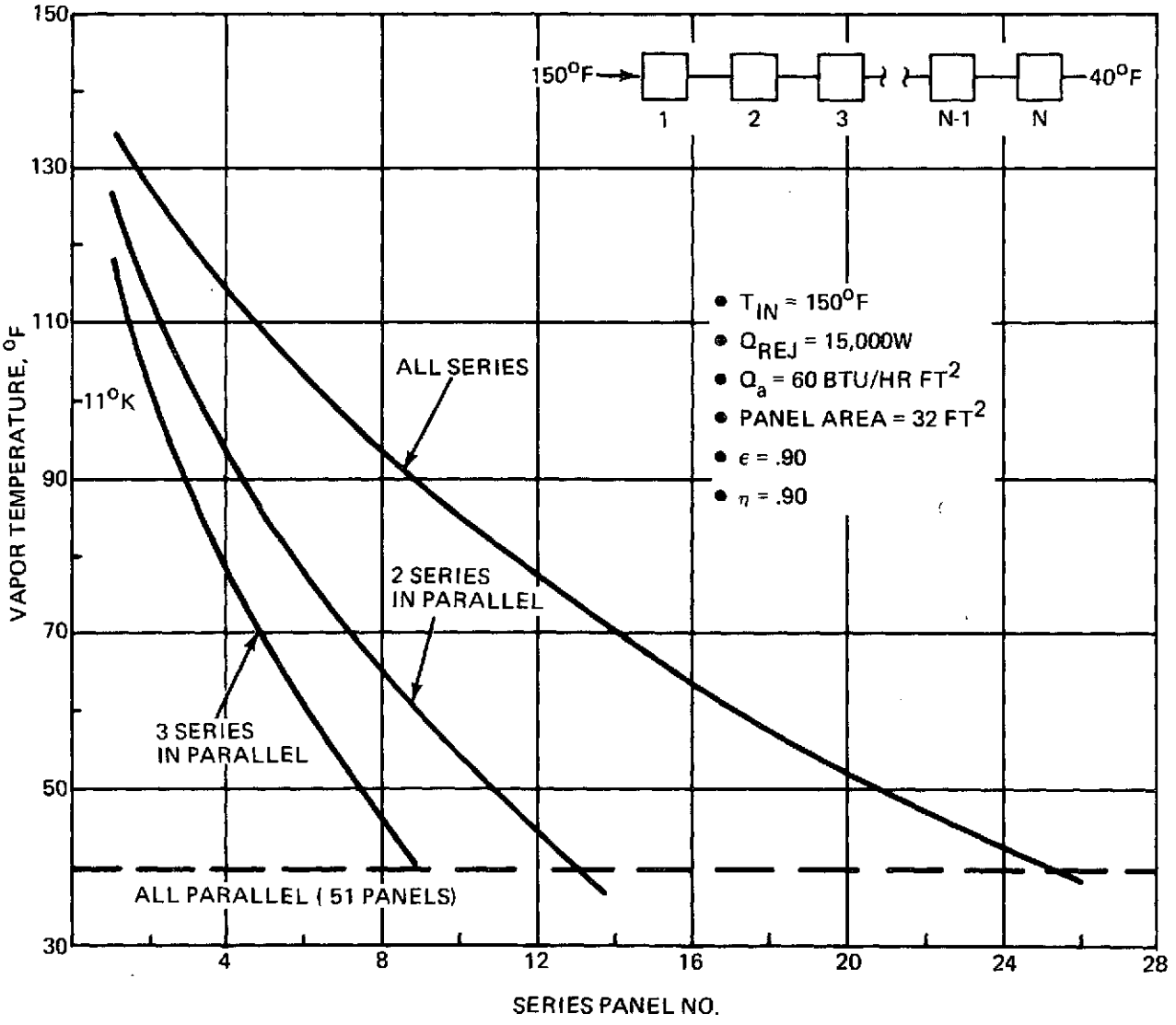

Figure 3-6 Panel Header Vapor Temperatures

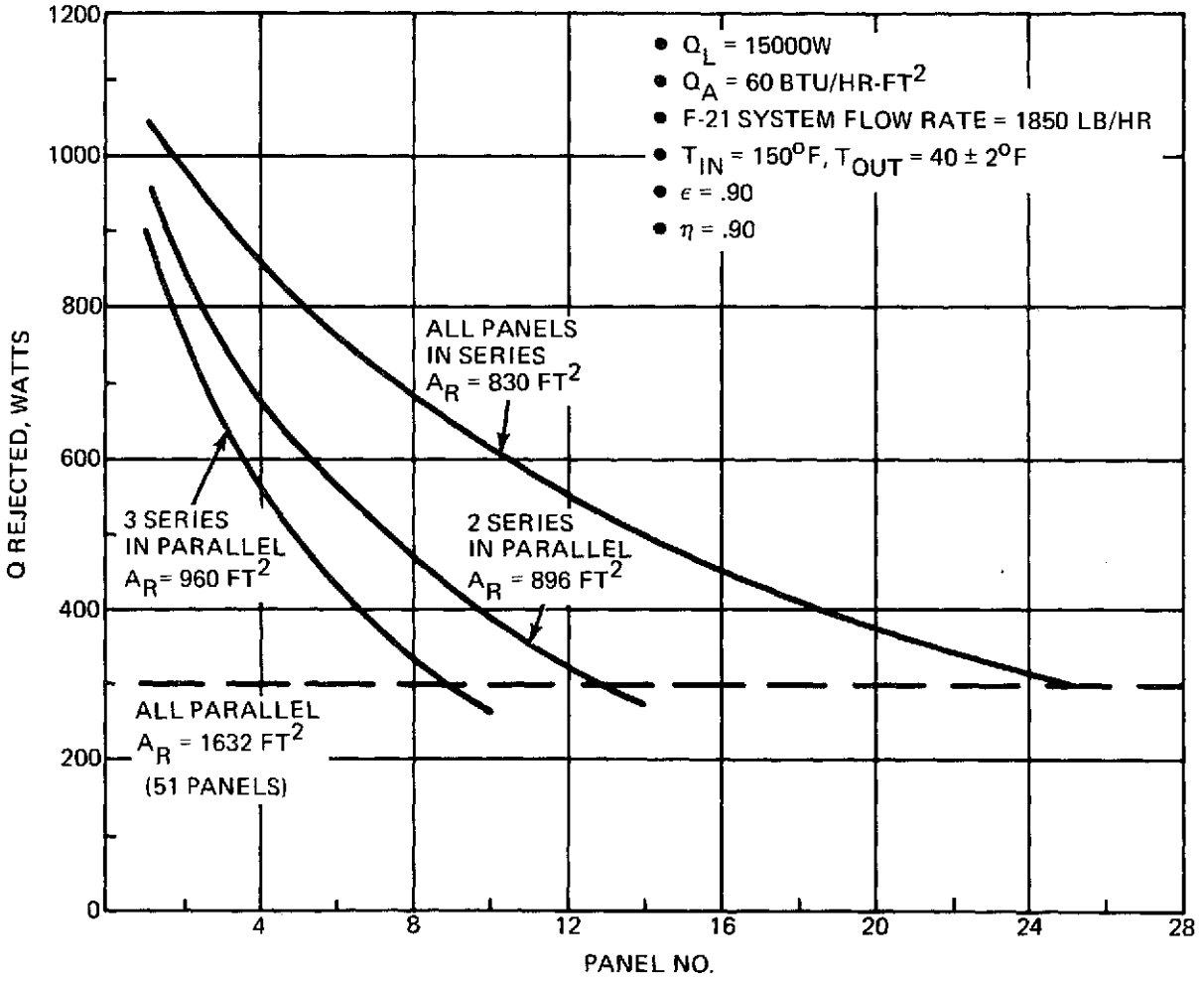

Figure 3-7 Heat Rejection Per Panel

Consider the simplified VCHP shown below which consists of ammonia as the working

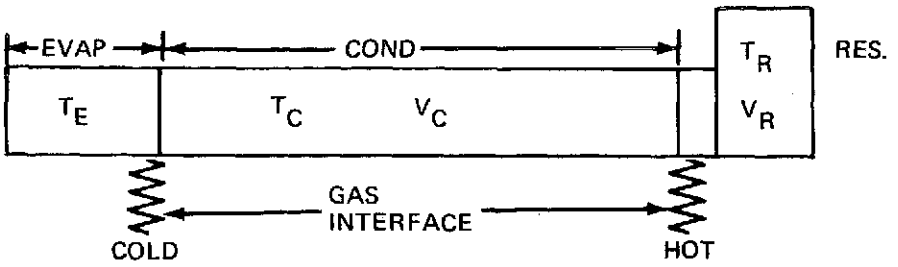

fluid and N_2 inert gas. During the cold or full close case, the gas fills the condenser with the interface located at the end of the evaporator. From the gas laws:

$$(mR)_G = \frac{P_G \; V_G}{T_G} \tag{3-7}$$

where

$$P_G = (P_{NH_3})_{\substack{\text{Cold}\\\text{Evap}}} - (P_{NH_3})_{\substack{\text{Cold}\\\text{Res}}} \tag{3-8}$$

$$V_G = V_C + V_R \tag{3-9}$$

and

$$T_G = (T_R)_{\text{Cold}} \tag{3-10}$$

During the hot or full open case, the gas interface is located at the end of the condenser with all of the gas in the reservoir and:

$$P_G = (P_{NH_3})_{\substack{\text{Hot}\\\text{Evap}}} - (P_{NH_3})_{\substack{\text{Hot}\\\text{Res}}} \tag{3-11}$$

$$V_G = V_R \tag{3-12}$$

and

$$T_G = (T_R)_{\text{Hot}} \tag{3-13}$$

Since the mass of gas mR is constant in the pipe, equations (3-8, -9, -10 and -11, -12, -13) can be substituted in equation (3-7) to give:

$$\left[(P_{NH_3})_{\substack{\text{Cold}\\\text{Evap}}} - (P_{NH_3})_{\substack{\text{Cold}\\\text{Res}}}\right] \frac{(V_C + V_R)}{(T_R)_{\text{Cold}}} = \left[(P_{NH_3})_{\text{Hot}_{\text{Evap}}} - (P_{NH_3})_{\substack{\text{Hot}\\\text{Res}}}\right] \frac{V_R}{T_{R(\text{Hot})}}$$

which can be rearranged to give:

$$\frac{V_C}{V_R} = \frac{\left[(P_{NH_3})_{\substack{\text{Hot}\\\text{Evap}}} - (P_{NH_3})_{\substack{\text{Hot}\\\text{Res}}}\right] (T_R)_{\text{Cold}}}{\left[(P_{NH_3})_{\substack{\text{Cold}\\\text{Evap}}} - (P_{NH_3})_{\substack{\text{Cold}\\\text{Res}}}\right] (T_R)_{\text{Hot}}} - 1 \tag{3-15}$$

where $(P_{NH_3})_{Evap}$ = pipe total pressure at evaporator temperature

$(P_{NH_3})_{Res}$ = ammonia partial pressure at reservoir temperature

P_G = inert gas pressure

T_R = reservoir temperature

V_C, V_R = condenser and reservoir vapor volumes, respectively

Vg = inert gas volume

m = moles of inert gas

R = gas constant

From equation (3-15), one can determine the VCHP reservoir size required for a given control condition. Figure 3-8 is a plot of V_R/V_C (ratio of reservoir to condenser volume) as a function of evaporator temperature control range (temperature difference between hot and cold cases). At T_{Hot} the panel is fully open and at T_{Cold} it is completely closed. Also shown is the affect of variation in reservoir temperature on reservoir size. A constant reservoir temperature results in a tighter control range for the same V_R/V_C ratio.

3.4 SYSTEM SELECTION

The heat pipe radiator system selected for detailed design was the all series system shown in Figure 3-1. Under the boundary conditions imposed, the series system required the least radiator area of the several systems studied (see Table 3-2) and required nominal VCHP reservoir sizes (<0.1 ft^3). The parallel system was rejected on the grounds that the area required for maximum load, maximum environment condition was almost double that of the series system. In addition, the size of the VCHP reservoirs required for control were impractical. The series/parallel systems considered were attractive from an area standpoint, but they required reservoir sizes approximately twice as large as the straight series system and were rejected for that reason.

For the radiator module under study, the VCHP condenser vapor volume was approximately 28 in.^{3} (.0055 m^3). A reasonable reservoir/condenser volume ratio was set at $V_R/V_C = 7$ which gives a $V_R = 196$ in.^{3} (.04 m^3). From Figure 3-8, curve A, for a $V_R/V_C = 7$, the minimum control range is 25°F for a varying reservoir temperature. This means a full-open panel at an evaporator temperature of 60°F and a fully closed panel at 35°F. For control spans less than 25°F, a fixed reservoir

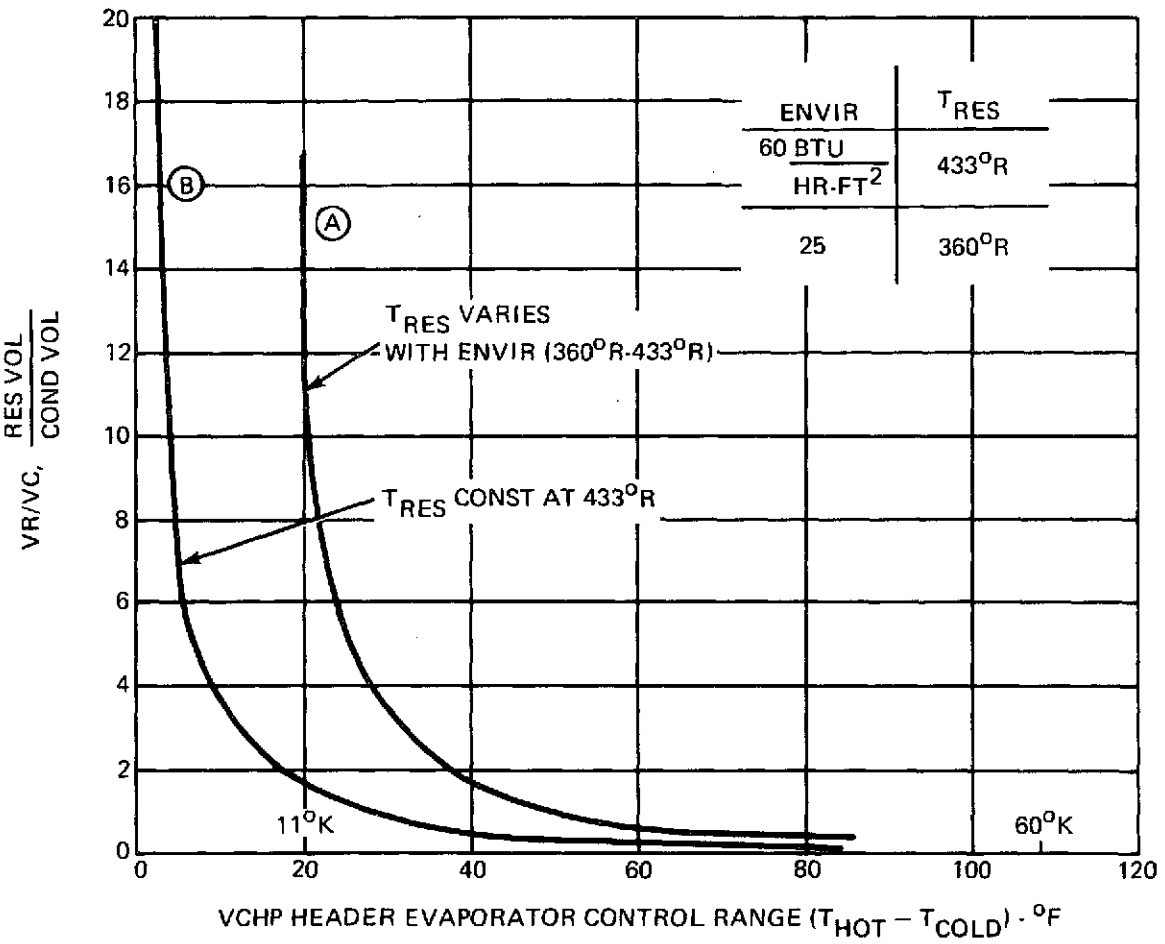

Figure 3-8 Reservoir Size vs Control Range (Based on 35°F Shutoff)

temperature is required, as seen in Figure 3-8, curve B. Referring to Figure 3-2, it can be seen that the all-parallel system operating vapor temperatures will be close to 40°F. This will be the nominal value for all load conditions since the fluid outlet temperature remains fixed at 40°F; thus, a relatively tight control range is needed ($T_{Hot} - T_{Cold} < 5^{o}F$). Even by keeping the reservoir temperatures constant, high reservoir volumes would be required as seen in Figure 3-8. However, in the series systems reasonable reservoir sizes can be used for most of the modules since the control spans can be expanded to 20 - 30°F. Only the last few panels in the series need be restricted to tighter control ranges to insure a nominal 40°F fluid outlet. The number of different size reservoirs can be minimized by varying the inert gas pressure as required to compensate for different "on/off" operating temperatures.

3.5 SYSTEM PERFORMANCE

The system selected for detailed design consisted of 26, 1.22m (4 ft) by 2.44 m (8 ft) panels with heat exchangers connected in series. The performance analysis neglected temperature drops through the tube walls and also across thermal interfaces since these should be small. The complete 15,000 watt system was divided into three zones; namely, zones A, B, and C. Table 3-3 shows the split.

Table 3-3 - Series System Reservoir Sizes

Zone	Panel No's.	Nominal Reservoir Size, V_R/V_C	Reservoir Temperature
A	1 - 14	5	Varies with environment
B	15 - 21	4	Constant @ 246°K (-16°F)
C	22 - 26	7	Constant @ 246°K (-16°F)

Each VCHP header was designed to be fully operational under maximum load and environment at the temperatures shown in Figure 3-9 by the solid curve. The fully closed temperature for each header is indicated by the dashed curve in the same figure. For example, the VCHP header on panel number 14 is fully open at a temperature of 297°K (74°F) and fully closed at 280°K (44°F). To keep the reservoir sizes reasonable ($V_R/V_C \approx 7$), the reservoirs in zones B and C must be kept at a constant temperature of approximately 246°K (-16°F). The last several panels close at temperatures less than 278°K (40°F). This is because the panels in zone C have an "on/off" temperature difference of 2.8°K (5°F) with a full open temperature of 278°K (40°F). If desired, the system can be designed for an "on" temperature of 279°K (42°F) and off at 277°K (38°F) but this scheme must be fully investigated.

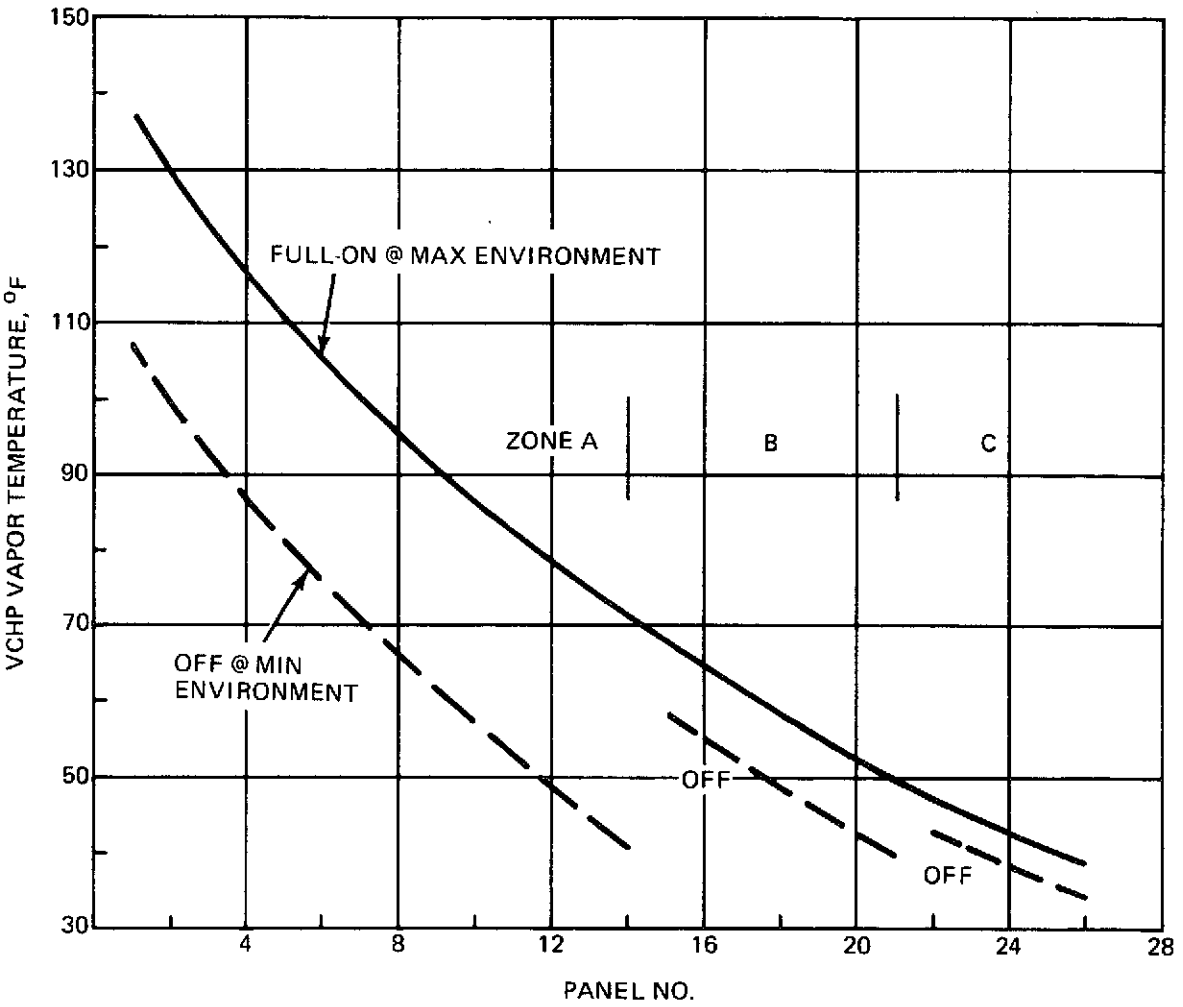

Figure 3-9 VCHP On and Off Temperatures, Series System, Ammonia Working Fluid and N_2 Gas

The 26-panel series system was investigated for several load conditions and environments. Figure 3-10 summarizes the data for the extreme environments. In Figure 3-10a, the system freon liquid loop outlet temperature is plotted as a function of the maximum and minimum environments. As shown, outlet temperature varies only 3.3°K (6°F) for a maximum-to-minimum load variation of 37.1. Figure 3-11 shows the heat rejection per panel for the two extreme load conditions. Under the low load condition (T_{in} = 55°F), panels 1 - 10 and 16 - 23 are fully closed as expected since the VCHP header vapor temperatures are below the cutoff temperatures shown in Figure 3-9.

3.6 FEASIBILITY PANEL SELECTION

Panel number 14 in the series system was selected to demonstrate the operational feasibility of a VCHP radiator. The reasons for selection were; (1) it required a nominal (500 watt) load capability; (2) it had a convenient operating temperature range between 72°F (full open, warm environment) and 41°F (full close, cold environment); and (3) it did not require a constant temperature reservoir to hold its control span. The design specifications established for this panel are summarized in Table 3-4. The V_R/V_C ratio was changed from 5 to 7 to compensate for slightly warmer reservoir temperatures than were originally estimated. This was a result of more comprehensive investigations that were done in support of the detailed design effort.

Table 3-4 Modular Panel Specifications

- Panel size - nominal 1.22 m x 2.44 m (4 x 8 ft)
- 1 - VCHP header - 1.83 m (6 ft) overall length
- Reservoir size - $V_R/V_C \approx 7$
- Heat exchanger length - .61 m (2 ft)
- 6 - Feeder heat pipes - nominal 2.75 m (9 ft) overall length
- VCHP full-open vapor temperature - 295°K (72°F) @ 190 w/m^2 (60 Btu/hr-ft^2)
- VCHP full close vapor temperature - 278°K (41°F) @ 79 w/m^2 (25 Btu/hr-ft^2)
- Reservoir temperature range - 200°K to 246.5°K (-100°F to -16°F)
- Operational environment - 79 - 190 w/m^2 (25-60 Btu/hr-ft^2)

Table 3-4 Modular Panel Specification (Cont'd)

- Nominal panel capacity - 500 watts
- Panel emittance, ϵ - .9
- Heat pipe working fluids
  - VCHP header: NH_3 + N_2 inert gas
  - Feeder pipes: NH_3

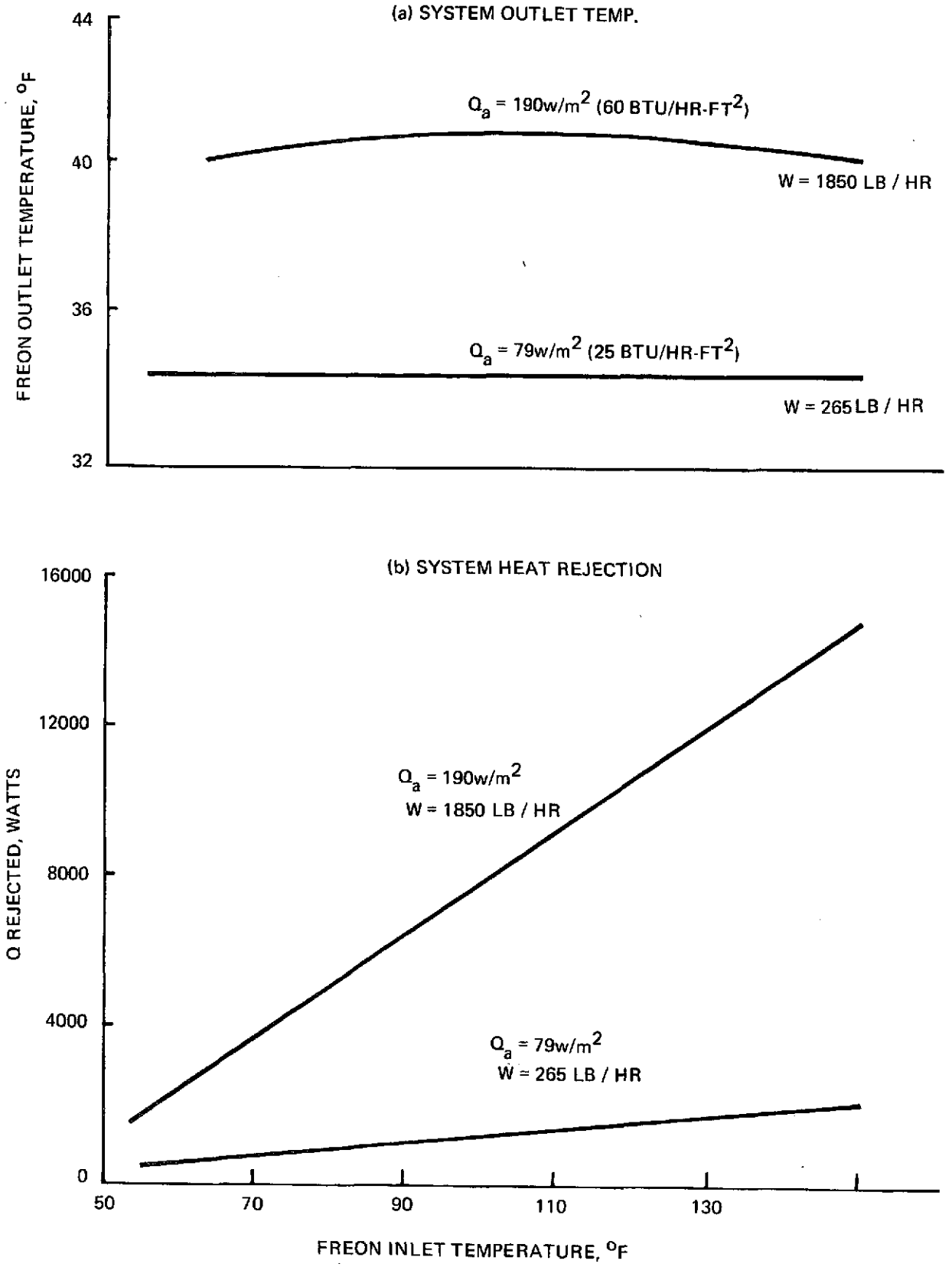

Figure 3-10 Series System Performance

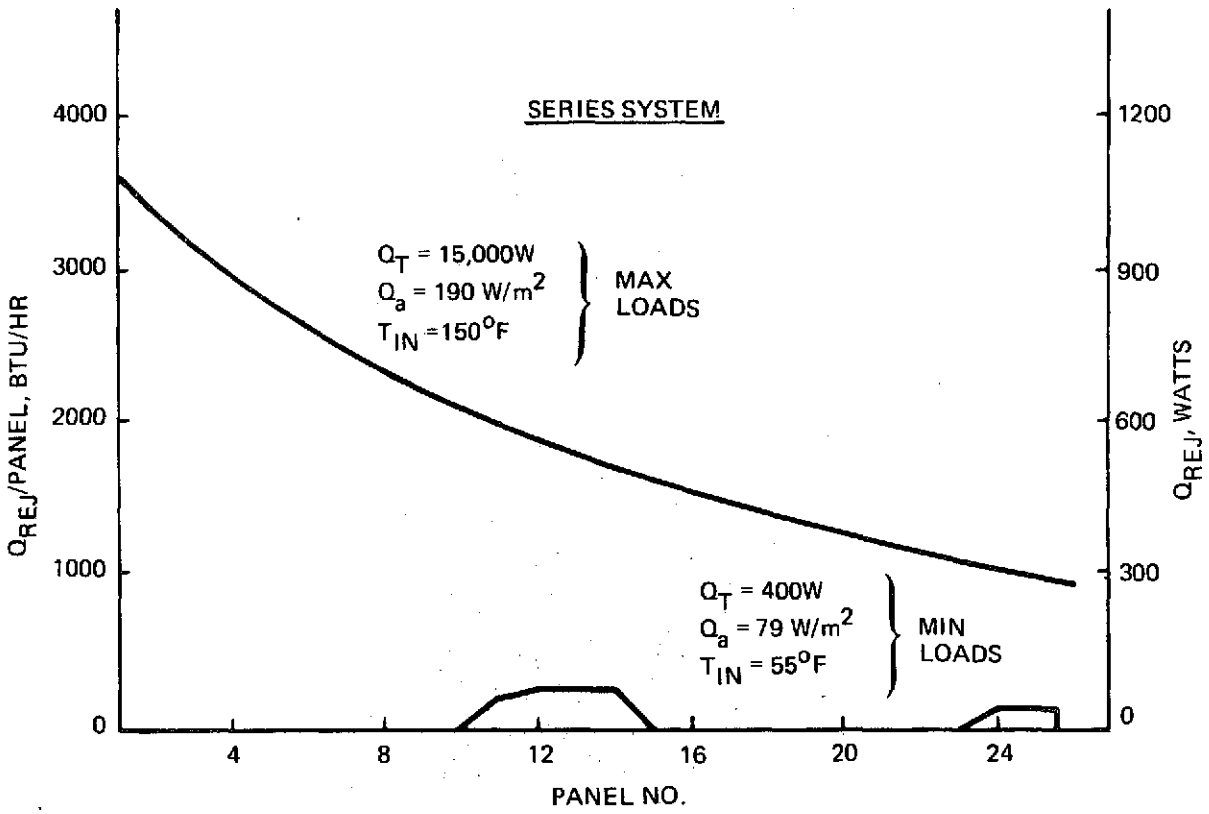

Figure 3-11 Heat Rejected Per Panel, Maximum and Minimum Loads

Section 4

DESIGN DETAILS

The objective of the hardware phase of this program was to design and build a typical VCHP radiator module that would demonstrate the feasibility of the technical approach. No attempt was made to weight-optimize the design. The basic panel, shown in Figure 4-1, has the VCHP header, fluid heat exchanger, panel feeder heat pipes and radiating fin as its major components.

The overall size of the panel was set by ground rules at 4 x 8 ft. The number of feeder heat pipes for the panel was determined by the required fin effectiveness, redundancy, ease of fabrication and cost. A large number of feeder pipes would certainly result in a more efficient panel but it would also unnecessarily complicate the manufacturing and assembly. Six feeder pipes, spaced on 8-in. centers, were chosen as a reasonable compromize. If any one pipe were lost due to a puncture, the panel's fin effectiveness would be only slightly affected.

For ease of manufacturing and assembly, the basic panel is formed from six finned subassemblies joined (riveted) along their common edges to form the complete panel. Each subassembly contains the condenser section of a feeder heat pipe cradled in a centrally located semicylindrical depression running the entire length of the fin. A polyurethane bonding agent (Crest Products Co.) is used to attach each heat pipe to its fin. The temperature drop between the condenser and the fin root is kept small (less than $1^{o}F$) due to the relatively thin .010-.015-in. bondline and the large heat transfer area. The evaporator sections of the feeder heat pipes are welded to the condenser of the VCHP header to minimize the temperature gradient across the interface. (There is not enough heat transfer area available to permit the use of a mechanical type of attachment without incurring excessive temperature drops.) Figure 4-2 shows details of the welded interface.

A .020 in. thick aluminum sheet was specified for the fin material primarily because it could be more readily formed than the larger thicknesses. The fin effectiveness for the panel as a function of root temperature is shown in Figure 4-3. The curve is based upon an assumed surface emittance of .90 which was provided by 3-M White Velvet paint.

FOLDOUT FRAME 1

FOLDOUT FRAME 2

NOTES (UNLESS OTHERWISE INDICATED)

1- ALL AL ALY WELDING SHALL BE IN ACCORDANCE WITH MIL-W-8604 USING FILLER WIRE ALLOY 5183, 5356 OR 5556.

2- DURING WELDING OPERATION, WELDING FIXTURES SHALL BE FULLY UTILIZED WHENEVER NECESSARY TO MINIMIZE DISTORTIONS AND TO MAINTAIN DIMENSIONS SHOWN. (COORDINATE WITH ENGR'G IN PROBLEM AREAS). SEE AD1411-1308X DWG FOR WELD HOLDING FIXTURE FOR FEEDER PIPES.

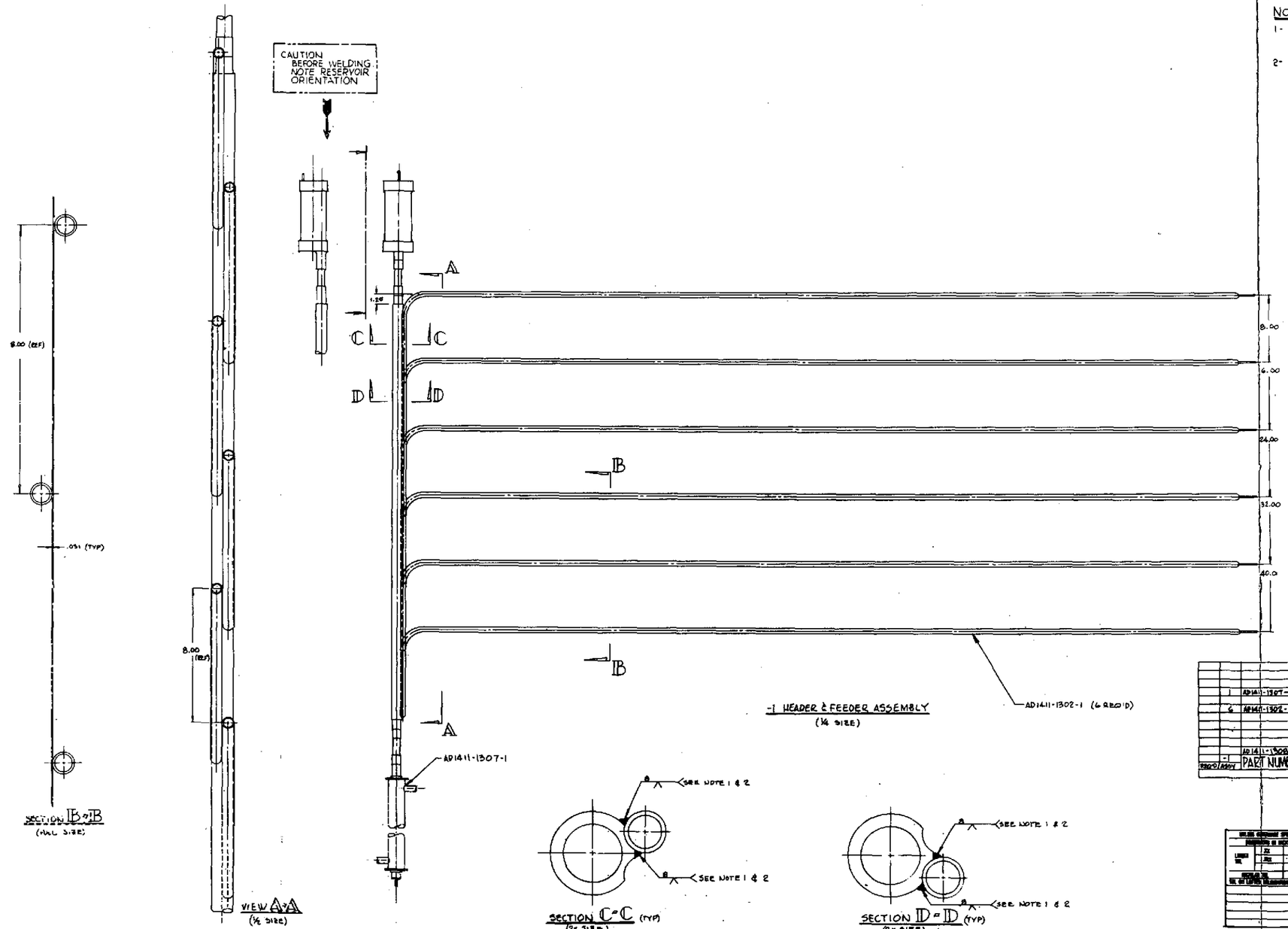

-1 HEADER & FEEDER ASSEMBLY
(1/4 SIZE)

QTY PER ASSY	PART NUMBER	NOMENCLATURE	MATERIAL	GOVT SPEC	COMM SPEC	STOCK SIZE	QTY REQ'D
1	AD1411-1307-1	HEADER ASSY					
6	AD1411-1302-1	FEEDER ASSY					
-	AD1411-1308-1	HEADER & FEEDER ASSY (WELDED)					

PARTS LIST

NEXT ASSY- AD1411-1309

	CONTRACT NO. NAS 9-12848	GRUMMAN AEROSPACE CORPORATION BETHPAGE, NEW YORK 11714
		HEADER & FEEDER ASSEMBLY RADIATOR HEAT PIPE
		SIZE 26512 AD1411-1308
		NONE NOTED

Figure 4-1 Panel Assembly

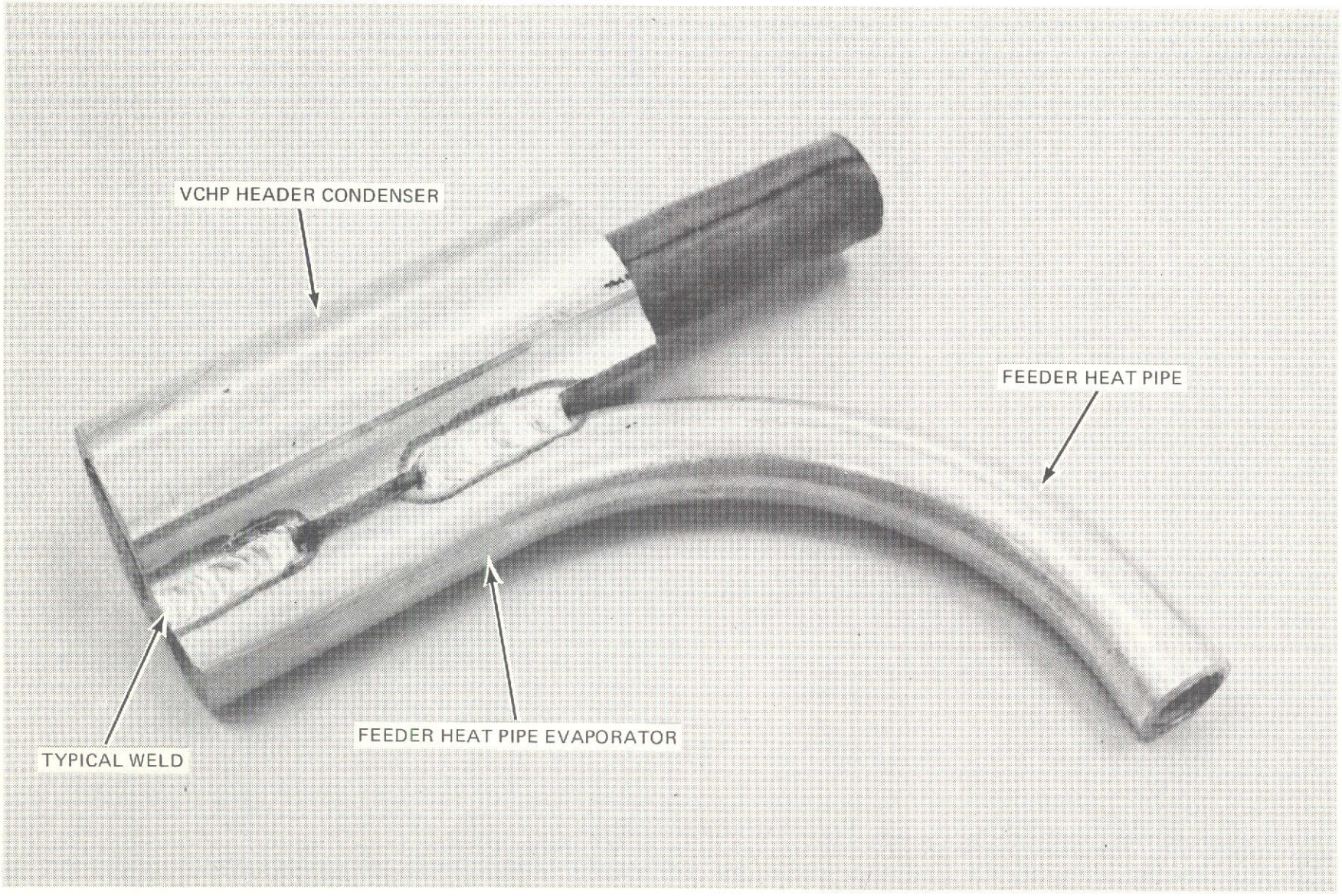

Figure 4-2 VCHP Header/Feeder Pipe Welded Interface

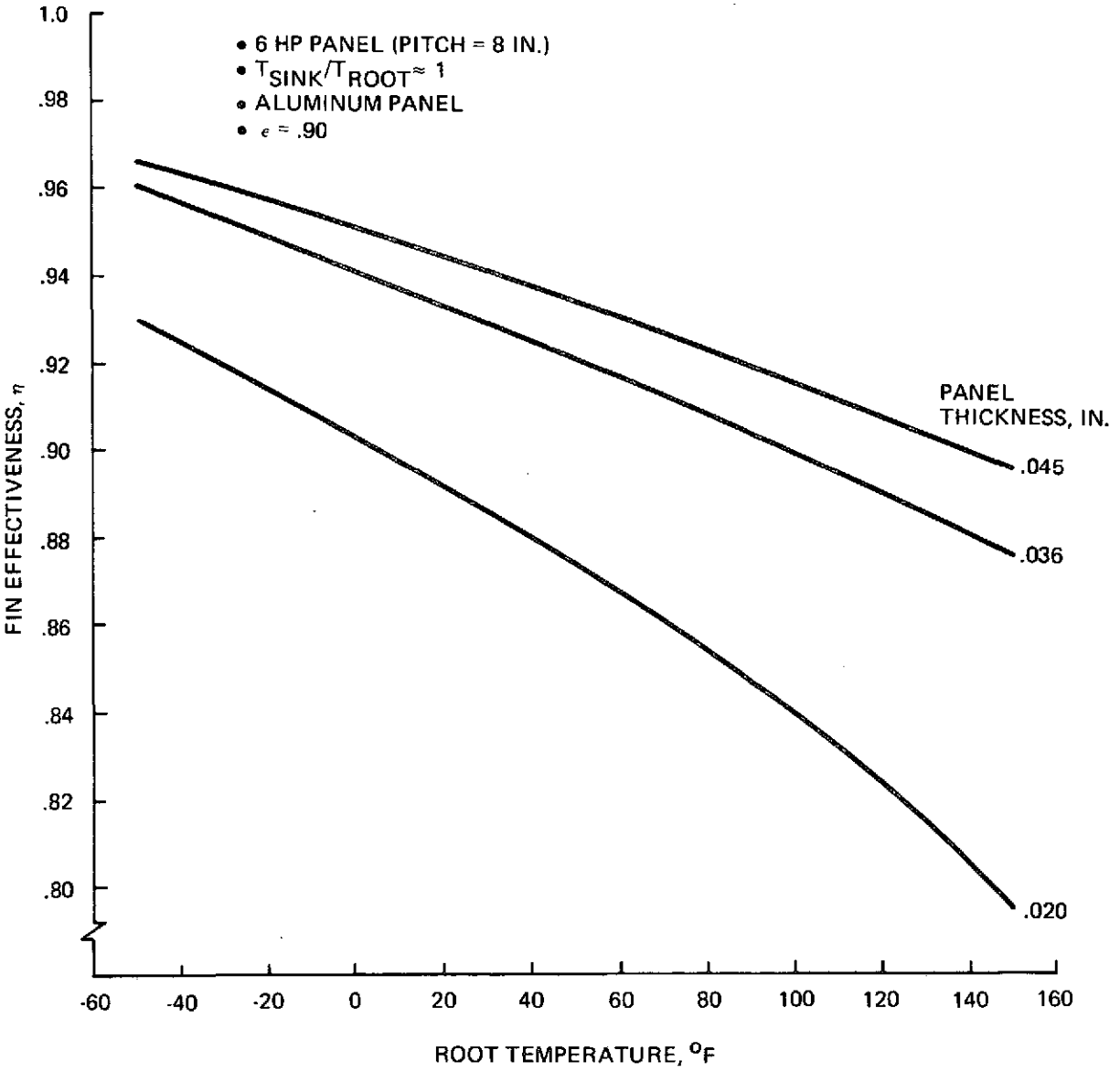

Figure 4-3 Heat Pipe Panel Fin Effectiveness

4.1 PANEL FEEDER HEAT PIPES

The overall dimensions of the feeder heat pipes were dictated by the fixed 4 x 8 ft panel area and the 8-in. center-to-center spacing. The condenser sections of the pipes were made equal to the panel length of 8 ft and the evaporator sections were made equal to the 8-in. spacing. This of course required the evaporator to be perpendicular to the condenser and resulted in an L-shaped configuration. An additional 2 in. were added to each pipe to accommodate the transition section (bend) between the evaporator and condenser; thus the overall length of each feeder pipe was 106 in. The pipe envelope was made from 6061 aluminum with a 0.625-in. o.d. and 0.500-in. i.d. since it was readily available and satisfied all structural and manufacturing requirements.

The feasibility panel needed a nominal 500 watt capacity at 70 - 75°F. The required capacity of each feeder pipe was therefore one-sixth of the panel capacity or approximately 85 watts. However, each feeder pipe was designed to handle at least 170 watts at an adverse tilt of 0.500 in. This was done to provide adequate margin in case the panel might be called upon to reject higher loads--as it would be if it were tested as the number 1 panel in the series system (1000 watt capacity at 135°F). Capacity at tilt was necessary to facilitate 1-g ground testing by minimizing the importance of panel alignment.

Ammonia was selected as the working fluid due to its high figure of merit and the performance margin that it offered. A basic spiral artery wicking system was decided upon because it promised superior performance at tilt than the simpler, longitudinally grooved extrusions that were available at the time. Results of computerized parametric analyses are presented in Figure 4-4 and give predicted capacity as a function of tilt and temperature. The decrease in capacity with increasing temature is related to the corresponding decrease in the liquid transport factor $(\sigma \rho \lambda / \mu)$ for ammonia over the 75°F-125°F range. As shown in Figure 4-4a, the feeder pipe design has more than adequate capacity over the temperature range of interest. Figure 4-4b indicates how the pipe will perform when tilted. The high tilt capability is due to the 170 mesh overwrap of the artery and relaxes possible test constraints.

Details of the pipe and artery design are given in Figure 4-5 and summarized in Table 4-1. The pipe has only two welds and is bent on a 2.5-in. radius. A 10-in. long biased wrapped flexible section is spliced to the normal artery to permit forming the bend after the artery is inserted in the pipe.

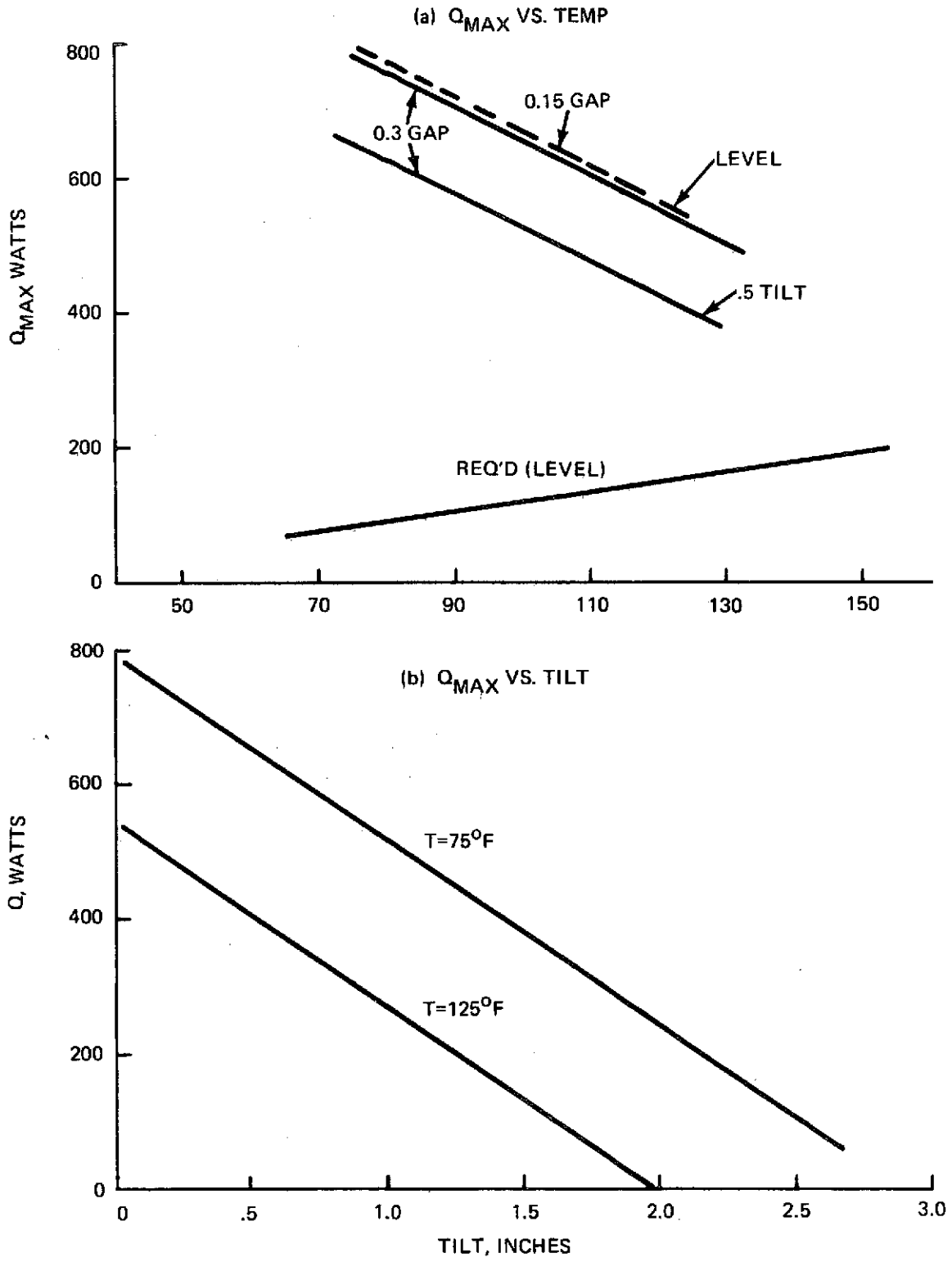

Figure 4-4 Feeder Pipe Performance

FOLDOUT FRAME

FOLDOUT FRAME 2

REVISIONS			
LTR	DESCRIPTION	DATE	APPROVED
A	1. REDRAWN & REDESIGNED	9/8/72	

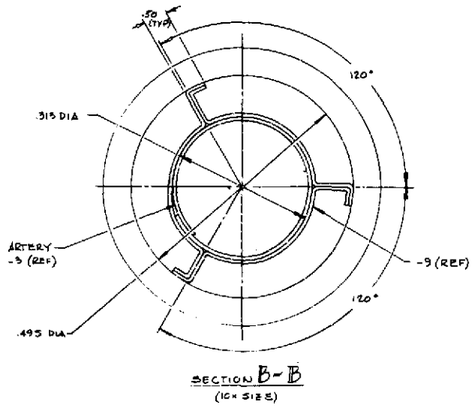

SECTION B-B
(10× SIZE)

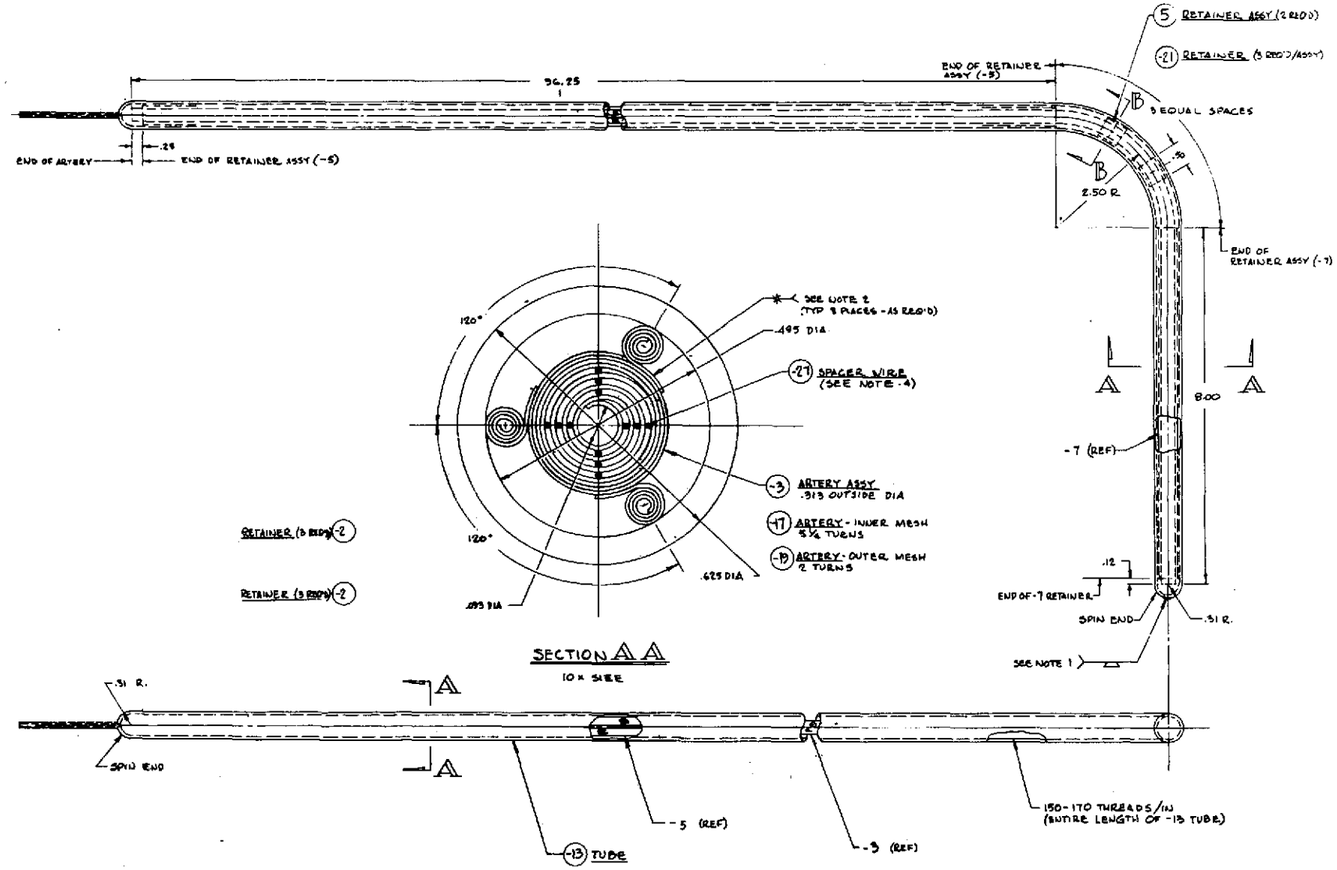

-1 HEAT PIPE ASSY

NOTES:
1. WELD PER SPEC MIL-W-8604
2. SPOT WELD PER SPEC MIL-W-6858 CLASS 'A'
3. PASSIVATE -3, -5, -7, & -9 ASSY'S PER MIL-S-5002.
4. .110 AND 100 MESH SCREEN STRIPS MAY BE SUBSTITUTED FOR WIRE IN THE BEND AREA.

ASSEMBLY PROCEDURE:
1. INSTALL ARTERY AND RETAINERS INTO TUBE
2. SPIN EACH END
3. FORM BEND
4. WELD TIP AT SHORT END
5. WELD IN CHARGE TUBE - LONG END
6. CHARGE TUBE WITH AMMONIA
7. PINCH OFF CHARGE TUBE

		✓		-35	AMMONIA (NH3)	ULTRA HIGH PURITY	PURITY (99.999 %)				REF
	✓			-27	SPACER WIRE	304 ST.STL. WIRE	.012-.014		.018 DIA		12 REQ'D
				-25	RETAINER	304 ST.STL. SCREEN	.014-.160				6
				-25	RETAINER	304 ST.STL. SCREEN					3
	3			-21	RETAINER	304 ST.STL. SCREEN					3
		1		-19	ARTERY (OUTER)	304 ST.STL. SCREEN	.014-.160				2
		1		-17	ARTERY (INNER)	304 ST.STL. SCREEN					4
		1		-15	CHARGE TUBE						1
		1		-13	TUBE	6L-ALLOY TUBE	WALL-.020/.16	6061-T6	.875x.065W x 110		1
		2		-9	RETAINER ASSY (SPACER)		SEE NOTE 3				2
		1		-7	RETAINER ASSY (SHORT)		SEE NOTE 3				1
		1		-5	RETAINER ASSY (LONG)		SEE NOTE 3				1
		1		-3	ARTERY ASSY		SEE NOTE 3				1
			AD1411-1302-1		HEAT PIPE ASSY						1
-5	-3	-1	PART NUMBER		NOMENCLATURE	MATERIAL	GOVT. SPEC	COMM. SPEC	STOCK SIZE		QTY REQ'D
REQUIRED PER ASSY			PARTS LIST								

NEXT ASSY AD1411-1308

	NAS9-12848	GRUMMAN AEROSPACE CORPORATION BETHPAGE, NEW YORK 11714
	DRAWN G. HALL 8-8-72	FEEDER ASSEM HEAT PIPE RADIATOR
	APPROVED	
	SIZE R	CODE IDENT NO. 26512
	DWG NO. AD1411-1302	REV A

Figure 4-5 Feeder Heat Pipes

Table 4-1 - Feeder Heat Pipe Design Details

Evaporator = 8.0 in. Condenser = 96.0 in. Overall Length = 106.0 in.
Pipe Envelope
• 6061 Aluminum tube, 0.625 in. x 0.500 in. • 150 Circumferential grooves/in.
Artery
• OD = .310 in. • Gap = 0.015 in. • Tunnel diameter = 0.093 in. • Material - 100 mesh SS/170 mesh outer wrap • Retainer - 170 mesh, 3 webs

4.2 VCHP HEADER

The VCHP header consists of a circumferentially grooved aluminum envelope, 1.00-in. OD nominal and 97.54 in. long. The main sections of the pipe are: the heat exchanger, 29.88 in. long; two low K sections, 4.31 in., condenser, 51.69 in. and reservoir 7.25 in. Additional dimensional information is given in Figure 4-6.

The inside diameter of the pipe is 0.867 in., grooved with 208 threads/in. The artery is a tunnel design (Ref. 12) with an overall outside diameter of .683 in. and a tunnel diameter of .200 in. The tunnel wick is fabricated in 100 mesh stainless steel screening and sealed in a 170 mesh stainless steel screen outer enclosure. The artery is supported in the heat pipe with an eight-web, 170 mesh retainer system in the condenser and evaporator sections of the pipe. The retainer outside diameter is covered (or shielded) with .002 in. nickle foil and one layer of 100 mesh screen in order to build up a .010 in. thick insulating layer of NH_3 on the outside of the retainer. The shield and insulator screen are incorporated to minimize the reheat of the subcooled fluid from the condenser wall as it travels down the artery system to the evaporator section of the pipe (Ref. 13).

The artery is terminated at the end of the condenser assembly. Two 170 mesh scrolls, .080 in. in diameter provide the capillary communication paths between the condenser retainer and the reservoir which is lined with 100 mesh stainless steel

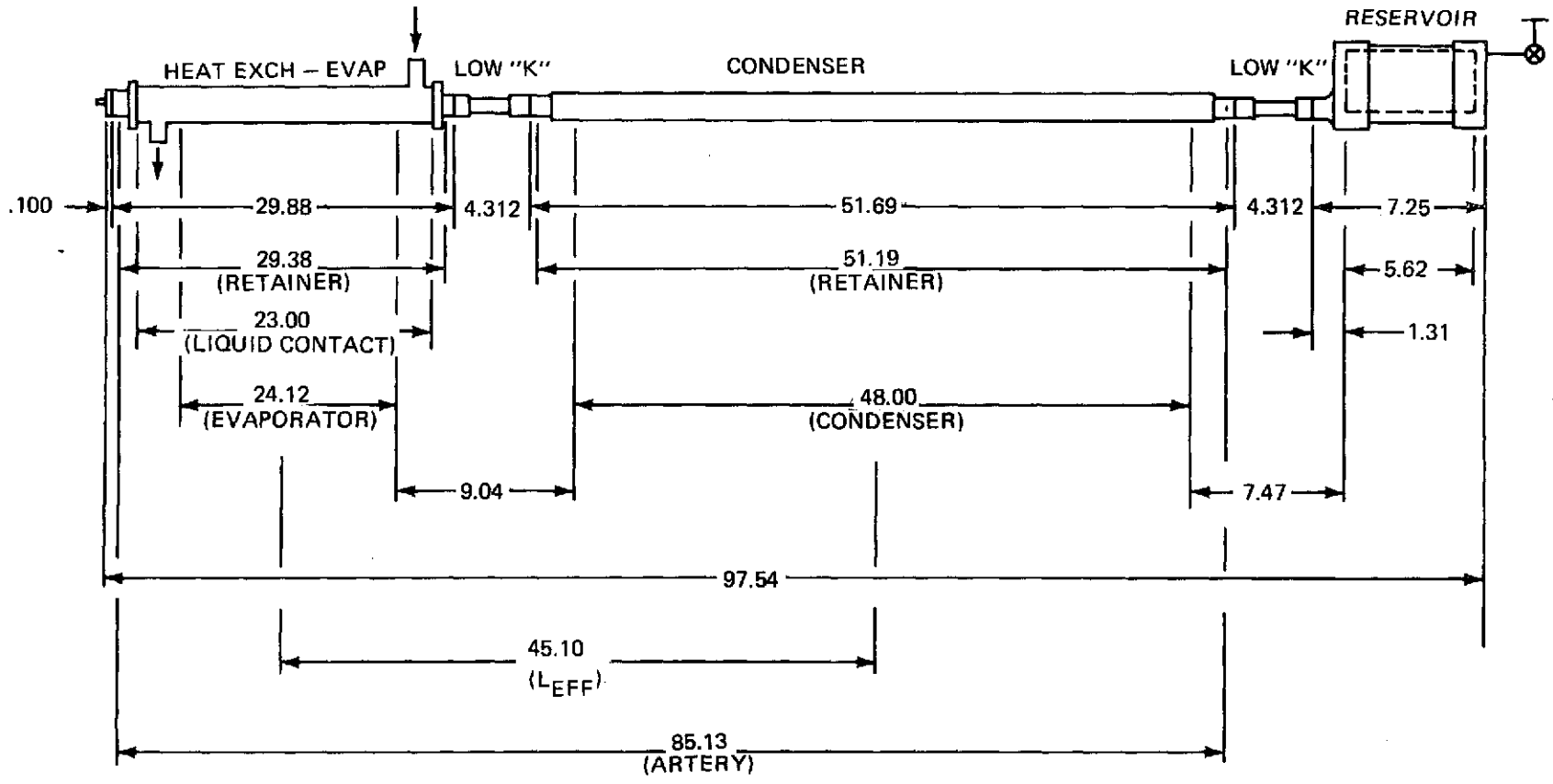

Figure 4-6 Header Heat Pipe Reference Dimensions (Inches)

screening. The condenser section envelope is grooved longitudinally with two .625 in. diameter slots to receive the evaporator sections of the feeder pipes as was shown in Figure 4-2. Figure 4-7 is a detailed drawing of the VCHP header assembly.

The design of the VCHP header was based on providing a maximum annulus flow area in the pipe. The annulus is defined as the area between the artery o.d. (.683 in.) and the tunnel diameter (.200 in). The intent of the maximum annulus design is to provide for vapor/gas bubble growth within the artery and still hold design capacity with fluid flow in the outer wraps of the artery (Ref. 13).

The theoretical performance of the above configuration (not optimized for Q_{max}) in the single fluid mode (no inert gas), is presented in Figure 4-8. The upper curves are the Q_{max} vs tilt performance with a fully primed tunnel. The lower curve is the performance based on annulus capacity only (tunnel deprimed).

The reservoir size and inert gas charge in a passive VCHP are determined by the temperature control range requirements and the variations in the sink environments for the condenser and reservoir radiator panels. Of course, the reservoir size and inert gas charge are also a function of the vapor space volume in the condenser.

The performance requirements for the VCHP header are included in the panel specifications which were given in Table 3-4. They specify a maximum capacity of 500 watts; a full open condenser at a pipe temperature of $72^{o}F$, while in a maximum environment defined by Q_a = 60 Btu/hr-ft^2, and a fully closed condenser at a pipe temperature of $41^{o}F$, while in a minimum environment of Q_a = 25 Btu/hr-ft^2.

The reservoir volume and N_2 inert gas charge for the above conditions, as determined by the VCHP computer program, are respectively 39.73 in.^{3} and .01498 lb.

To meet the volume requirement the reservoir was designed as a cylinder, 5.62 in. long, with a 3.00 in. i.d.

The predicted locations of the interface separating the N_2 gas and NH_3 in the condenser of the VCHP are plotted in Figure 4-9. The curve for maximum environment (60 Btu/hr-ft^2) and the curve for minimum environment (25 Btu/hr-ft^2) define the full operating range of the pipe. Thus, even though the overall operating range of the pipe is 41 - $72^{o}F$, the control span for a fixed environment (fixed reservoir and full off condenser temperature) is approximately $7^{o}F$.

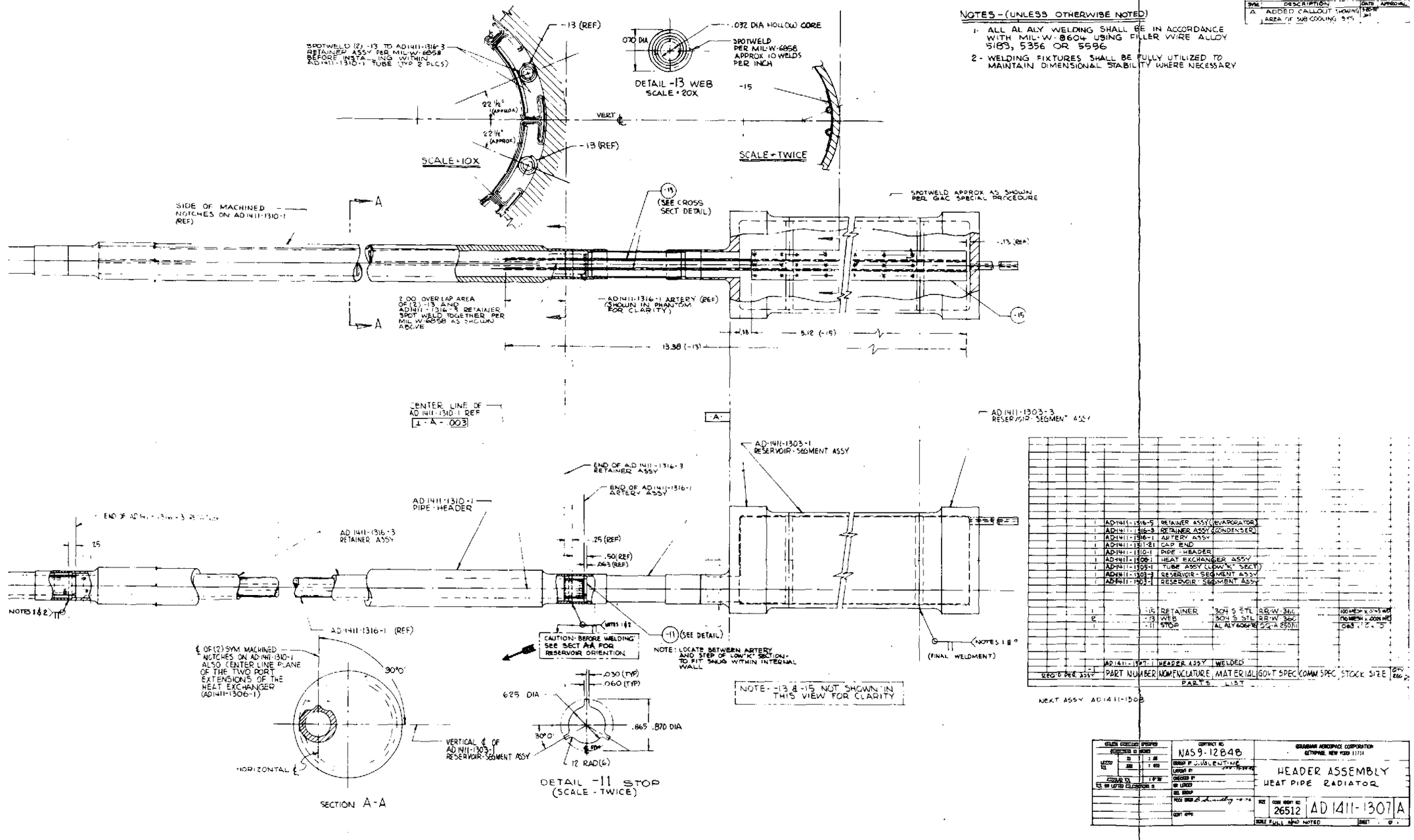

REVISIONS

SYM	DESCRIPTION	DATE	APPROVAL
A	ADDED CALLOUT SHOWING AREA OF SUB-COOLING SYS		

NOTES - (UNLESS OTHERWISE NOTED)

1. ALL AL ALY WELDING SHALL BE IN ACCORDANCE WITH MIL-W-8604 USING FILLER WIRE ALLOY 5183, 5356 OR 5556
2. WELDING FIXTURES SHALL BE FULLY UTILIZED TO MAINTAIN DIMENSIONAL STABILITY WHERE NECESSARY

ITEM	QTY	PART NUMBER	NOMENCLATURE, MATERIAL	GOVT SPEC	COMM SPEC	STOCK SIZE
1		AD1411-1316-5	RETAINER ASSY (EVAPORATOR)			
1		AD1411-1316-3	RETAINER ASSY (CONDENSER)			
1		AD1411-1316-1	ARTERY ASSY			
1		AD1411-1311-21	CAP END			
1		AD1411-1310-1	PIPE-HEADER			
1		AD1411-1306-1	HEAT EXCHANGER ASSY			
1		AD1411-1305-1	TUBE ASSY (LOW 'K' SECT)			
1		AD1411-1303-3	RESERVOIR-SEGMENT ASSY			
1		AD1411-1303-1	RESERVOIR-SEGMENT ASSY			
1		-15	RETAINER	304 S STL	QQ-W-366	100 MESH x .0045 WIRE
2		-13	WEB	304 S STL	QQ-W-366	150 MESH x .0024 WIRE
1		-11	STOP	AL ALY 6061-T6	QQ-A-250/11	.063 x .10 x 5
1		AD1411-1307	HEADER ASSY	WELDED		
REQ'D PER ASSY		PART NUMBER	NOMENCLATURE, MATERIAL	GOVT SPEC	COMM SPEC	STOCK SIZE

PARTS LIST

CONTRACT NO	NAS9-12848	GRUMMAN AEROSPACE CORPORATION BETHPAGE, NEW YORK 11714
		HEADER ASSEMBLY HEAT PIPE RADIATOR
SIZE	CODE IDENT NO 26512	AD1411-1307 A
SCALE FULL AND NOTED		SHEET

Figure 4-7 Header Assembly (Sheet 1 of 2)

FOLDOUT FRAME

FOLDOUT FRAME 2

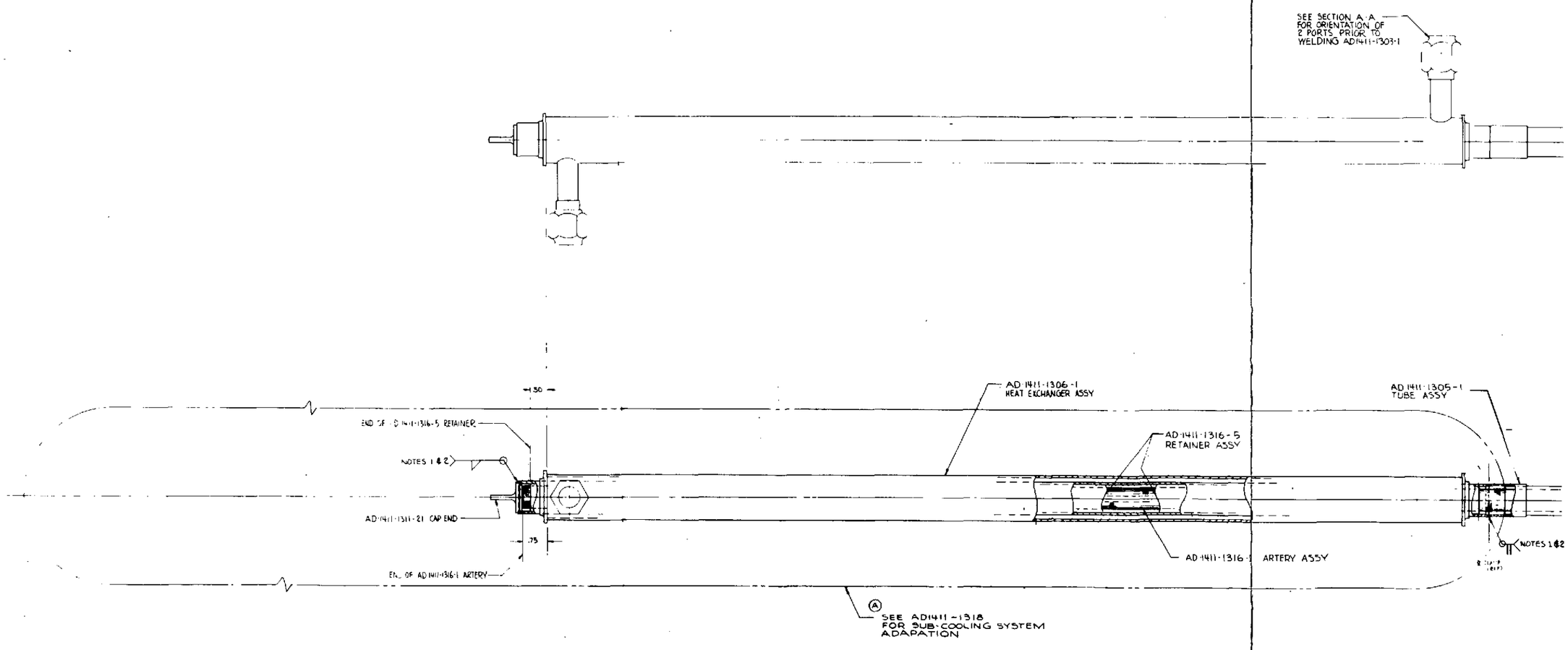

-1 HEADER ASSEMBLY

Figure 4-7 Header Assembly (Sheet 2 of 2)

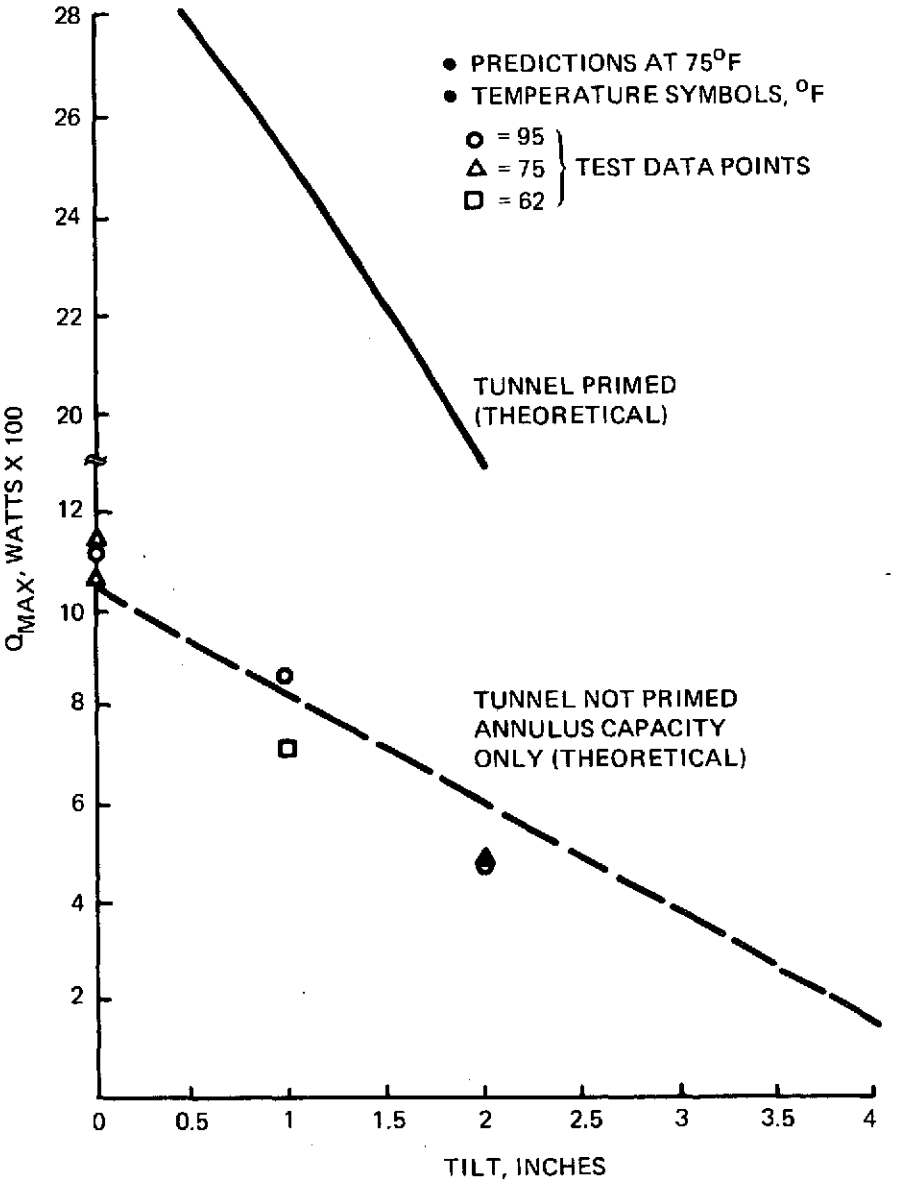

Figure 4-8 Radiator Header Performance Without Control Gas

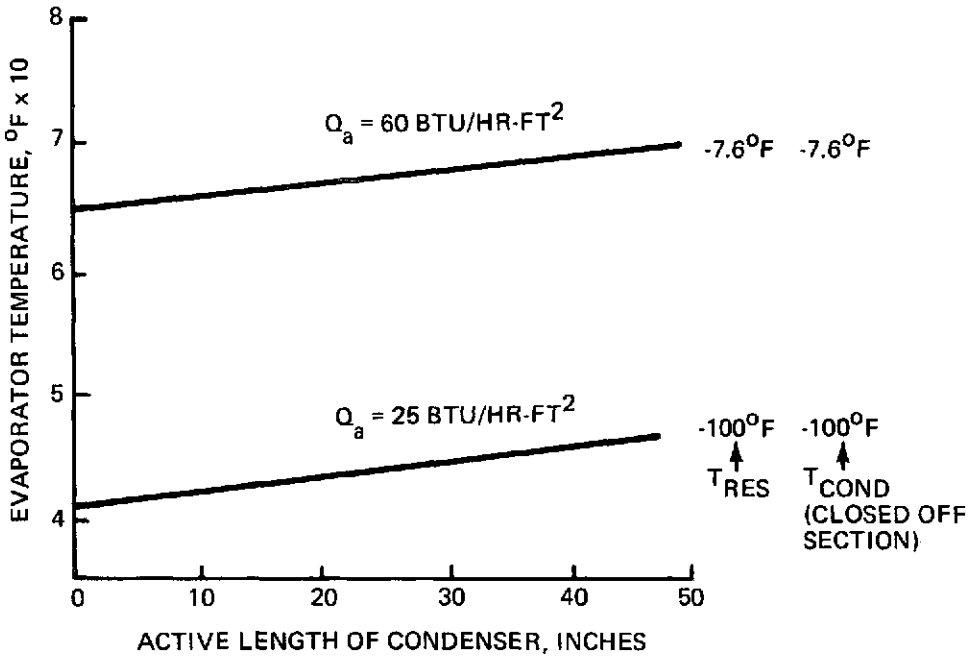

Figure 4-9 Header Interface Location For Design N_2 Charge of 0.01498 Lb

If the fluid temperature in the circulating loop exceeds 72°F (neglecting heat exchanger ΔT's) the VCHP will open fully. The panel will reject 500 watts until the fluid loop inlet temperature decreases to within the control range 65 - 72°. If the loop load decreases further and the temperature falls below 65°, the VCHP will shut off completely.

Two conditions will advance the interface back into the condenser: (1) an increasing fluid loop load, or (2) a decrease in the environment (Q_a). Following the later case the VCHP will modulate with a 7° span at a lower pipe temperature rejecting a little less than 500 watts. Reducing the fluid loop load will again lead to a pipe shut off condition; reducing Q_a will open it again. This process can be continued until Q_a = 25 Btu/hr-ft^2 (the minimum). At this point the control range will be 41-47°F.

4.3 HEAT EXCHANGER

The heat exchanger is designed to transfer heat from a Freon-21 heat transport loop to the evaporator section of the VCHP header. It is 24 in. long with an o.d. = 1.25 in. and i.d. = 1.00 in. The core of the exchanger is made of 48 circumferential aluminum strip fins that are brazed to the o.d. of the VCHP header. Brazing was required to provide good thermal contact which increased the available heat exchanger effectiveness. The actual exchanger core is shown in Figure 4-10 and a detailed assembly drawing is given in Figure 4-11.

The required number of fins was dictated by the available core material (15 fins/in.) and the pipe i.d.

$$N_{Fins} = {}^{Fins}/_{in.} \times \pi D_i$$

$$N = 15 \times \pi \times 1.0 = 48$$

From the fin dimensions, the free flow area was calculated to be A_c = 0.24 in.^{2} = 0.00167 ft^2. The hydraulic diameter D_h was determined from:

$$D_h = \frac{4 \times \text{Flow Area}}{\text{Wetted Perimeter}} = 0.0734 \text{ in.} = 0.0061 \text{ ft}$$

The Reynolds number was found from:

$$R_e = \frac{D_h G}{\mu}$$

where $G = m/A_c$

μ = freon viscosity

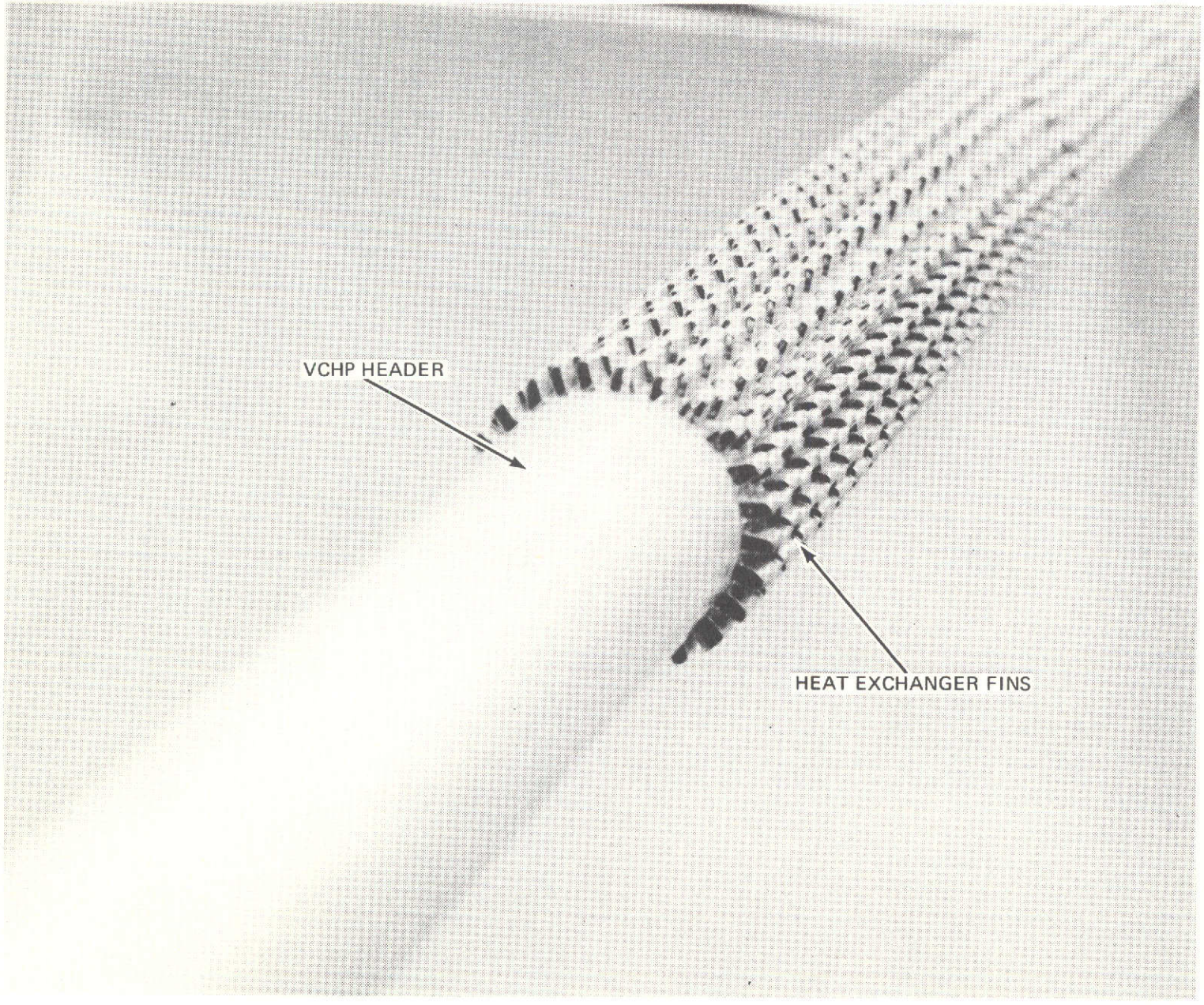

Figure 4-10 Heat Exhanger Core

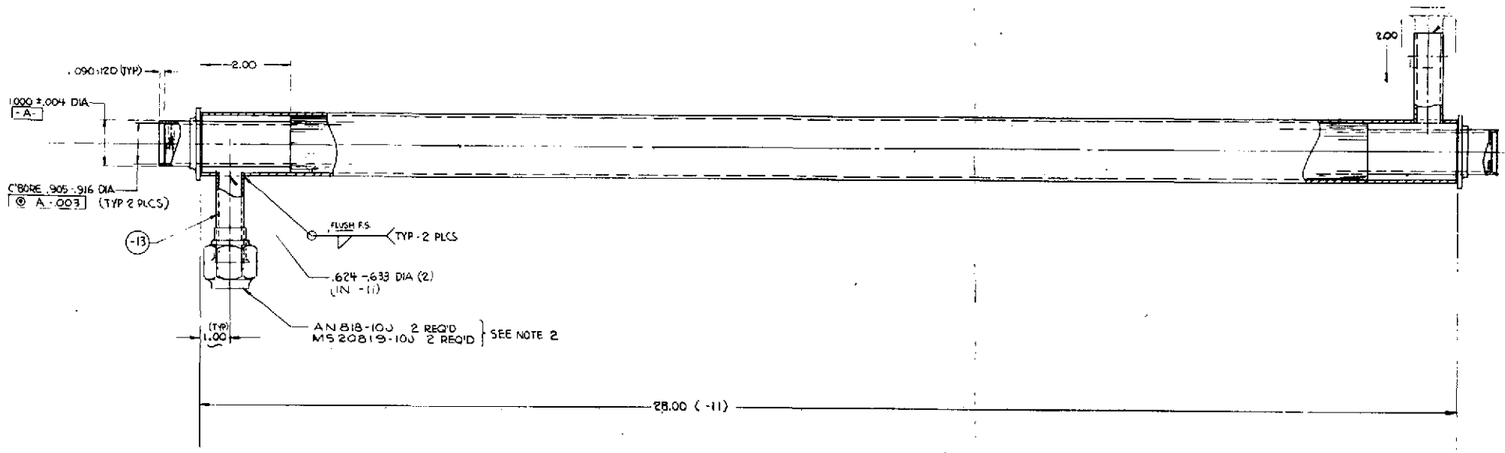

NOTES:

1- ALL AL ALY WELDING SHALL BE IN ACCORDANCE WITH MIL-W-8604 USING FILLER WIRE ALLOY 5183, 5356 OR 5556.

2- AN818-10K & MS20819-10K MAY BE USED IN LIEU OF -10J FOR NUT AND SLEEVE

3- INSTALL AD1411-1304-1 FIN ASSY WITHIN -3 SHELL ASSY SO THAT NO GAP EXIST BETWEEN RESPECTIVE PARTS. TO ACHIEVE THIS, CONCENTRIC SHIMMING AND/OR MACHINING INSIDE DIA OF -11 IS PERMITTED.

REQ'D PER ASSY		PART NUMBER	NOMENCLATURE/MATERIAL	GOVT. SPEC	COMM. SPEC	STOCK SIZE	KEY REQ'D
2		AN818-10J	NUT	STD. PARTS	SEE NOTE		2
2		MS20819-10J	SLEEVE	STD. PARTS	1 & 2		2
	1	AD1411-1304-1	FIN ASSEMBLY	SEE DWG			1
	2	AD1411-1311-19	FLANGE				
2		AD1411-1306-13	TUBE	ALUM ALY TUBE	WW-T-700/6	6061-T6	.609 D x .035 WALL	2
1		AD1411-1306-11	OUTER SHELL	ALUM ALY TUBE	WW-T-700/6	6061-T6	1.750 D x .028 WALL	1
	1	AD1411-1306-3	OUTER SHELL ASSY (AS WELDED)					1
	1	AD1411-1302-1	HEAT EXCHANGER ASSY (AS WELDED)					1

PARTS LIST

NEXT ASSY AD1411-1307 FOR -1

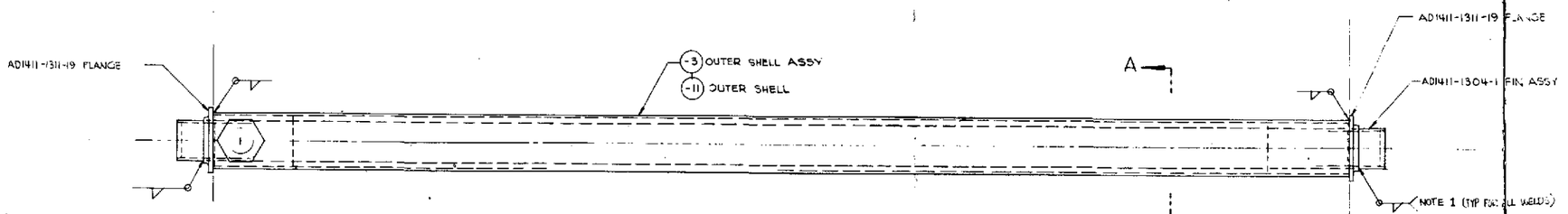

-1 HEAT EXCHANGER ASSY

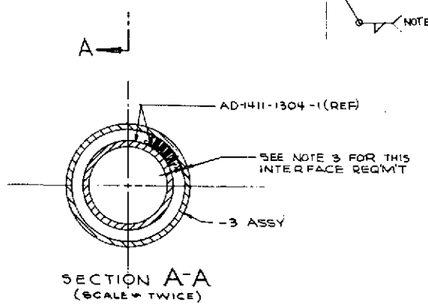

SECTION A-A
(SCALE = TWICE)

	CONTRACT NO. NAS 9-12848	GRUMMAN AEROSPACE CORPORATION BETHPAGE, NEW YORK 11714
		HEAT EXCHANGER ASSEMBLY HEAT PIPE RADIATOR
		SIZE A CODE IDENT NO. 26512 DWG NO. AD1411-1306
		SCALE 1/1 SHEET 1 OF 1

Figure 4-11 Heat Exchanger Assembly

At a flow rate m = 1850 lb/hr, the Reynolds number was calculated to be 8900.

From a similiar fin, (Ref. 14) the "Colburn" J-factor was estimated to be 0.0063.

The J" factor is defined as:

$$J = (h_f/GC_p)\ (N_{pr})^{2/3} \qquad (4\text{-}1)$$

where h_f = fluid conductance

C_p = fluid specific heat = 0.25

N_{pr} = Prandt'l number = 3.46

Using equation (4-1), the fluid conductance h_f is calculated to be:

$$h_f = 767\ \frac{\text{Btu}}{\text{hr-ft}^2{}^{o}\text{F}} = 5.33\ \frac{\text{Btu}}{\text{hr-in.}^{o}\text{F}}$$

However, where an extended surface is used, temperature gradients along the fins extending into the fluid reduce the temperature effectiveness of the surface. To account for this, a surface effectiveness η_o is determined from:

$$\eta_o = 1 - \frac{A_f}{A_t}\ (1 - \eta_f) = 0.685$$

where $\frac{A_f}{A_t}$ = ratio of total fin area to total heat transfer area = 0.870

η_f = fin effectiveness = 0.638

The heat transfer or conductance from the freon to the header wall can now be determined from:

$$U_1A_T = \eta_o A_T h_f = 1150\ \frac{\text{Btu}}{\text{hr-}^{o}\text{F}}$$

where A_T, the total heat transfer area is 2.18 ft^2

The effectiveness of the system can be determined from

$$\eta = 1 - e^{-\text{NTU}}$$

where NTU is the number of heat transfer units of the heat exchanger $= \frac{(UA)_x}{mc_p}$

$$(UA)_x = \frac{1}{\frac{1}{U_1A_T} + \frac{1}{U_2A_H}}$$

U_2A_H = header conductance = $\frac{\pi D L_{ev} h_{ev}}{144} = 1230 \frac{Btu}{hr^oF}$

Therefore $(UA)_x = 588 \frac{Btu}{hr^oF}$ and NTU = 1.27

and $\eta_x = 1-e^{-1.27} = .72$ at a flow rate of 1850 lb/hr.

η_x as a function of flow rate is shown in Figure 4-12.

The temperature drops through the heat exchange system can be related to η_x by:

$$\eta_x = \frac{T_{in} - T_{out}}{T_{in} - T_v} \tag{4-2}$$

where T_{in} = freon inlet temperature

T_{out} = freon outlet temperature

T_v = header vapor temperature

Equation (4-2) can be rearranged as:

$$\eta_x (T_{in} - T_v) = (T_{in} - T_{out}) = Q/mC_p$$

Both $(T_{in} - T_v)$ and $(T_{in} - T_{out})$ are plotted as a function of Q in Figure 4-13.

The pressure drop through the heat exchanger was estimated from

$$\Delta P = \frac{G^2}{2 g_c \rho} \frac{(f A_t)}{A_c}$$

Where: g_c = gravitational constant

ρ = liquid density

f = friction factor

The entrance and exit loss coefficients have been neglected since they are small compared to the friction loss. At the design flow rate of 1850 lb/hr, the pressure drop is approximately one-half psi. The details of the final heat exchanger design are presented in Table 4-2.

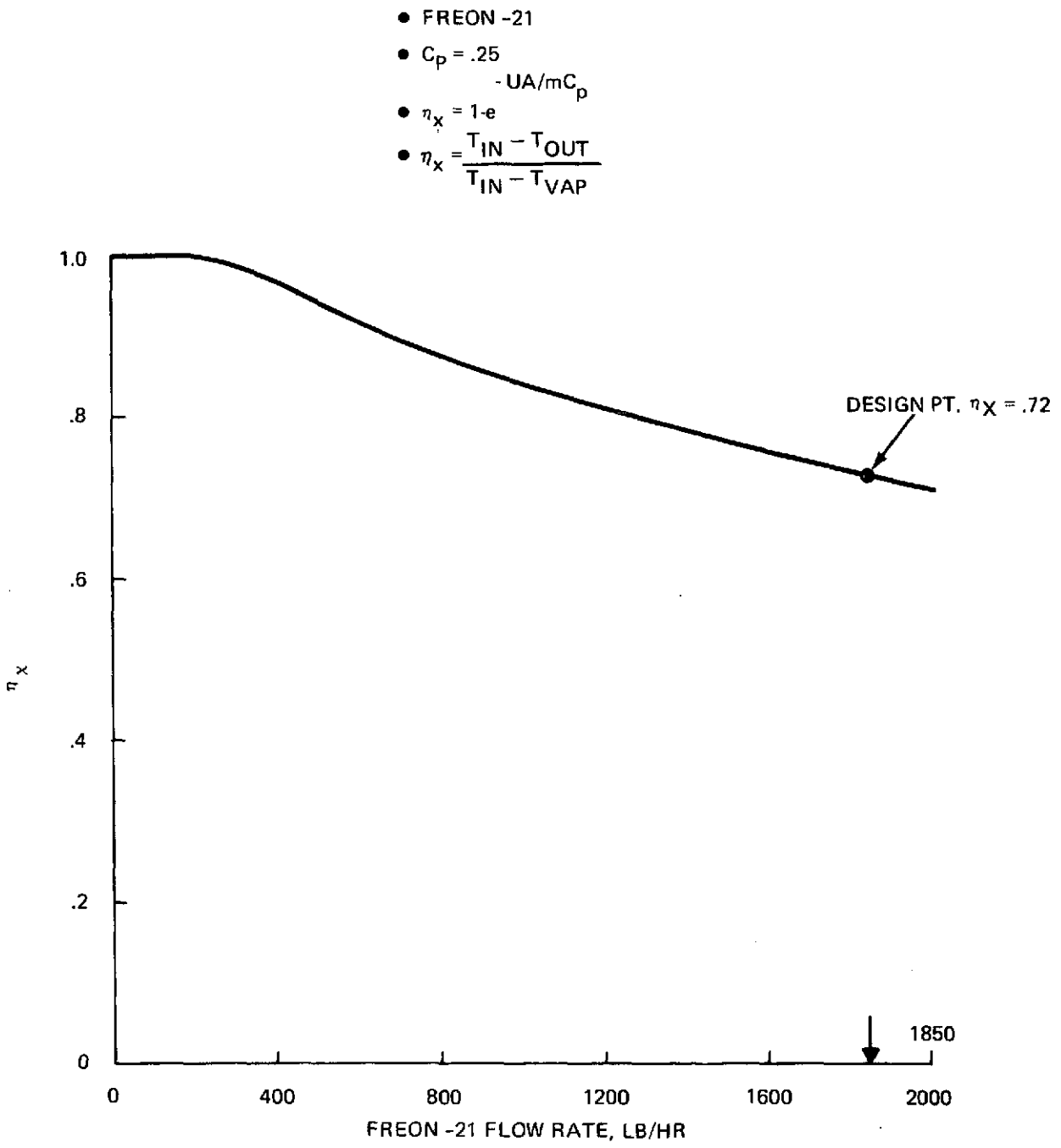

Figure 4-12 Heat Exchanger Effectiveness

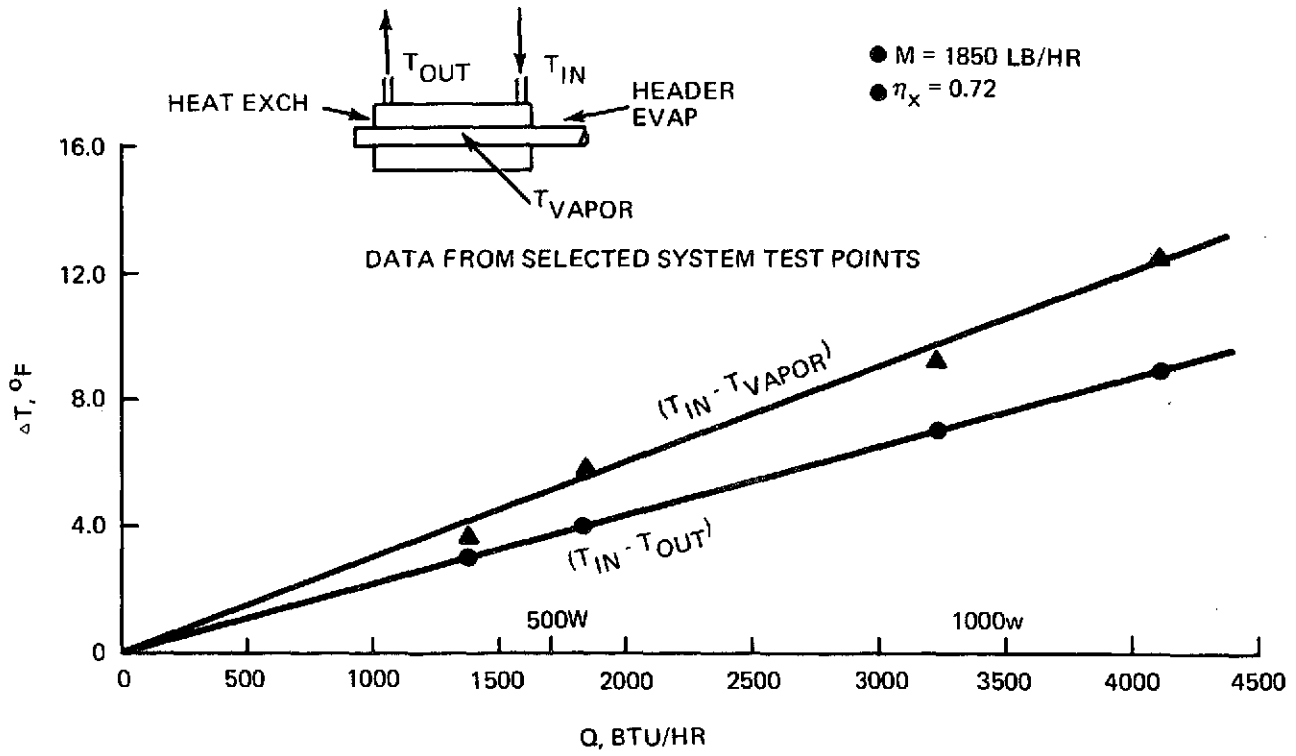

Figure 4-13 ΔT vs. Q Heat Pipe Radiator Heat Exchanger

Table 4-2 Heat Exchanger Details

Length (fins)	24 in.
I.D.	1.00 in.
O.D.	1.250 in.
Number of Fins, N	48
Fin Thickness, t	0.006 in.
Fin Height, w	0.10 in.
Fin Material	3003 Aluminum
Fluid	Freon 21
Mass Flow Rate, m	1850 lb/hr
Max. Allowable Pressure	150 psi

4.4 PHOTOGRAPHS

This subsection contains photographs showing the major hardware components of the heat pipe radiator panel during various stages of fabrication.

Figure 4-14: VCHP Header Assembly

Figure 4-15: VCHP Header Components with Attached Feeder Heat Pipes

Figure 4-16: Radiator Panel Components Before Assembly

Figure 4-17: Assembled Heat Pipe Radiator

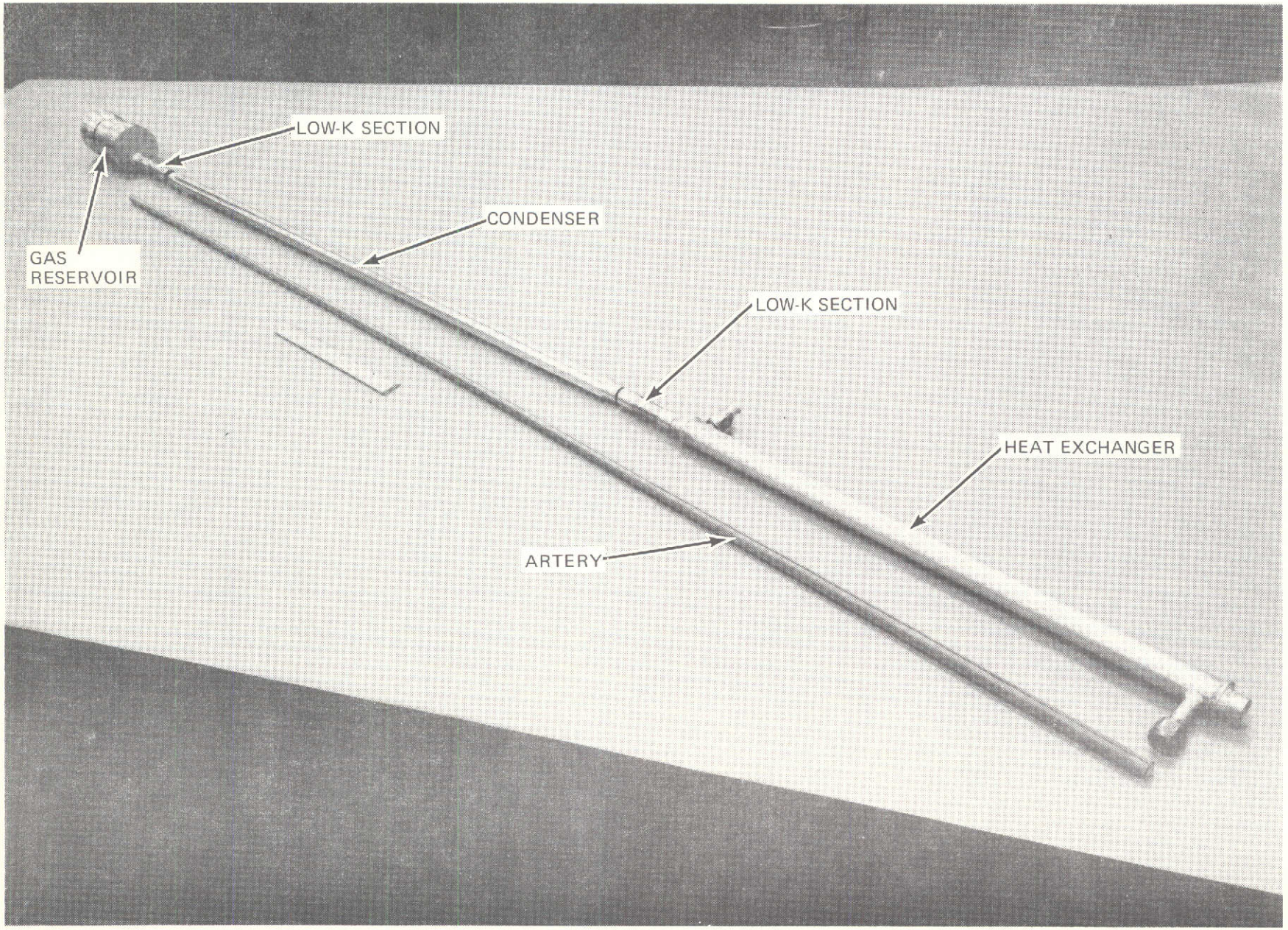

Figure 4-14 VCHP Header Assembly

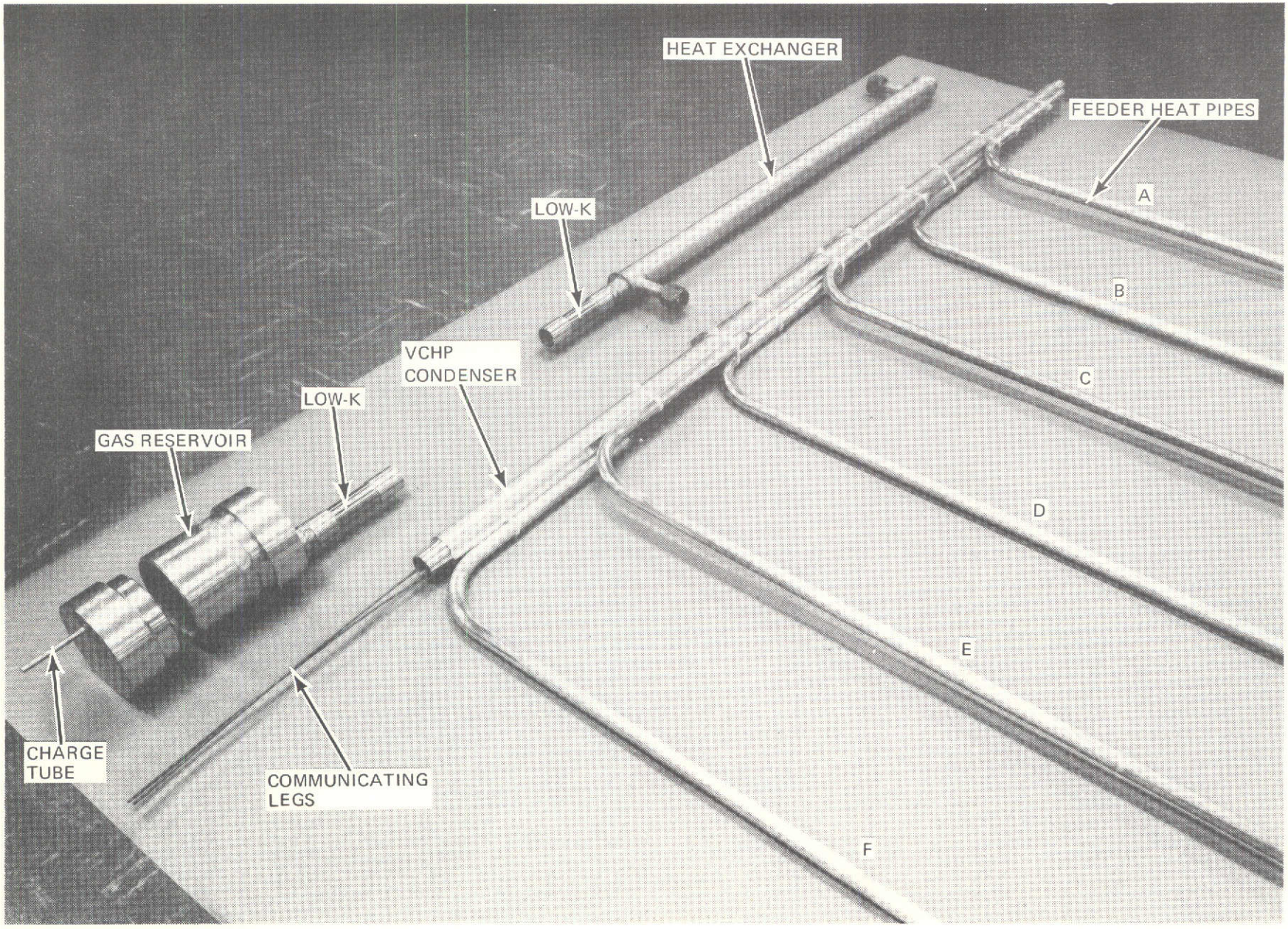

Figure 4-15 VCHP Header With Feeder Pipes

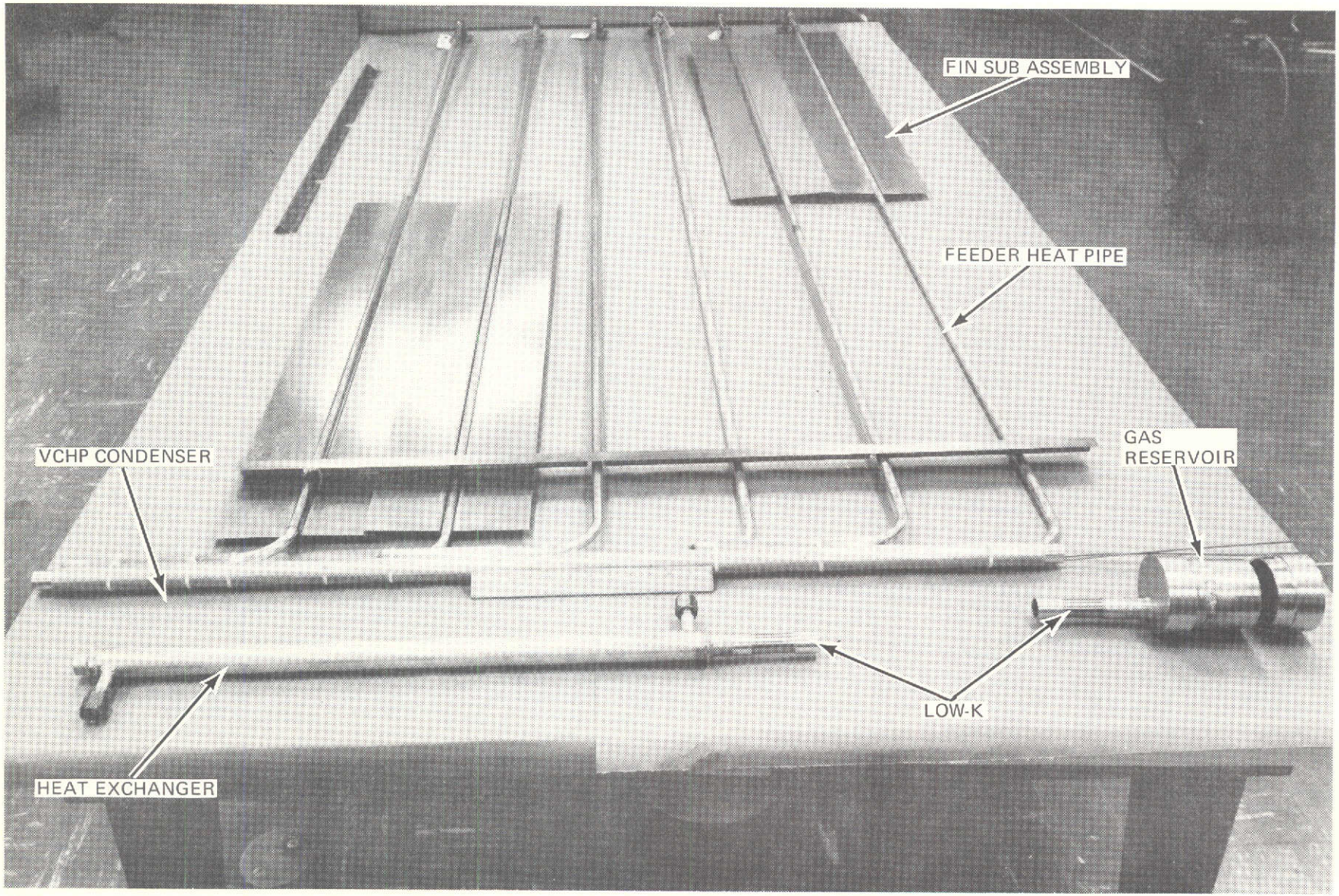

Figure 4-16 Radiator Panel Components

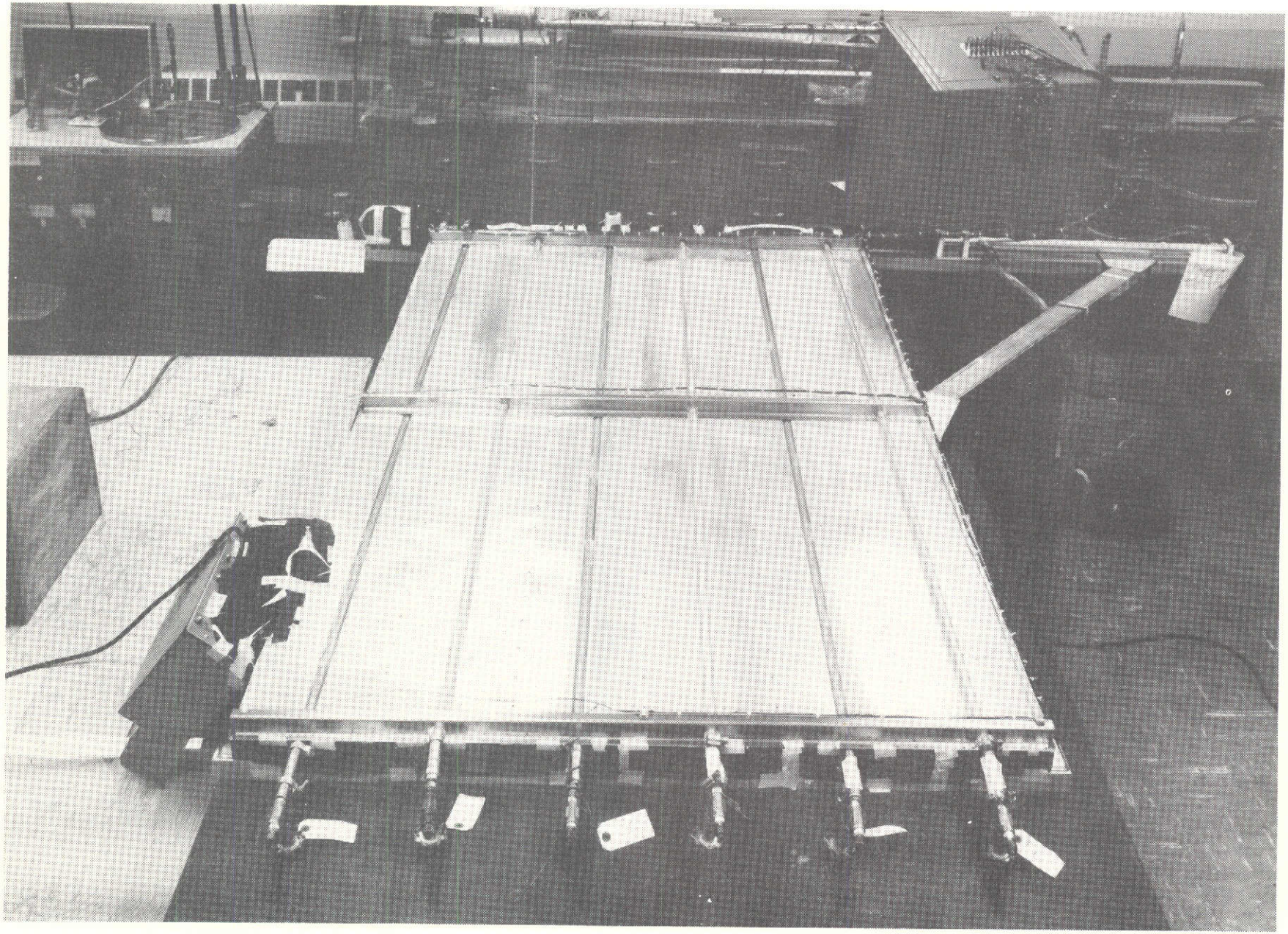

Figure 4-17 Assembled Radiator Panel

Section 5

BENCH TEST DATA

This section contains the results of the thermal bench tests that were performed on the three major components of the heat pipe radiator prior to panel assembly. Data are presented for the feeder heat pipes, VCHP header and heat exchanger.

5.1 FEEDER HEAT PIPES

The feeder heat pipes were individually tested at a tilt of at least 0.5 in. and 75°F. However, one feeder pipe (S/N 06) was tested at tilts of .50 in., .75 in. and 1.0 in. and at temperatures ranging from 60 - 125°F. Power was applied to the pipes via electrical heaters wrapped circumferentially around the 8-in. evaporators. Each 8-ft long condenser was cooled by a variable temperature water bath. The pipes were instrumented with 13 copper-constantan thermocouples as indicated in Figure 5-1. After installation of the thermocouples, both the 8-in. evaporator and 4-in. adiabatic sections were insulated, with 1-in. thick Armaflex insulation.

During testing, it was noticed that the tunnel in the artery was fairly sensitive to the type of condenser cooling. Initially, a high velocity spray bath was used, but spray velocity variations over the 8-ft long condenser caused the tunnel to deprime, resulting in Q_{max} values of about 150 watts of 0.5 in. tilt. A cooling trough was then substituted for the spray bath and pipes S/N 02, 03, 04 and 06 were retested. The data then obtained indicated that the tunnel was priming and capacities equal to or greater than 400 watts at 0.5 in. tilt were obtained. Capacities much greater than 400 watts could not be tested due to heater failures.

Figure 5-2 is a summary of the maximum capacities vs tilt for the six feeder heat pipes. Also shown is the predicted performance at 75°F. Figure 5-3 shows the average temperature drop of several of the pipes as a function of power input. The temperature drop, which is defined as the average evaporator temperature minus average condenser temperature, was approximately 4°F at 200 watts. However, it really should be considered to be smaller since the evaporator thermocouples were influenced by their close proximity to the electrical heater, which resulted in higher than actual readings.

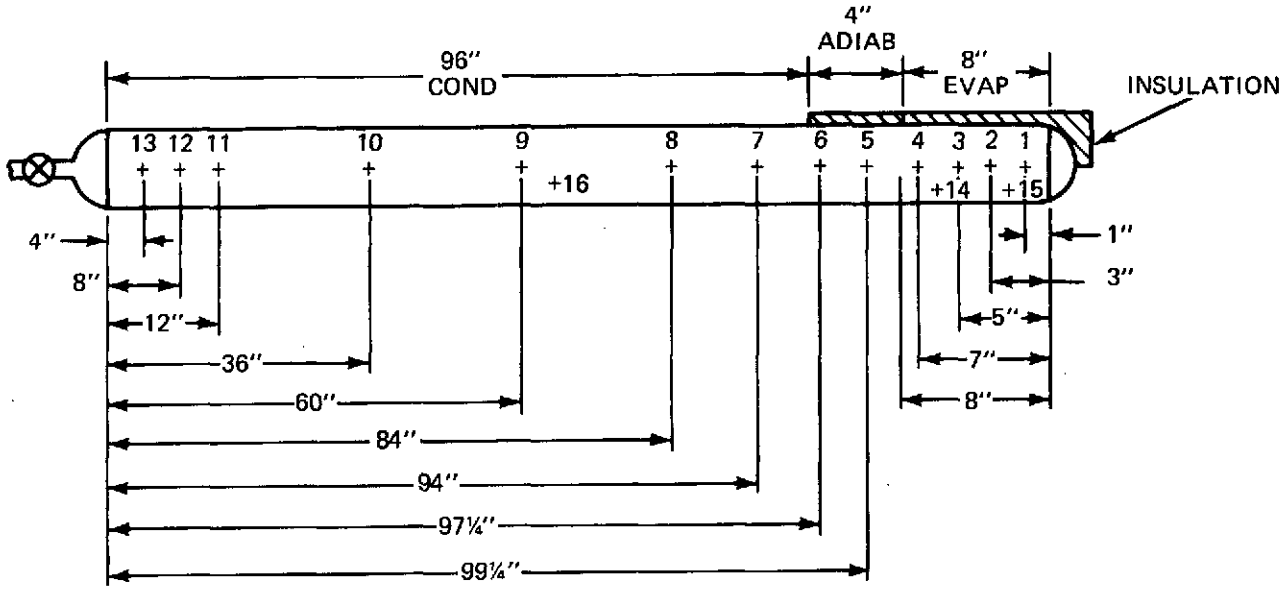

Figure 5-1 Feeder Pipe Instrumentation

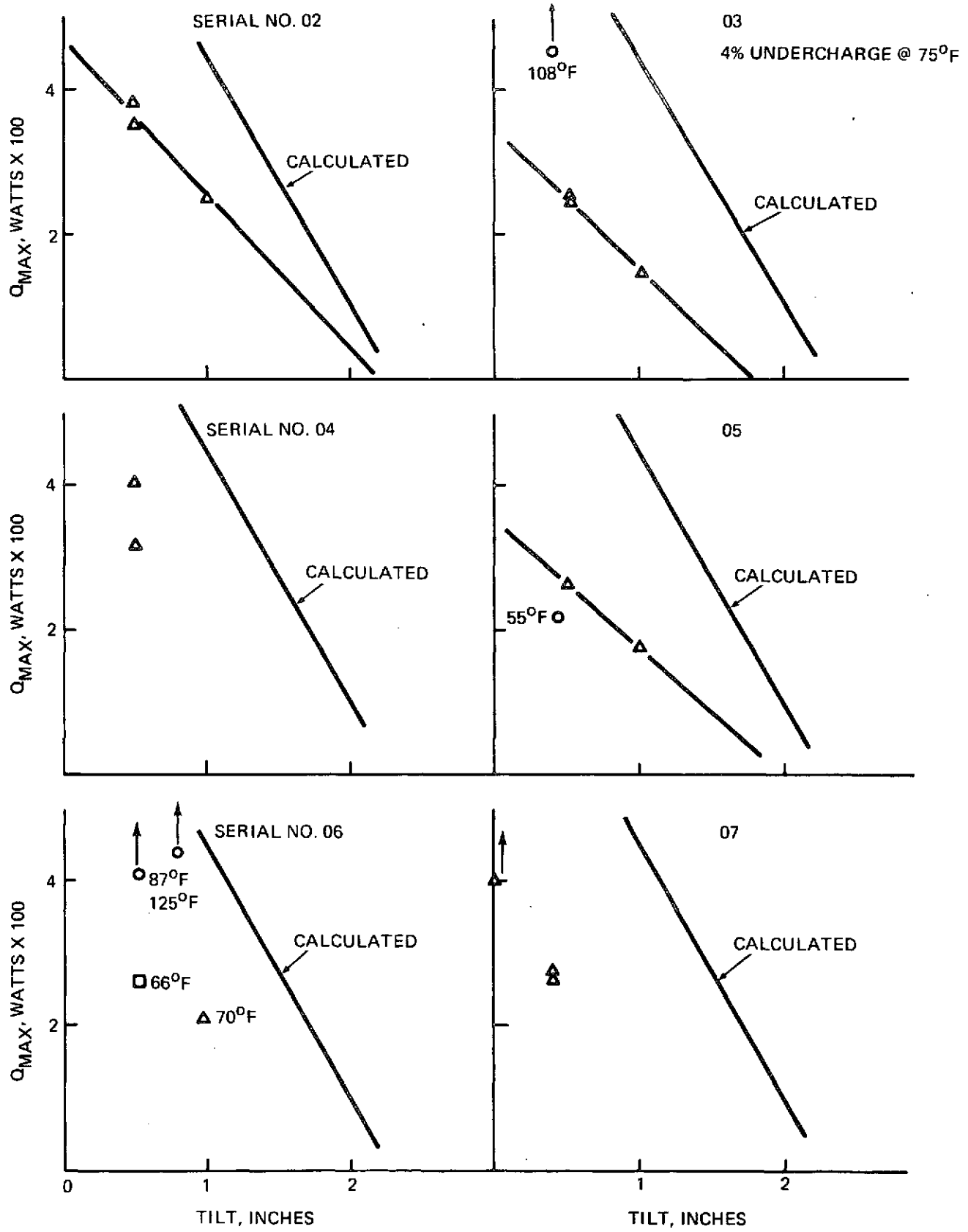

Figure 5-2 Feeder Heat Pipe Test Data, Maximum Loads vs Tilt (Temperature, 75 ± 5°F Unless Otherwise Noted)

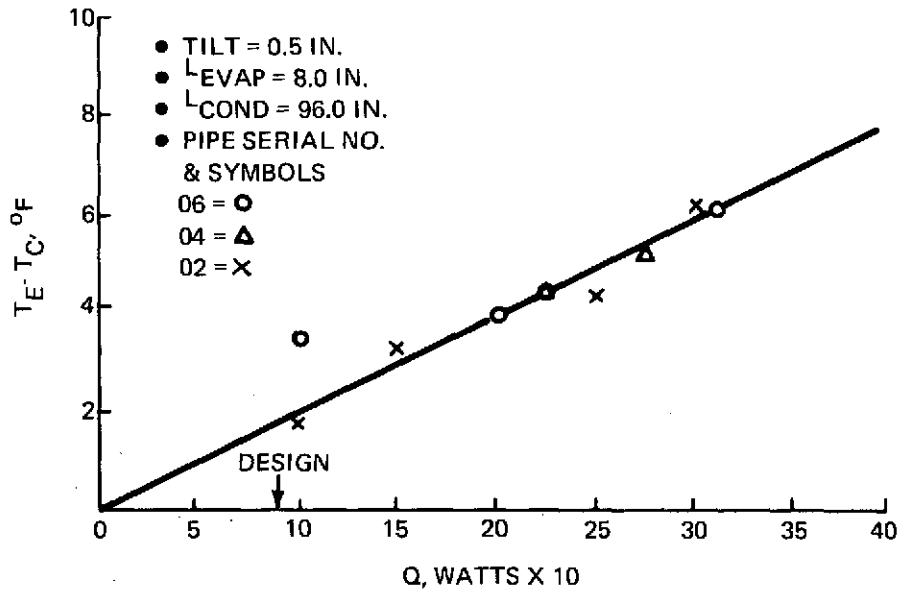

Figure 5-3 Feeder Pipe Overall Temperature Differential

5.2 VCHP HEADER

The three areas of performance that were evaluated during the bench test of the VCHP were: (1) single fluid maximum capacity; (2) VCHP maximum capacity, and (3) temperature control span. The header was instrumented with 33 copper constantan thermocouples as shown in Figure 5-4. The heat exchanger inlet and outlet temperatures were measured with immersion type thermocouples instrumented to give both absolute and differential millivolt readings. The latter was used to determine the heat input to the header by a $WC_p \Delta T$ calculation.

The header was first tested as a single fluid (NH_3), fixed conductance heat pipe by omitting the inert gas (N_2) charge. Tests were conducted at 0.5 in. adverse tilt and at vapor temperatures of 75 and 115°F. After completion of these tests, the header was tested as a VCHP with two different amounts of N_2 control gas, 0.00557 and 0.01498 lb; the latter is the design operational charge. The smaller charge was used for initial checkouts which were done at reservoir temperatures of 55°F and above.

The single fluid performance test results are plotted in Figure 4-7. The burnout point for a heat pipe being loaded by a fluid heat exchanger is determined by plotting the temperature difference between the fluid outlet and the heat pipe vapor as a function of load, Q. An abrupt increase in the slope of the ΔT vs Q curve indicates the end of effective heat pipe action and marks the burnout point. As indicated, the experimental Q_{max} (burnout) points follow the theoretical artery annulus performance line. These results indicate that the tunnel portion of the artery did not hold prime during the single fluid bench test series. Several factors may be responsible for this condition. They are: (1) a strong non-uniform coupling between the heat exchanger and the evaporator section of the heat pipe; (2) a screen discrepancy in the internal capillary structure of the pipe, or (3) a small quantity of residual inert gas in the artery. As mentioned earlier the required header pipe capacity was designed into the artery annulus, therefore, the tunnel prime condition did not impact the program goals.

The header pipe was tested in the VCHP mode with a partial N_2 charge of 0.00557 lb and with the design N_2 charge of 0.01498 lb. The expected degradation in Q_{max} when the control gas was present in the pipe was the same for both the partial and design N_2 quantities. Typical performance of the header with control gas is shown in Table 5-1. Some of the data shown are those obtained after thorough mixing of the N_2 and NH_3 (or after several dryouts following gas injection). Q_{max}

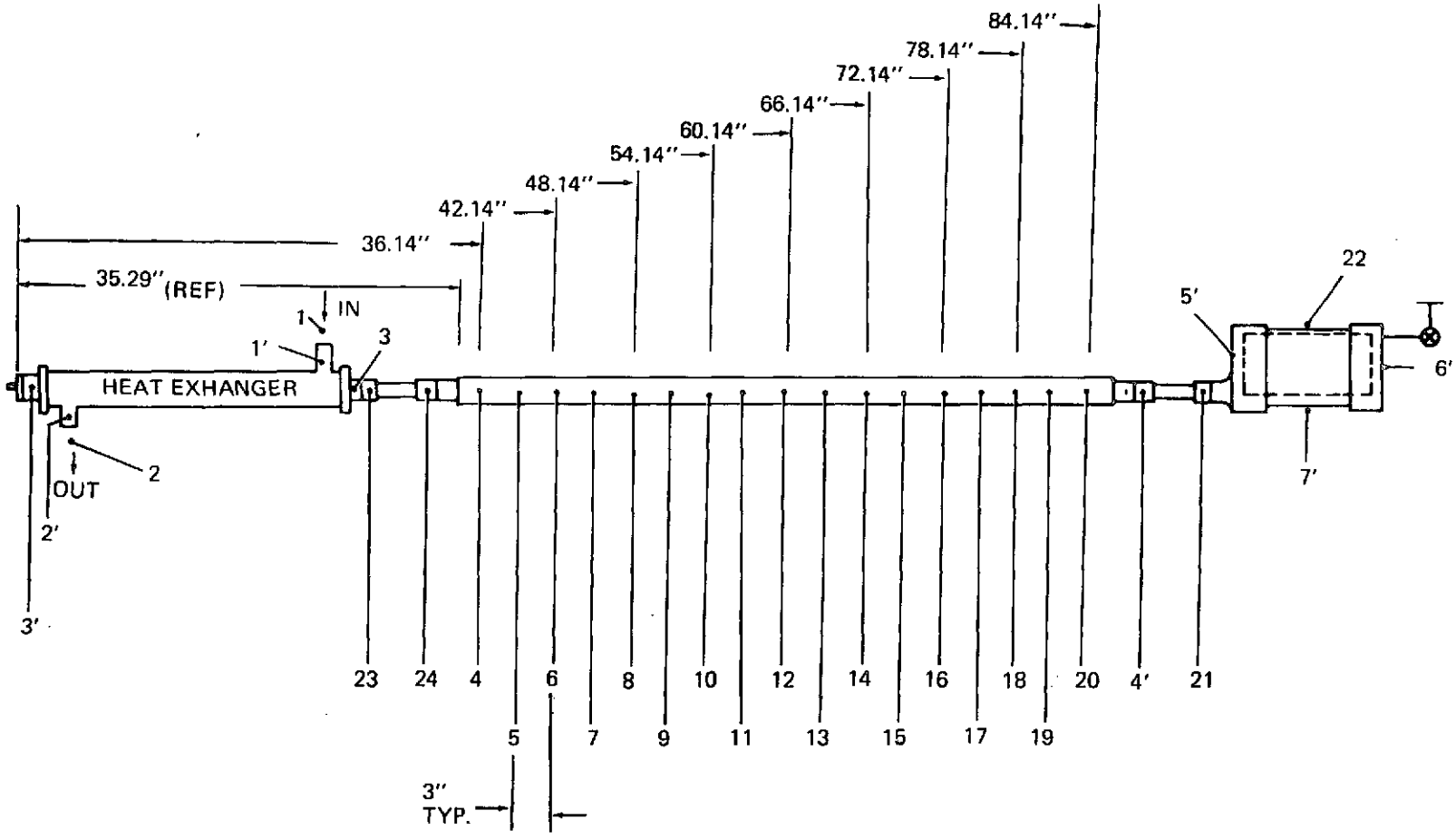

NOTES

1.) T/C'S ARE CU/CON
2.) T/C 1 & 2 ARE IMMERSION TYPE THERMOCOUPLES
3.) T/C 8' RESERVED FOR CONDENSER SPRAY
4.) T/C 23 & 24 ARE PIPE TEMP CONTROL POINTS
5.) T/C 9' RESERVED FOR RESERVOIR SPRAY

Figure 5-4 VCHP Header Instrumentation

Table 5-1 - VCHP Q_{max} Test Data, Reservoir Temperature = 57°F

Q_{max}, W	L_c = Open Cond. Length, in.	L' = Effective Length, in.	Q_{max} x L' (W-in.)	Comments
896	27	34	30,464	Right after gas injection
314	24	32	10,048	
350	44	42	14,700	
640	48	44	28,160	Right after gas injection
400	33	37	14,800	
830	21	31	25,730	Right after gas injection
916	38	39	35,274	Four days after gas injection
516	36	38	19,610	
480	33	37	17,760	

values close to single fluid performance were consistently obtained on the first run-up of the pipe following gas injection. The data presented in the table tend to be minimum values for VCHP operation. The time to complete an average Q_{max} run was about 30 minutes. When this time was increased, thus providing for more thorough dissolution of N_2 from the vapor/gas bubble region within the artery, higher Q_{max} values could be realized, as evidenced by the 916 watt point obtained after a total test time of approximately one hour.

Temperature control span studies were conducted with both partial and design N_2 charges in the pipe. Figure 5-5 gives both test data and predictions for the gas interface location as a function of vapor temperature.

Two main features of the experimental curve for the partial charge should be noted. First, the actual temperature control span is greater than predicted. The explanation of the increase in temperature control span involves again the vapor/gas bubble in the artery. It is postulated that when the interface advances in the condenser, as a result of an evaporator load increase, or more precisely an increase in pipe

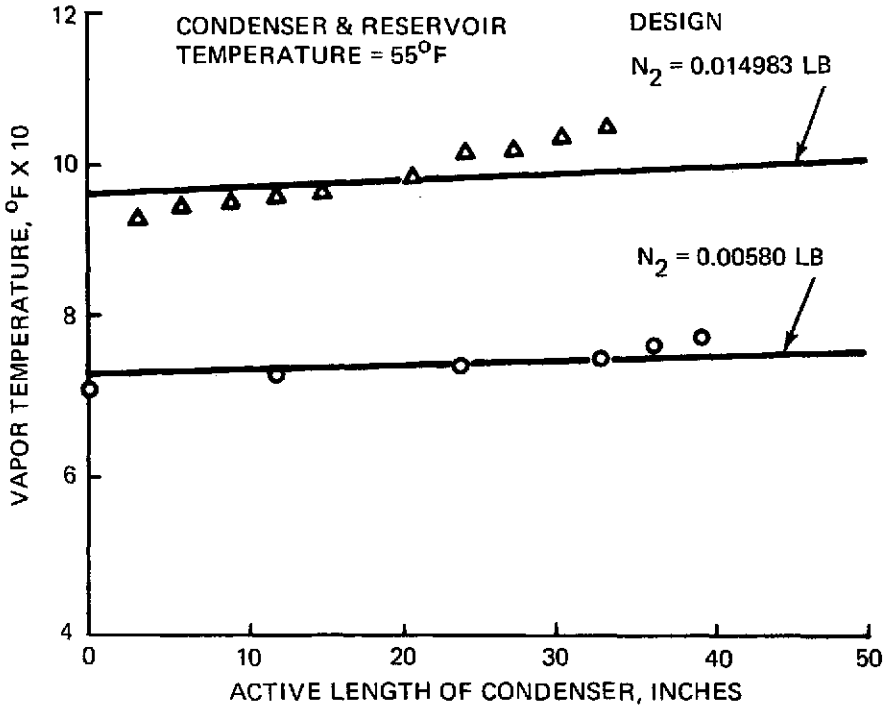

Figure 5-5 VCHP Test Data, Partial and Design Gas Charge

temperature, the vapor/gas bubble grows in length to the new interface location while the fluid expelled from the artery collects in the reservoir. This fluid collection reduces the reservoir volume and in turn increases the theoretical condenser opening temperature and the temperature control span.

The second observation in the experimental control span curve is the sudden break in the curve at 75°F. The break indicates the start of dryout in the evaporator and full artery depriming. Complete dryout of the evaporator was seldom noticed. After what seemed to be a start of dryout, the heat exchanger inlet to outlet temperature difference would decrease and the temperature difference between the heat exchanger outlet temperature and header vapor temperature would increase. For a given load, these ΔT's would eventually stabilize. However, control of the pipe was lost. Increasing the inlet temperature caused the outlet temperature to increase, while still maintaining a constant load of several hundred watts.

Figure 5-6 details the interface progression with increasing heat load for the design charge case. The corresponding vapor temperature is also plotted on the ordinate. Notice that the heat pipe action began at a vapor temperature of close to 97°F which was identical with the predicted value. This is indicated by the fact that the condenser temperature is within 2°F of the vapor temperature at this point. At lower vapor temperatures the difference between them is much greater, which means no heat piping.

5.3 HEAT EXCHANGER

At a Freon 21 design flow rate of 1850 lbs/hr, the estimated heat exchanger effectiveness is 72% and the calculated pressure drop is 0.5 psi. Figure 5-7 presents some typical test data obtained for the heat exchanger using Freon 113 instead of Freon 21 which was not available. To maintain the 72% effectiveness and compensate for the difference in fluid properties, a Freon 113 flow rate of 3300 lb/hr (WCp = 206 w/°F) was used.

The temperature differences between the Freon inlet and header vapor and the Freon inlet and outlet are plotted as a function of load. Also shown is the predicted inlet to vapor differential.

5.4 PANEL ASSEMBLY

After the panel was assembled and the feeder heat pipes pinched-off, a rudimentary thermal test was conducted in a 85°F room temperature environment. The objective of this basic performance test was to establish that all heat pipe components

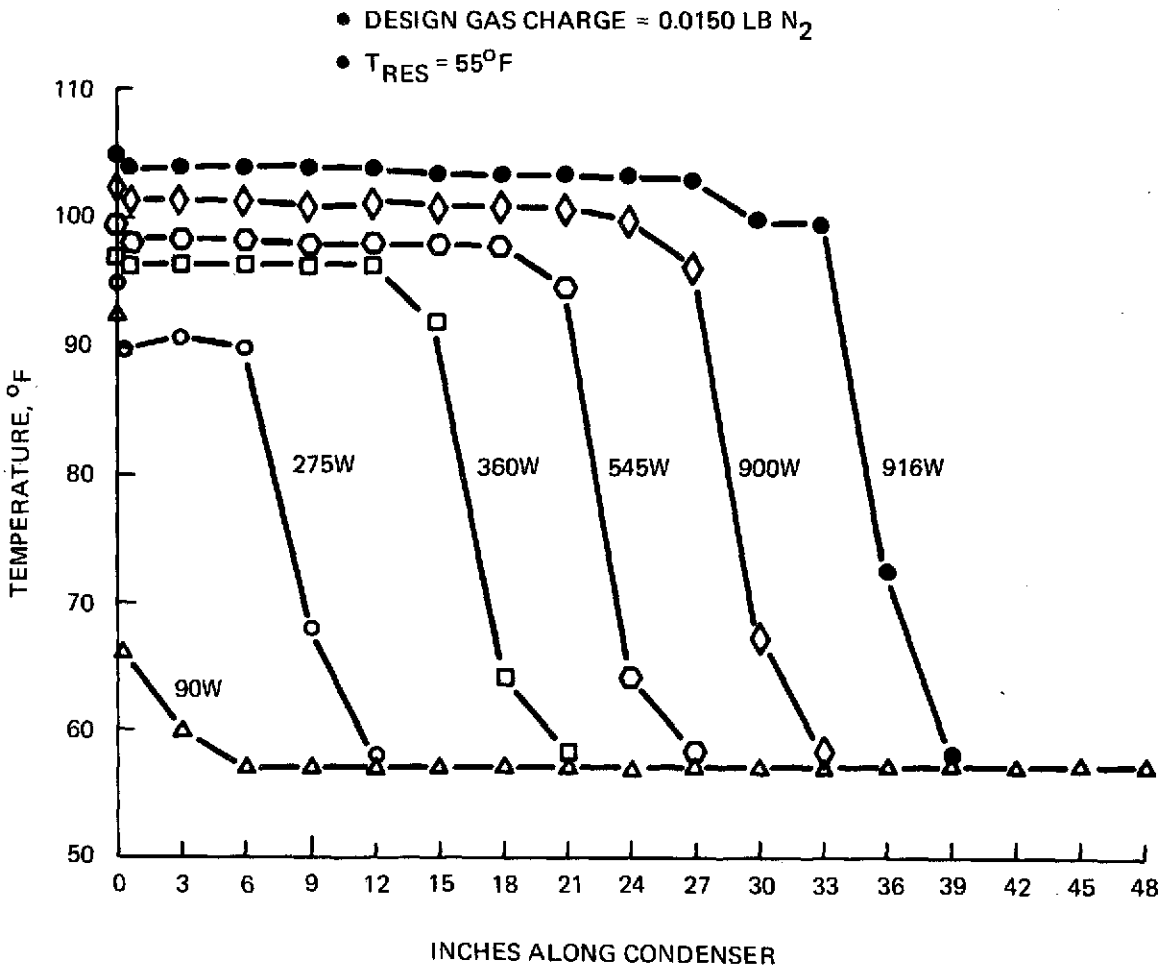

Figure 5-6 VCHP Header Bench Test Data

were operating prior to shipping the panel to NASA/JSC. A fan was used to blow air across the panel to help dissipate the heat load. Also, in order to obtain movement of the gas interface at room termperatures, the reservoir of the VCHP was cooled to $6^{o}F$.

Figure 5-8 shows the temperature distribution along the VCHP header and temperatures at the adiabatic section and mid-condenser fin root point of the six feeder pipes. The gas interface within the VCHP can be seen to move toward the reservoir end of the condenser as the heat load increases, as expected.

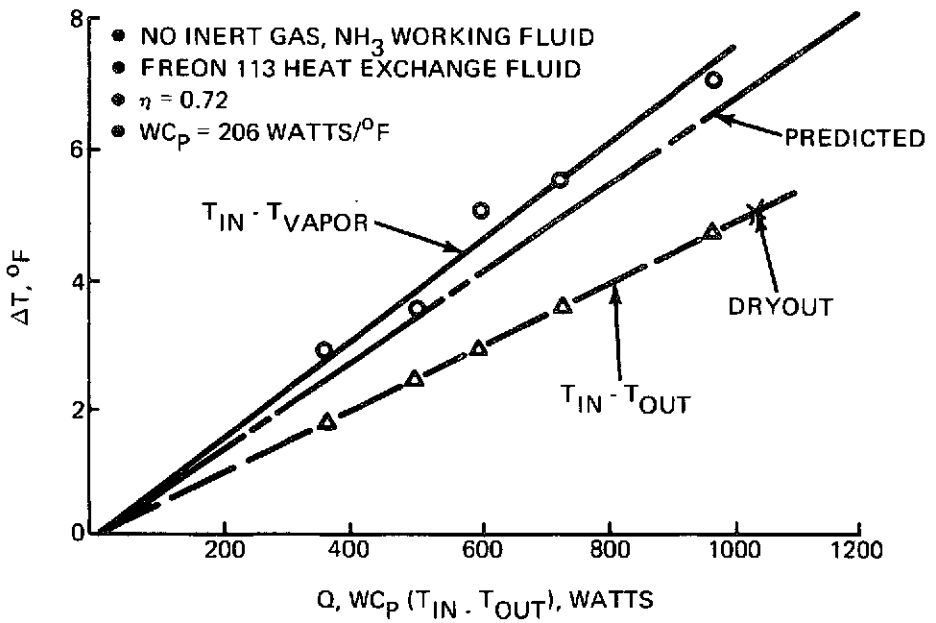

Figure 5-7 Heat Pipe Radiator Heat Exchanger Data

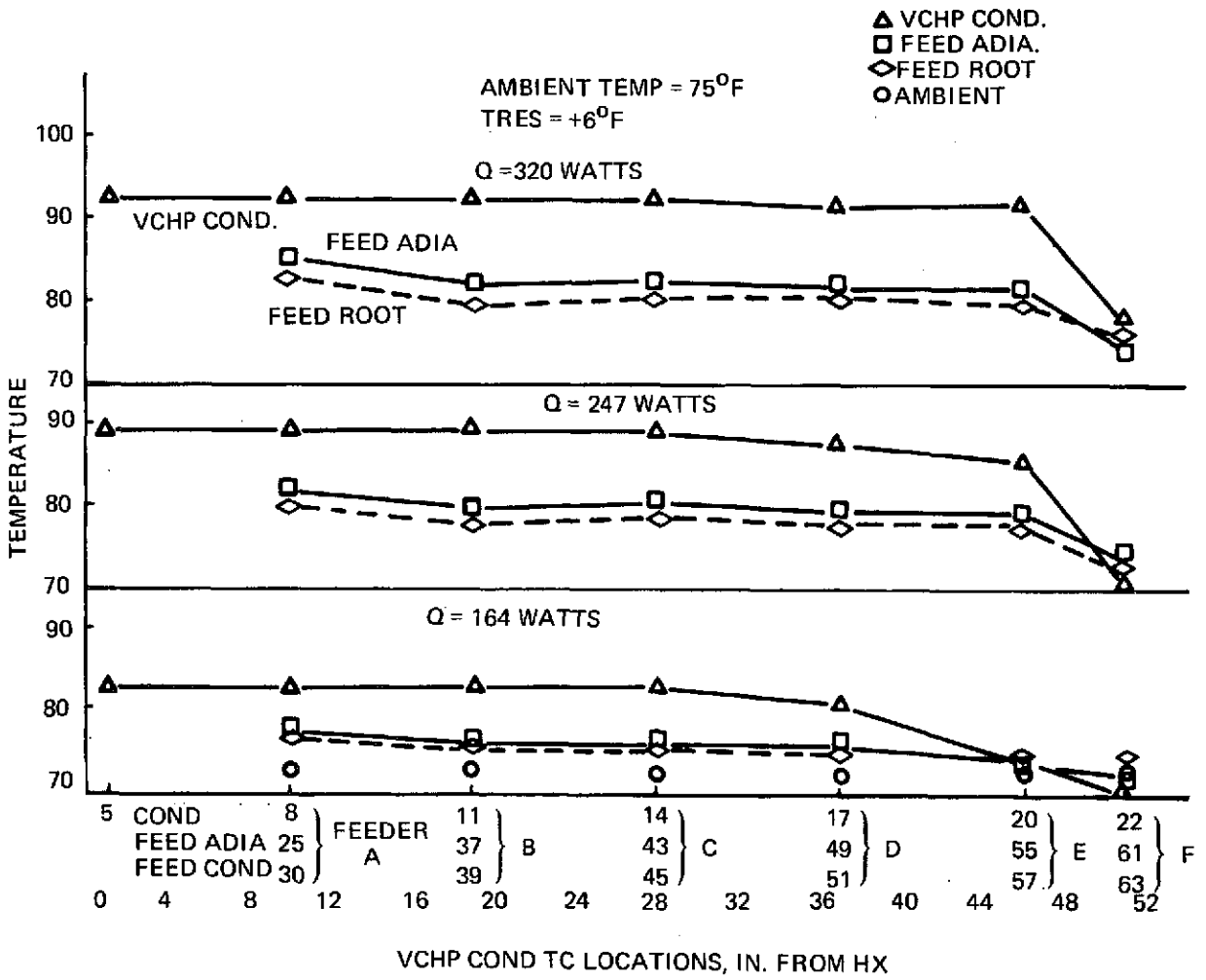

Figure 5-8 Ambient Functional Test, Heat Pipe Radiator

Section 6

SYSTEM TEST

This section presents the results of the thermal vacuum test that was performed in Chamber A of the NASA/JSC-SESL facility. The primary test objective was to determine the feasibility of using a VCHP radiator, in conjunction with a fluid heat source, to reject waste heat to a space environment. The test was designed to evaluate the performance of the VCHP header and the heat pipe radiating fin when both components are integrated into one radiator panel.

6.1 DISCUSSION

The heat pipe radiator was installed in the test chamber on five insulated bars that supported the periphery and the center of the panel approximately 5 ft above the chamber floor. It was positioned so that the VCHP header was level, while the feeder pipe evaporators were 1/2 in. above the end of their condensers. A 12 ft by 12 ft environment simulator panel, painted black, was mounted about 6 to 10 in. below the radiating surface of the heat pipe panel. The surface temperature of the simulator was controlled by attached cooling coils using either liquid nitrogen or Freon 12, depending on the desired thermal environment. As an economy measure, the simulator panel was used to provide the environment instead of the chamber cold walls, resulting in greatly reduced liquid nitrogen requirements.

The backside of the heat pipe radiating fin and the entire VCHP header, except for the front of the reservoir, were insulated with 25 layers of aluminized mylar superinsulation. Another 25-layer insulation blanket enclosed both the simulator panel and the radiator in a cocoon.

The radiator was instrumented with 87 copper/constantan thermocouples and 8 thermistors, the latter providing specific ΔT measurements during testing. Copper/constantan immersion thermocouples were used to measure the inlet and outlet temperatures of the VCHP heat exchanger. An instrumentation drawing for the radiator is given in Figure 6-1 and a description of the thermocouple locations is contained in Table 6-1.

The basic test plan called for measuring VCHP header and heat pipe panel temperatures for various combinations of environment, heat exchanger flow rate and

FOLDOUT FRAME 1

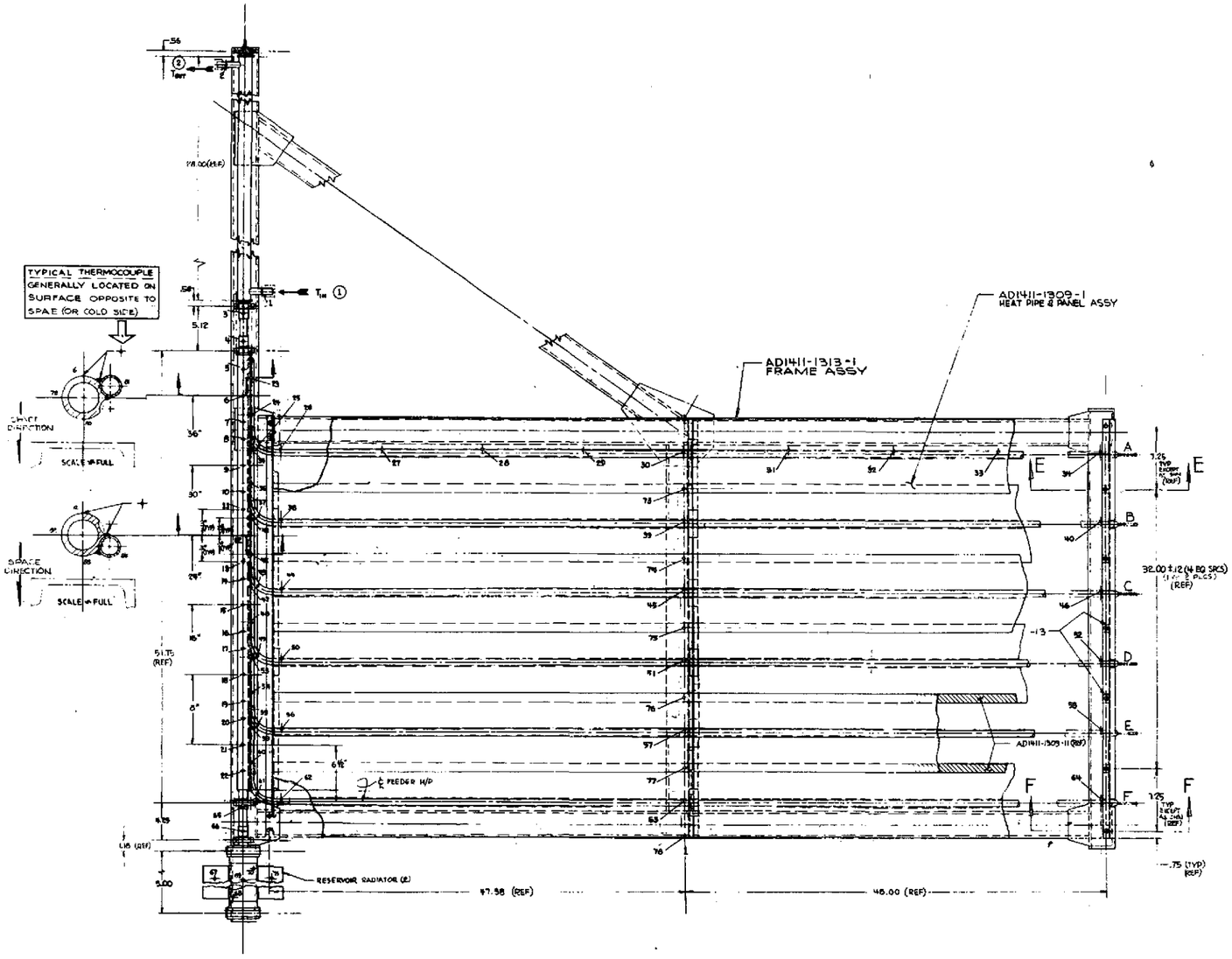

-1 RADIAIOR PANEL & SUPPORT ASSEMBLY

VIEW LOOKING DOWN WITH SIMULATED SPACE (OR COLD SIDE) ON FAR SIDE OF RADIATOR

FOLDOUT FRAME 2

THERMOCOUPLE DISTRIBUTION

HEADER SYSTEM	
HEAT EXCHANGER (T_{IN} & T_{OUT})	2
LOW 'K' SECTION (2 EA)	4
HEADER (CONDENSER SECT)	18
RESERVOIR BODY	3
RESERVOIR FINS	2
FEEDER PIPES	
EVAPORATOR (2 EA)	12
CONDENSER	24
ADIABATIC (1 EA)	6
RADIATOR PANEL	
DISTRIBUTED AS SHOWN	7
TOTAL	78

	CONTRACT NO. NAS-9-12848	GRUMMAN AEROSPACE CORPORATION BETHPAGE, NEW YORK 11714
		THERMOCOUPLE DISTRIBUTION HEAT PIPE RADIATOR
	SIZE E	CAGE CODE NO. 26512 AD1411-1317

Figure 6-1 Panel Instrumentation

Table 6-1 Heat Pipe Radiator Thermocouples

REF: AD 1411-1317

TC No.	Code	Location	TC No.	Code	Location
1	EN01	Freon inlet tube strap-on	33	FA33	Feeder A, condenser
1a	AJ0020	Freon inlet, immersion	34	FA34	Feeder A, condenser
2	EX02	Freon outlet tube strap-on	35	FB35	Feeder B, evaporator
2a	AJ0024	Freon outlet, immersion	36	FB36	Feeder B, evaporator
3	LK03	Low conduction section	37	FB37	Feeder B, adiabatic section
4	LK04	Low conduction section	38	FB38	Feeder B, condenser
5	HC05	Header condenser	39	FB39	Feeder B, condenser
6	HC06	Header condenser	40	FB40	Feeder B, condenser
7	HC07	Header condenser	41	FC41	Feeder C, evaporator
8	HC08	Header condenser	42	FC42	Feeder C, evaporator
9	HC09	Header condenser	43	FC43	Feeder C, adiabatic section
10	HC10	Header condenser	44	FC44	Feeder C, condenser
11	HC11	Header condenser	45	FC45	Feeder C, condenser
12	HC12	Header condenser	46	FC46	Feeder C, condenser
13	HC13	Header condenser	47	FD47	Feeder D, evaporator
14	HC14	Header condenser	48	FD48	Feeder D, evaporator
15	HC15	Header condenser	49	FD49	Feeder D, adiabatic section
16	HC16	Header condenser	50	FD50	Feeder D, condenser
17	HC17	Header condenser	51	FD51	Feeder D, condenser
18	HC18	Header condenser	52	FD52	Feeder D, condenser
19	HC19	Header condenser	53	FE53	Feeder E, evaporator
20	HC20	Header condenser	54	FE54	Feeder E, evaporator
21	HC21	Header condenser	55	FE55	Feeder E, adiabatic section
22	HC22	Header condenser	56	FE56	Feeder E, condenser
23	FA23	Feeder A, evaporator	57	FE57	Feeder E, condenser
24	FA24	Feeder A, evaporator	58	FE58	Feeder E, condenser
25	FA25	Feeder A, adiabatic section	59	FF59	Feeder F, evaporator
26	FA26	Feeder A, condenser	60	FF60	Feeder F, evaporator
27	FA27	Feeder A, condenser	61	FF61	Feeder F, adiabatic section
28	FA28	Feeder A, condenser	62	FF62	Feeder F, condenser
29	FA29	Feeder A, condenser	63	FF63	Feeder F, condenser
30	FA30	Feeder A, condenser	64	FF64	Feeder F, condenser
31	FA31	Feeder A, condenser	65	LK65	Low conduction section
32	FA32	Feeder A, condenser	66	LK66	Low conduction section

Table 6-1 Heat Pipe Radiator Thermocouples (Cont.)

TC No.	Code	Location	TC No.	Code	Location
67	RR67	Reservoir radiator	73	PA73	Panel assembly
68	RR68	Reservoir	74	PC74	Panel assembly
69	RR69	Reservoir	75	PD75	Panel assembly
70	RR70	Reservoir	76	PE76	Panel assembly
71	RR71	Reservoir radiator	77	PF77	Panel assembly
72	PA72	Panel assembly	78	PG78	Panel assembly

inlet temperature. Table 6-2 gives the nominal values for these test conditions. Major emphasis was given to evaluating performance at the panel design point of 60 Btu/hr-ft^2, Q_a, and 1850 lb/hr, flow rate. For this condition the inlet temperature was varied in 5^o increments between 40^{o}F and 140^{o}F. In addition to the basic test envelope, the panel's response from a frozen condition was also investigated.

6.2 TEST RESULTS

It was evident early in the test program that the VCHP header would not function exactly as anticipated. The condenser section opened at the predicted inlet temperatures whenever the reservoir temperature was equal to, or colder than, the shutoff portion of the condenser. But, no matter what the environment and flow rate, the condenser could never be made to open completely -- even when inlet temperatures were increased well beyond the predicted full-open value. Many of the planned test points were sacrificed in an attempt to obtain a fully operative VCHP condenser and this resulted in obtaining a fewer number of valid steady state performance points than scheduled.

An example of this behavior is given in Figure 6-2 which shows the temperature distribution along the VCHP header for several values of inlet temperature for the design condition. At an inlet temperature of 74^{o}F, the condenser should have been fully open but it is actually only about half open (24 in.). Increasing the inlet to 90^{o}F opens it further, to about 32 in. But another increase to 95^{o}F has no effect; the interface has stabilized at about 32 in. from the end of the evaporator. Figures 6-3 and 6-4 give the corresponding temperatures of the panel feeder heat pipes for the 74^{o}F inlet and 95^{o}F inlet cases, respectively. In general, the temperature difference between a feeder condenser root and the VCHP condenser wall is less than 20^{o}F. Most of this drop occurs between the VCHP condenser and the feeder evaporator due to the much smaller heat transfer area that is available.

Failure of the VCHP header to completely open can be explained by two factors. First, since the tunnel never primed, there was excess fluid in the reservoir that resulted from the deprimed tunnel plus artery fluid that was displaced by gas/vapor bubbles trapped in the spiral. This has the effect of decreasing the reservoir gas volume, and the V_R/V_C ratio, and results in a much wider control span. That is, a much greater increase in vapor temperature is needed for a fully open condenser. This same observation was previously noted in the discussion of the VCHP bench test data (see Section 5.2). The second contributing factor impeding the gas interface from moving through the last third of the condenser is a reservoir temperature that was

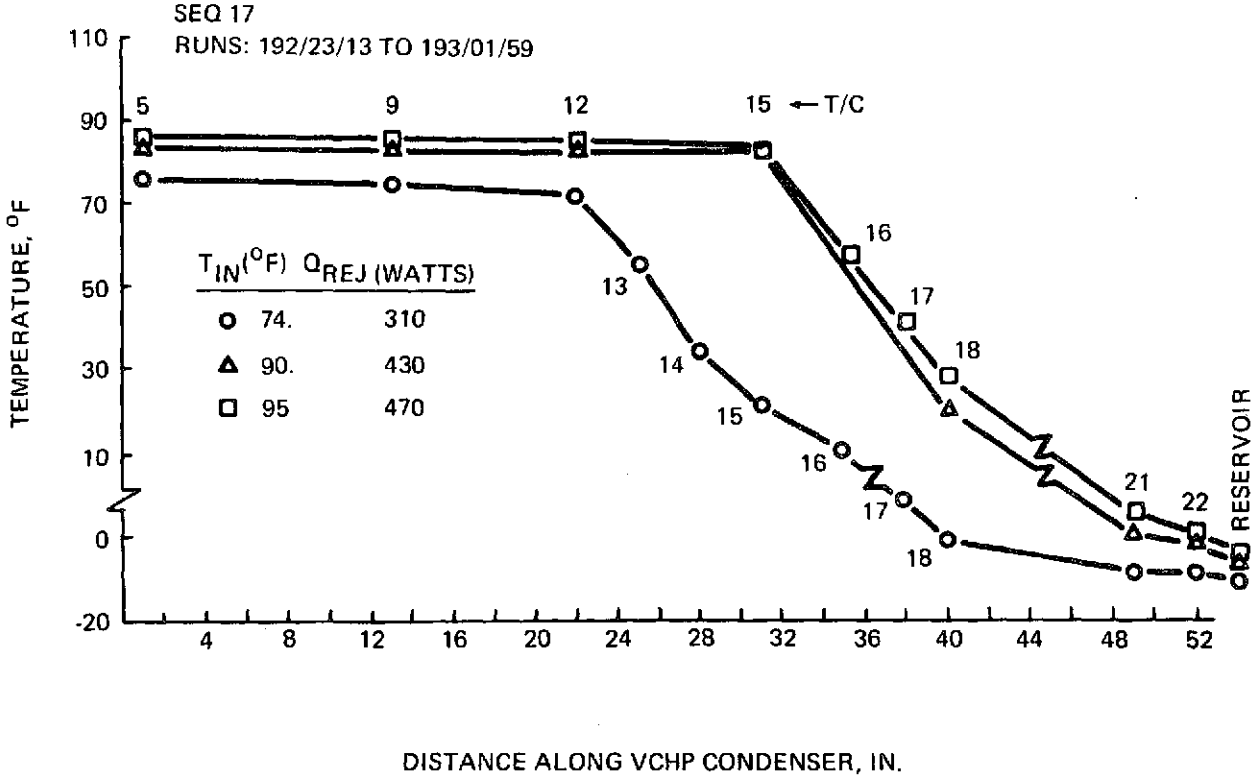

Figure 6-2 T/V Test Results VCHP Condenser Temperatures

Table 6-2 Heat Pipe Radiator Thermal Vacuum Test Conditions

Test parameter	Nominal values
1. Environment, Q_a, Btu/hr-ft^2	25, 43, 60*, 100, 150
2. Freon-21 Flow Rate, lb/hr	265, 1060, 1850*
3. Inlet Temperature, ^{O}F	40, 80, 120, 140

*DESIGN POINT. Inlet temperature varied in 5^{O}F increments between 40^{O}F and 140^{O}F, for this point only.

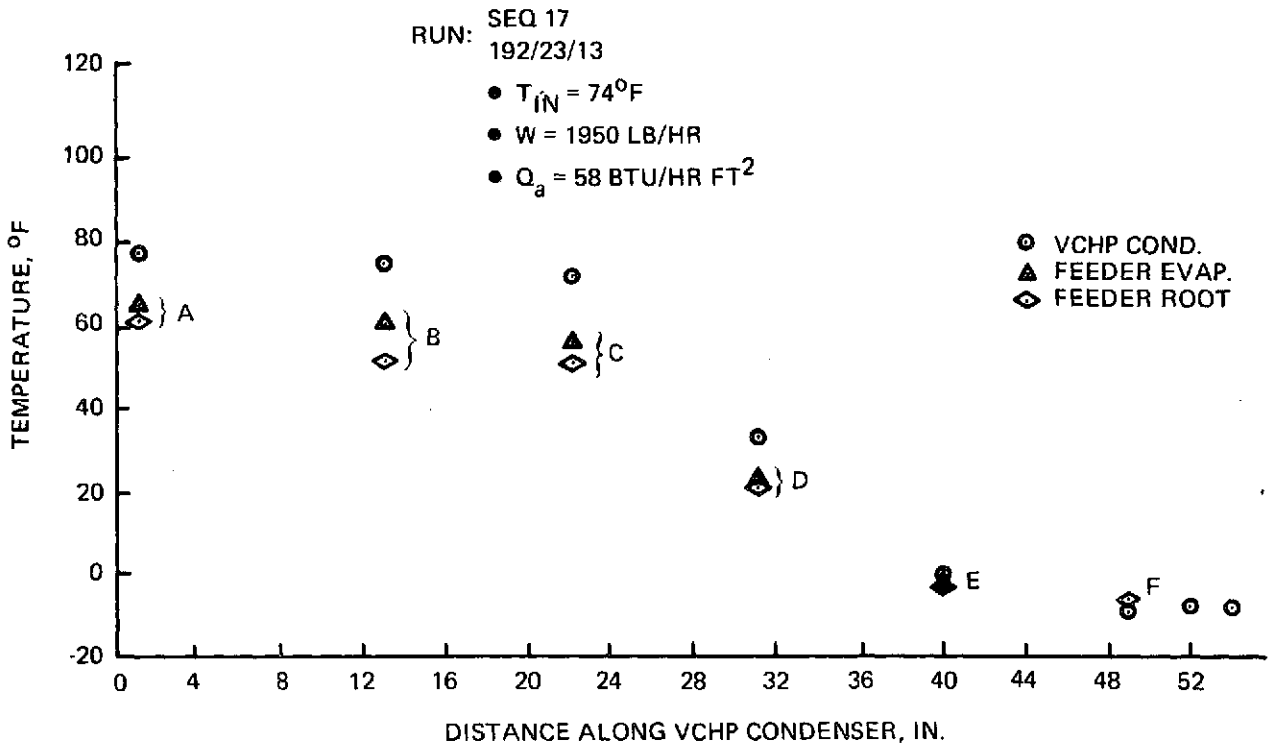

Figure 6-3 T/V Test Results, ΔT Header to Feeder Heat Pipes

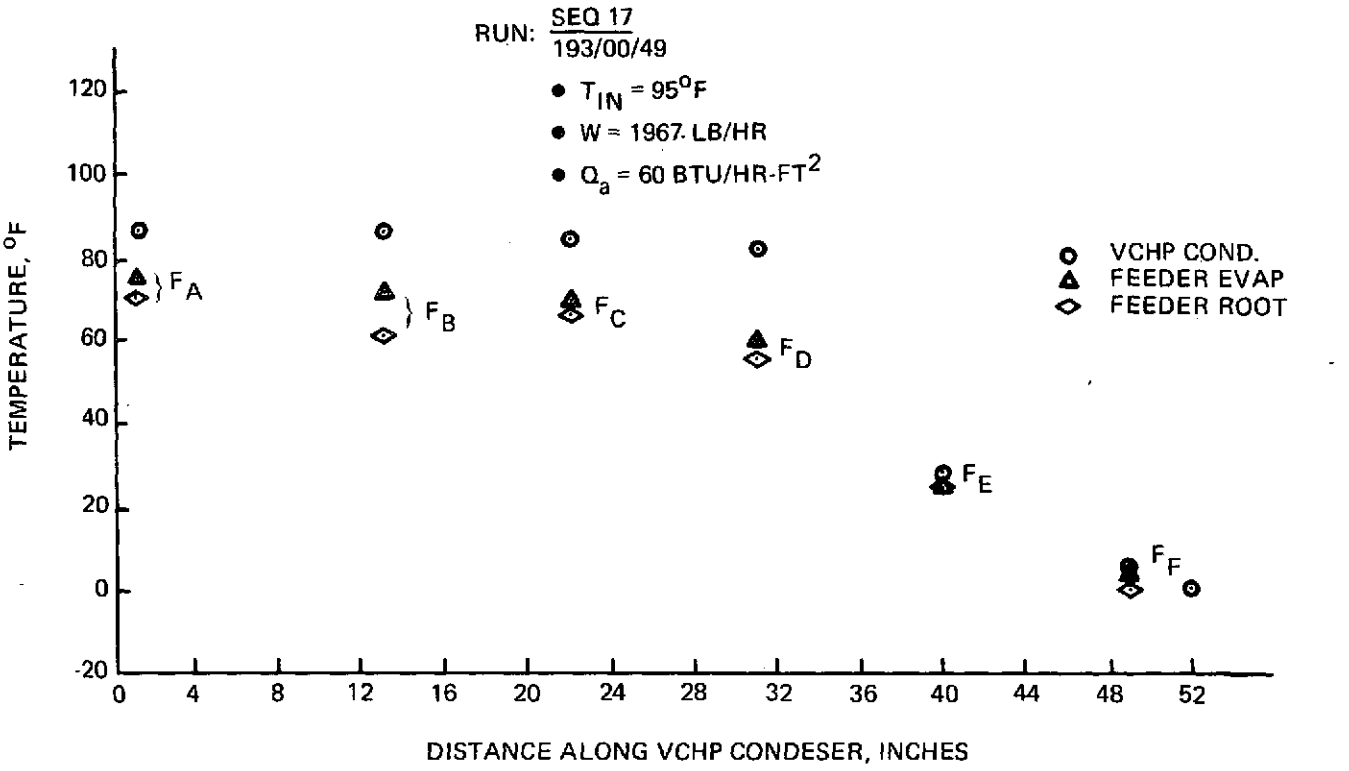

Figure 6-4 T/V Test Results, ΔT Header to Feeder Heat Pipes

warmer than the design value. The ideal reservoir radiation equilibrium temperatures that correspond to the test environments are given below.

Q_a, Btu/hr-ft^2	T_{Res}, ^oF
25	-103
60	- 16
100	45
140	89

For an inlet temperature of 74^{o}F and a 60 Btu/hr-ft^2 environment, an increase in reservoir temperature of only 6^{o}F from the ideal results in a theoretical change in blocked length of 7.2 in. This highly sensitive behavior is due to the relatively narrow condenser vapor space of .09 in. which results from having an overly large spiral annulus.

The fact that the reservoir temperatures were, in general, running warmer than the design values was largely due to a conduction heat gain of several Btu/hr through the leads of a reservoir heater and also to 4-in.^{2} of unpainted (low emittance) reservoir area. The reservoir heater was used only during a room temperature bench check of the VCHP to determine if it was operational. It was never used during the actual system tests. The effect on reservoir temperature of even a small heat gain can be seen in Figure 6-5 which shows reservoir temperature as a function of environment and an additional heat gain. The point of intersection between the environment curve and the X-axis locates the ideal radiation equilibrium temperature of the reservoir. As seen, in a 60 Btu/hr-ft^2 environment a gain of only 2 Btu/hr causes an increase in reservoir temperature of 12^{o}F, from -16^{o}F to -4^{o}F. The effect at the colder 25 Btu/hr-ft^2 environment is even more pronounced with an increase of 21^{o}F.

Detailed data for the steady state test points are given in Appendix B. A temperature map of the panel and temperature profiles along the VCHP header and feeder pipe A are provided for each test condition. A summary of these steady state test points is given in Table 6-3 along with the corresponding net heat rejection of the panel. Two values for heat rejection are given; one based on the measured fluid heat loss (WCp ΔT) and the other based on the panel temperatures ($\Sigma\sigma T^4$) and the environment. Ideally, in a system without losses, both values should be the same, but as seen from the table this is not the case.

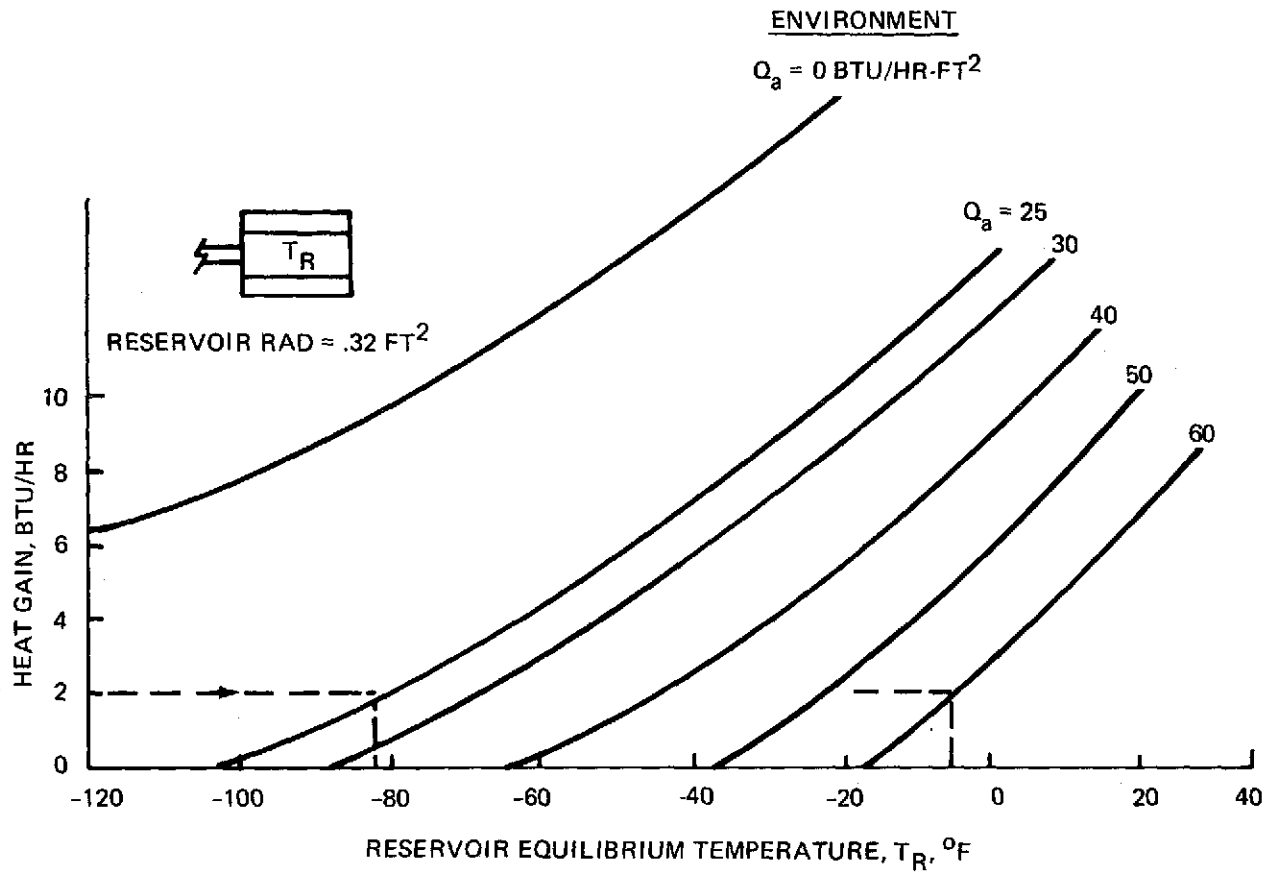

Figure 6-5 Reservoir Temperature vs Heat Gain

Table 6-3 Summary of Results

(1) Figure No.	Run No.	Q_a, Btu/Hr-Ft^2	Flow Rate, Lb/Hr	T_{in}, ^oF	T_{out}, ^oF	Q_{REJ}, (Btu/Hr)	
						WCp ΔT	$\Sigma\sigma T^4$ (2)
B-1a,b,c	193/08/30	56	1850	71	67.9	1435	980
B-2a,b,c	193/01/10	60	1990	96	92	1990	1331
B-3a,b,c	192/10/50	55	1064	71	67.9	855	813
B-4a,b,c	192/15/30	58	276	106.5	88	1240	1293
B-5a,b,c	191/21/40	41	276	71	57.4	938	945
B-6a,b,c	191/18/05	23	284	88.3	70.1	1300	1197
B-7	191/18/45	23	276	94	75	1310	1217
B-8a,b,c	193/10/25	93	1976	93	90	1482	753
B-9a,b,c	193/14/50	137	1985	129.6	127.7	943	1058

(1) Figures are in Appendix B. (a)= radiator panel temperature map

(b)= VCHP temperature distribution

(c)= temperature distribution along feeder pipe A

(2) $\Sigma\sigma T^4$ values courtesy of Dr. J. Sellers, Jr., Tuskeegee, Univ.

Agreement is fairly good (within 8%) at the low flow rate (276 lb/hr) but very poor at the high flow rate ($\approx$1850 lb/hr). There is evidence of a definite heat leak through the insulation blanket at the start of the condenser of feeder pipe A. This can be seen by looking at any of the plots of the temperature distribution and observing that the temperature for thermocouple no. 26 is far below the rest of the condenser readings. The environment is having a stronger influence on it than the others. For example, consider run 193/08/30 (Figures B-1a,c). Agreement between T/C 26 and the others becomes better when the environment is higher and the effective sink temperature is closer to the panel temperature, as seen in Run 193/14/50 (Figures B-9a,c). The possibility of a faulty thermocouple at no. 26 is disallowed since it gave the same reading as the others when the panel was in a no-load, frozen condition.

However, if the disagreement in the net heat rejection calculations was entirely due to a heat leak then the error should be completely dependent on the panel temperature and the environment. Yet for two cases with similar conditions, but different flow rates, this does not appear to be true. Consider Figures B-1a, c with the higher 1850 lb/hr flow and Figures B-4a, c with the lower 276 lb/hr flow. Agreement in the former case is poor but in the latter case it is good. This evidence would seem to minimize the influence of the heat leak.

The only other plausible explanation for the difference in heat rejection rates is an error in the immersion thermocouple readings, estimated at $\pm 1/2^{\circ}F$ for each thermocouple. This would have a much more pronounced affect at the higher flow rates since the difference between inlet and outlet temperatures is much smaller than at the lower flow rate. The fact that these readings were absolute measurements doesn't help either. A more accurate determination of ΔT would have been possible with a differential millivolt measurement between the inlet and outlet.

The steady state performance of the radiator, as measured by its heat rejection capability, is compared to predictions in Figure 6-6. The indicated test points correspond to the net heat rejection as determined by the actual panel temperatures. These data were previously given in Table 6-3. The agreement between test and prediction is fairly decent for the 1850 lb/hr flow rate--especially at inlet temperatures that are within, or close to, the design temperature control range. When the inlet temperature exceeds the higher bound of that range, as for the $96^{\circ}F$ inlet point at $Q_a = 60$ Btu/hr-ft^2, the test value, falls far short of the prediction. This is due to the fact that the VCHP header is not fully opened and thus all of the available panel surface area is not being used. The agreement for the lower flow rate is good only

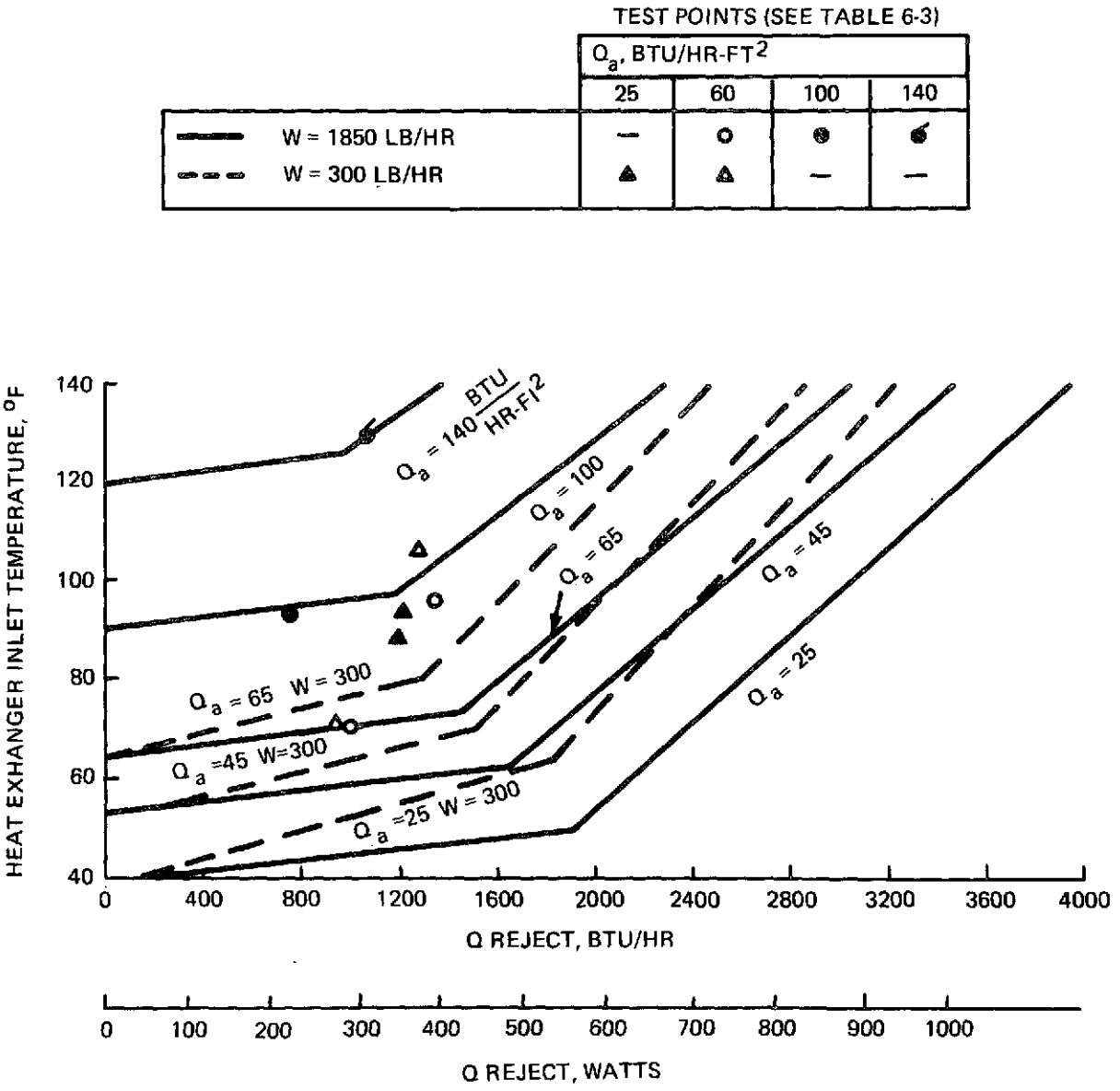

Figure 6-6 Heat Pipe Radiator Performance

for the 60 Btu/hr-ft^2 environment, also because the inlet temperature is close to the design control range. At the lower 25 Btu/hr-ft^2 environment the agreement is especially poor because the inlet is so far removed from the 40 - 60°F control range. Once again the panel is throttled by the inability of the VCHP to fully open.

As a general observation, complete dryout of the VCHP header was seldom witnessed during the performance testing. This would have been indicated by the outlet temperature converging toward the inlet temperature. What was noticed were partial evaporator dryouts, as indicated by an increasing outlet to vapor temperature difference. After the partial dryout began, the vapor temperature would remain fairly constant with a corresponding constant heat rejection rate.

The liquid to heat pipe heat exchanger worked as predicted and duplicated the performance of the previous bench tests. An effectiveness of 72%, at a flow rate of 1850 lb/hr. was verified from the measured fluid and vapor temperature differences. Selected test points are plotted in Figure 4-13. However, the pressure drop across the heat exchanger was higher than expected. At 1850 lb/hr flow the ΔP was about 3.5 psi compared to the estimated value of 0.5 to 1.0 psi.

After the radiator performance tests were run, a freezing test was performed by reducing the simulated environment to 1 Btu/hr-ft^2 and stopping the Freon flow. After several hours, the feeder pipes were at -259°F (NH_3 freezes at -108°F) and the header condenser reached temperatures below -110°F. The thermal inertia of the Freon in the heat exchanger kept the evaporator section of the header from going below -90°F. A start-up from this frozen condition was attempted by slowly increasing the flow rate to 265 lb/hr with an inlet temperature of 25°F.

Movement of the inert gas interface within the VCHP was noticed very quickly. As seen in Figure 6-7, the interface was completely out of the first low "K" section in about 22 minutes from the start of the sequence. The VCHP was completely thawed in about 70 minutes at a vapor temperature of 65°F and an inlet temperature of 78°F.

However, during this time period the feeder pipes never thawed. Because of a restricted test schedule, and considering the cold 1 Btu/hr-ft^2 environment, there was not enough time available to wait for thawing to occur. Therefore, a test deviation was initiated to increase the environment to 25 Btu/hr ft^2. However, the technique used in changing the environment, involved draining the LN_2 from the simulator plate

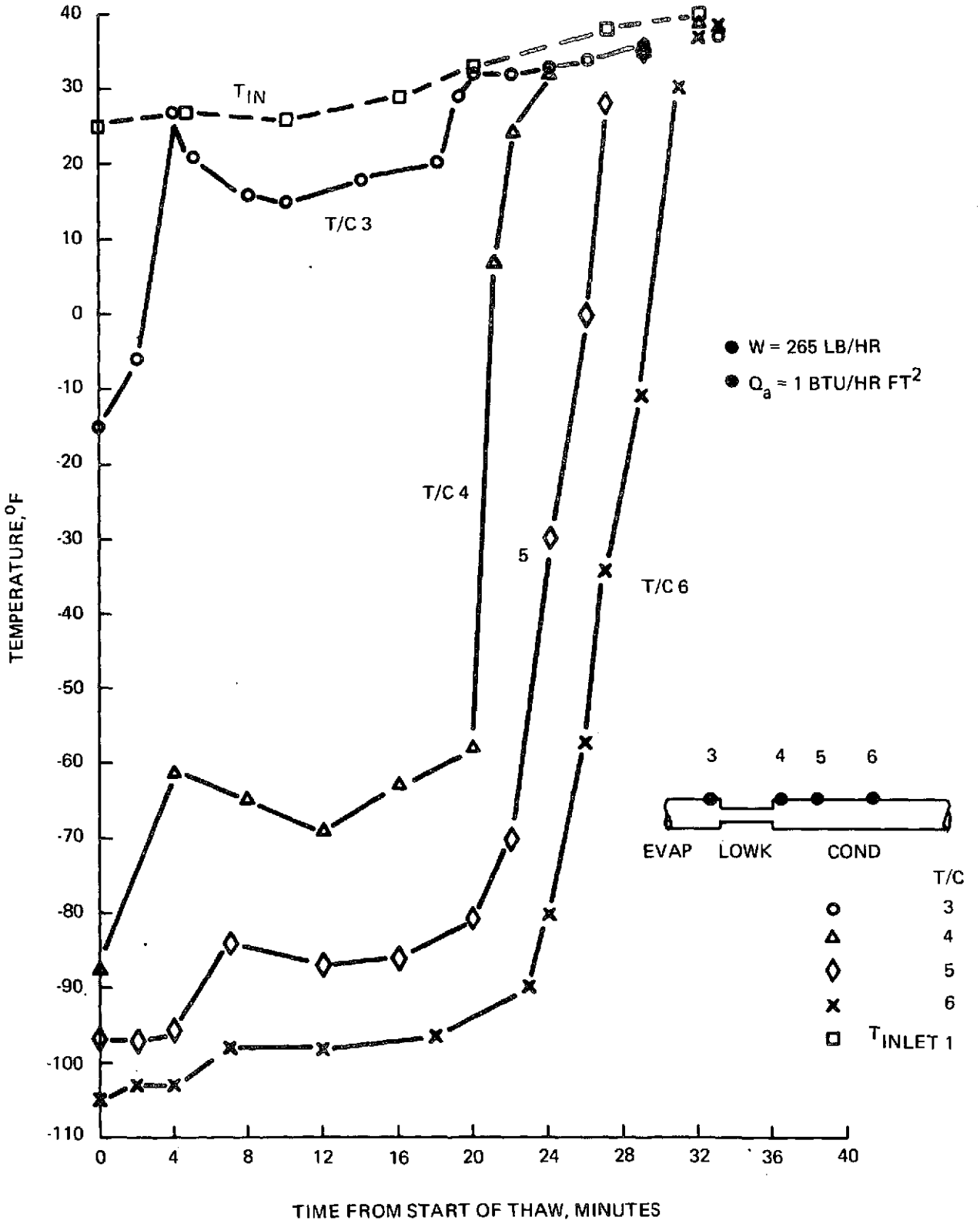

Figure 6-7 Heat Pipe Radiator Thaw Test, VCHP Header Response

and replacing it with Freon 12. In the process of clearing the LN_2 the simulator increased to a temperature equivalent to $Q_a = 50$ Btu/hr-ft^2. At this level, the feeder pipes thawed. Once thawed, however, the feeder pipes did not initially operate since the load imposed on them was probably beyond their reprime limit. In order to prime the feeder pipes after they thawed the flow to the heat exchanger was stopped for 10 - 15 minutes, thereby removing most of the heat load. They then primed and functioned normally, as demonstrated by a repetition of the data point previously cited in Figure B-2.

6.3 CONCLUSIONS

The significant conclusions that can be drawn from this program are:

- Heat pipe radiators are feasible for waste heat rejection to space. Heat pipes are extremely effective in uniformly distributing energy and maintaining an isothermal surface
- VCHP control of the panel is also feasible. The panel came "on-line" at the predicted inlet temperatures and partial VCHP control was demonstrated
- The net heat rejection capability of the panel was limited to about 400 watts because only about half of its available area could be activated. This was a problem of the VCHP header and not the radiating fin. Full panel capacity was not achieved due to the restricted VCHP control span
- Close control over reservoir temperature is particularly important for predictable VCHP operation and more careful attention must be paid to eliminating unaccounted for heat leaks. Also, the header design, with its narrow vapor space, was too sensitive to slight variations in reservoir behavior. It must be made less sensitive for more reliable VCHP operation
- Heat pipes can be reliably coupled to fluid loops, with predictable performance, using integral heat exchanger units
- The panel can not be thawed within a reasonable time period in a deep space environment. If this is a definite mission requirement the use of low freezing point feeder pipes in conjunction with the higher capacity ammonia pipes would be necessary
- Successful heat pipe operation was demonstrated after the panel had been completely frozen for an extended period and then thawed. The freeze/thaw cycle had no lingering adverse effects on the performance of the ammonia heat pipes.

Section 7

RECOMMENDATIONS

The feasibility of using variable conductance heat pipe radiators for waste heat rejection has been established. But this was only a first step toward their eventual implementation as flight hardware. Before that goal can be attained there are several intermediate steps that are necessary.

- The problem experienced with the restricted operating span of the VCHP header must be solved and a higher, 1000-2000 watt, VCHP capacity must be demonstrated. If the solution is not quickly in hand, an alertnate control concept must be identified and the hardware built and tested
- The VCHP radiator panel must be weight optimized and realistic flight weight designs must be tested
- Mission requirements must be more clearly defined before realistic solutions to the freeze/thaw problem can be formulated
- Finally, several VCHP radiator panels must be assembled and tested as a waste heat rejection system to verify overall system performance.

Section 8

REFERENCES

1. Feldmanis, C.J.: Application of Heat Pipes to Electronic Equipment Cooling. AIAA 7th Thermophysics Conference, 72-269, 1972.

2. Basiulis, A. and Hummel, T.A.: The Application of Heat Pipe Techniques to Electronic Component Cooling. ASME, 72-WA/HT-42, 1973.

3. Corman, J.C. and McLaughlin, M.H.: Thermal Development of Heat Pipe Cooled IC Packages. ASME 72-WA/HT-44, 1973.

4. McIntosh, R., Knowles, G., and Hembach, R,J.: Sounding Rocket Heat Pipe Experiment. AIAA 7th Thermophysics Conference, 72-259, 1972.

5. Edelstein, F., Swerdling, B., and Kossen, R.: Development of a Self-Priming High-Capacity Heat Pipe for Flight on OAO-C. AIAA 7th Thermophysics Conference, 72-258, 1972.

6. Edelstein, F., et. al.: The Development of a 150,000 Watt-Inch VCHP for Space Vehicle Thermal Control. ASME Paper 72-ENAV-14, 1972.

7. Scallon, T.R. Jr.: Heat Pipe Thermal Control System Concept for the Space Station. AIAA 7th Thermophysics Conference, 72-261, 1972.

8. Tawil, M., et. al.: Heat Pipe Applications for the Space Shuttle. AIAA 7th Thermophysics Conference, 72-272, 1972.

9. Barker, R.S. and Nicol, S.W.: Parametric Thermal Control Requirements for Future Spacecraft. AIAA 4th Thermophysics Conference, 69-621, 1969.

10. Tufte, R.J.: Wide Heat Load Range Space Radiator Development. ASME, 71-AV-5, 1971.

11. Morris, D.W., et. al.: Modular Radiator System Development for Shuttle and Advanced Spacecraft. ASME, 72-ENAV-34, 1972.

12. Kossen, R., et. al.: A Tunnel Artery 100,000 Watt-Inch Heat Pipe. AIAA Paper No. 72-273

REFERENCES (Cont.)

13. Kossen, R., et. al.: Development of a High Capacity VCHP. AIAA Paper No. 73-728

14. Kays and London: Compact Heat Exchangers. McGraw-Hill Book Co.

Appendix A Radiator Sizing Program

```
// JOB T
// FOR
*ONE WORD INTEGERS
*IOCS (CARD,TYPEWRITER,KEYBOARD,1132 PRINTER)
      REAL LEVP, NFEED, LFEED, LCOND
      MW=3
      MR=2
      NT=1
      NR=6
C  INPUT
  218 READ (MR,100) NPAN
      READ (MR,101) TIN, W, ETA, QABS1, EPS, AREA, ODIAM
      READ (MR,101) DFEED, NFEED, LFEED, HEVAP, HCOND, LEVP, LCOND, D3
  100 FORMAT (I3)
  101 FORMAT (8F10.4)
  216 SUMQ=0.0
      TP=100.
C  DEFINE CALCULATED VARIABLES
      FINS=11.1*3.1416*(ODIAM+.25)
      NFIN=IFIX(FINS+.5)
      FINS=NFIN
      FLOWA=3.1416*((ODIAM+.5)**2-ODIAM**2)-FINS*.006*.25
      WPER=3.1416*(ODIAM+.5+ODIAM)+2.*FINS*.25
      DHYD=4.*FLOWA/WPER
      G=W/FLOWA
      RE=DHYD*G*12./.760
      QABS=QABS1*AREA/ETA
      AREA2=LCOND*D3*3.1416/(2.*144.)
      AREA3=NFEED*DFEED*3.1416*LFEED/144.
C  CALCULATE 'COLBURN J FACTOR' FROM KAYS + LONDON  CURVE
      IF (RE-1000.) 5,5,10
    5 COLBJ=.0051*(RE/1000.)**(-.743)
      GO TO 25
   10 IF (RE-10000.) 11,11,12
   11 IRE=IFIX(RE/1000.)
      GO TO 13
   12 IRE=10
   13 GO TO (15, 16, 17, 18, 19, 20, 21, 22, 23, 23), IRE
   15 COLBJ=1.4E-3*(RE/1000.)**2-.0051*RE/1000.+.0089
      GO TO 25
   16 COLBJ=.0041+.0002*(RE-3000.)/1000.
      GO TO 25
   17 COLBJ=.0039+.0002*(RE-4000.)/1000.
      GO TO 25
   18 COLBJ=.0037+.0002*(RE-5000.)/1000.
      GO TO 25
   19 COLBJ=.0035+.0002*(RE-6000.)/1000.
      GO TO 25
   20 COLBJ=.0034+.0001*(RE-7000.)/1000.
      GO TO 25
   21 COLBJ=.0033+.0001*(RE-8000.)/1000.
      GO TO 25
   22 COLBJ=.0032+.0001*(RE-9000.)/1000.
      GO TO 25
   23 COLBJ=.0031+.0001*(RE-10000.)/1000.
   25 CONTINUE
      HFLU=COLBJ*G*.25/2.125
      AREA1=(3.1416*ODIAM+FINS*2.*.25)*LEVP
      ETAF=TANH(SQRT(2.*HFLU/(10.67*.006))*.25)/(SQRT(2.*HFLU/(10.67*.00
     A6))*.25)
      ETAO=1.-(FINS*2.*.25/(3.1416*ODIAM+FINS*2.*.25))*(1.-ETAF)
      R1=1./(ETAO*AREA1*HFLU)
```

```
      R2=1./((HEVAP*3.1416*D3*LEVP)/144.)
      COND1=1./(R1+R2)
      R3=1./(HCOND*AREA2)+1./(HEVAP*AREA2*DFEED/D3)+1./(HCOND*AREA3)
      COND2=1./R3
C  OUTPUT OF INPUT, CALCULATED VARIABLES
      WRITE (MW,107) NPAN, TIN
  107 FORMAT(1H1,2X,'INPUT VARIABLES',//,5X,'NUMBER OF PANELS = ',I3,2X,
     1'WITH FLUID INLET TEMP = ',F6.2,' DEG F',/)
      WRITE (MW,108)
  108 FORMAT (7X,'W',9X,'ETA',7X,'QABS1',6X,'EPS',7X,'AREA',7X,'ODIAM',/
     A)
      WRITE (MW,109) W, ETA, QABS1, EPS, AREA, ODIAM
  109 FORMAT (5X,F6.1,5X,F5.2,5X,F6.2,5X,F5.2,5X,F6.2,5X,F6.3,/)
      WRITE (MW,110)
  110 FORMAT (5X,'DFEED',5X,'NFEED',5X,'LFEED',7X,'HEVAP',7X,'HCOND',6X,
     1'LEVAP',5X,'LCOND',7X,'D3',/)
      WRITE (MW,111) DFEED, NFEED, LFEED, HEVAP, HCOND, LEVP, LCOND, D3
  111 FORMAT (5X,F5.2,5X,F5.2,5X,F5.2,5X,F7.2,4X,F7.2,5X,F5.2,5X,F5.2,
     15X,F5.2,///)
      WRITE (MW,112)
  112 FORMAT (2X,'CALCULATED VARIABLES',//)
      WRITE (MW,113) COLBJ, HFLU, RE, QABS
  113 FORMAT (5X,'COLBJ',4X,'HFLU',8X,'RE',8X,'QABS',/,5X,F6.4,5X,F6.4,
     15X,F8.3,5X,F8.3,//)
      WRITE (MW,114) AREA1, AREA2, AREA3, COND1, COND2
  114 FORMAT (5X,'AREA1',5X,'AREA2',5X,'AREA3',5X,'COND1',5X,'COND2',/,
     14X,F7.3,3X,F7.3,3X,F7.3,3X,F7.2,3X,F7.2,////)
      WRITE (MW,115)
  115 FORMAT (5X,'NPANEL',4X,'TOUT',8X,'TVAP',8X,'TROOT',14X,'QREJ',17X,
     A'SUM Q',17X,'QREJ (WATTS)',/)
C  BEGIN EXECUTION OF CAPACITY CALCULATIONS
      WCP=.25*W
      EX=EXP(COND1/WCP)
      Z=(ETA/WCP)*(EX/(1.-EX))-ETA/COND2
      I=0
      TPR=TP+460.
      RTP=EPS*AREA*.1713E-8*TPR**4-QABS
      F=TIN-TP+Z*RTP
   35 I=I+1
   30 FP=-1.+Z*4.*EPS*AREA*.1713E-8*TPR**3
      TPN=TP-F/FP
      TPNR=TPN+460.
      RTPN=EPS*AREA*.1713E-8*TPNR**4-QABS
      F=TIN-TPN+Z*RTPN
      IF (ABS(F)-.001) 50,50,40
   40 TP=TPN
      TPR=TP+460.
      GO TO 30
   50 QREJ=RTPN*ETA
      TVAP=TPN+QREJ/COND2
      SUMQ=QREJ+SUMQ
      TOUT=TIN-(ETA/W)*RTPN
      QREJW=QREJ/3.413
      WRITE (MW,103) I, TOUT, TVAP, TPN, QREJ, SUMQ, QREJW
  103 FORMAT (5X,I3,3(5X,F7.2),3(5X,E19.9),/)
      TIN=TOUT
      IF (I-NPAN) 35, 60, 60
   60 CONTINUE
      WRITE (NT,104)
  104 FORMAT (5X,'READY FOR PARAMETRIC CHANGES',/)
  200 READ (NR,105) NPAR
```

```
  105 FORMAT (I3)
      GO TO (201,202,203,204,205,206,207,208,209,210,211,212,213,214,215
     A,216,217,218,219), NPAR
  201 READ (NR,105) NPAN
      GO TO 200
  202 READ (NR,106) TIN
  106 FORMAT (F10.5)
      GO TO 200
  203 READ (NR,106) W
      GO TO 200
  204 READ (NR,106) ETA
      GO TO 200
  205 READ (NR,106) QABS1
      GO TO 200
  206 READ (NR,106) EPS
      GO TO 200
  207 READ (NR,106) AREA
      GO TO 200
  208 READ (NR,106) DFEED
      GO TO 200
  209 READ (NR,106) NFEED
      GO TO 200
  210 READ (NR,106) LFEED
      GO TO 200
  211 READ (NR,106) HEVAP
      GO TO 200
  212 READ (NR,106) HCOND
      GO TO 200
  213 READ (NR,106) LEVP
      GO TO 200
  214 READ (NR,106) LCOND
      GO TO 200
  215 READ (NR,106) D3
      GO TO 200
  219 READ (NR,106) ODIAM
      GO TO 200
  217 CONTINUE
      CALL EXIT
      END
// XEQ
 30
  150.      2000.      .9       45.       .9        32.      1.125
  0.5        6.       96.       2700.     3500.    24.       48.       1.
```

TYPEWRITER CODES

Code	Name	Description
001	NPAN	# of panels (I3)
002	TIN	fluid inlet temp, °F
003	W	mass flow rate, lb m/hr
004	ETA	radiator efficiency
005	QABS1	ambient absorbed heat, $\frac{btu}{hr\ ft^2}$
006	EPS	e ~ emissivity
007	AREA	area of one panel, ft^2
008	DFEED	I.D. of feeder heat pipe
009	NFEED	number of feeder pipes per panel
010	LFEED	length of feeder condenser, in.
011	HEVAP	h_{evap} , $\frac{btu}{hr\ ft^2 °F}$
012	HCOND	$h_{condenser}$, $\frac{btu}{hr\ ft^2 °F}$
013	LEVP	evaporator length of header, in.
014	LCOND	condenser length of header, in.
015	D3	inside diam. of header, in.
016	execute with new parameters	
017	end computer session ~ kill program	
018	read new set of data cards, then execute	
019	ODIAM outside diameter of header evaporator, in.	

Appendix B

System Test Results

The data that are presented correspond to definite steady state conditions. The results for each test point are described by three data plots.

(a) Radiator panel temperature map

(b) Temperature distribution along VCHP header

(c) Temperature distribution along feeder pipe A

Appendix B Contents

Figure No.	Run No.	$Q_{Absorbed}$ BTU/Hr Ft^2	Flow Rate lb/Hr	T_{Inlet} °F
	Day/Hr/Min			
B-1a,b,c	193/08/30	56	1850	71
B-2a,b,c	193/01/10	60	1990	96
B-3a,b,c	192/10/50	55	1064	71
B-4a,b,c	192/15/30	58	276	106.5
B-5a,b,c	191/21/40	41	276	71
B-6a,b,c	191/18/05	23	284	88.3
B-7	191/18/45	23	276	94
B-8a,b,c	193/10/25	93	1976	93
B-9a,b,c	193/14/50	137	1985	129.6

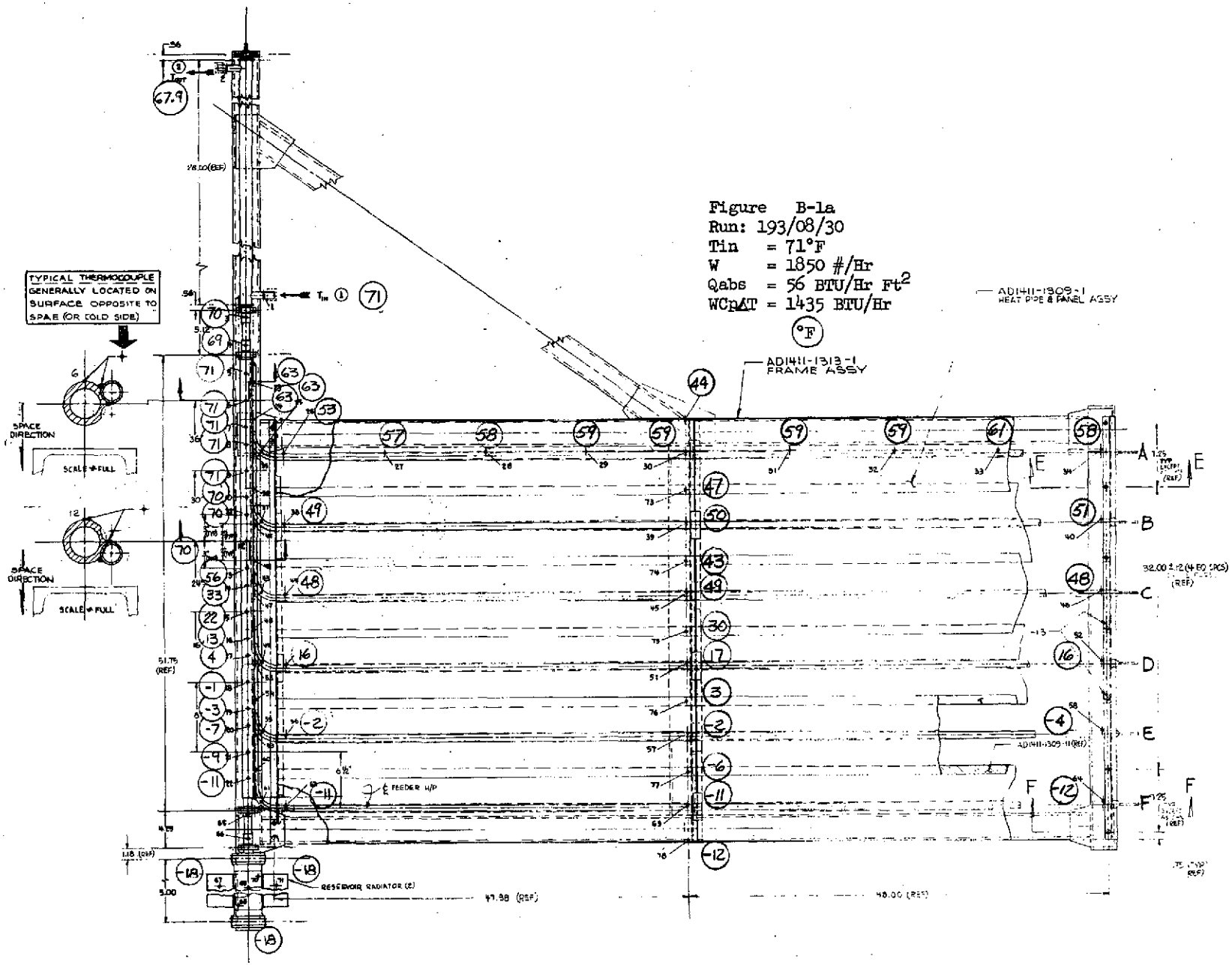

Figure B-1a
Run: 193/08/30
Tin = 71°F
W = 1850 #/Hr
Qabs = 56 BTU/Hr Ft^2
WCpΔT = 1435 BTU/Hr

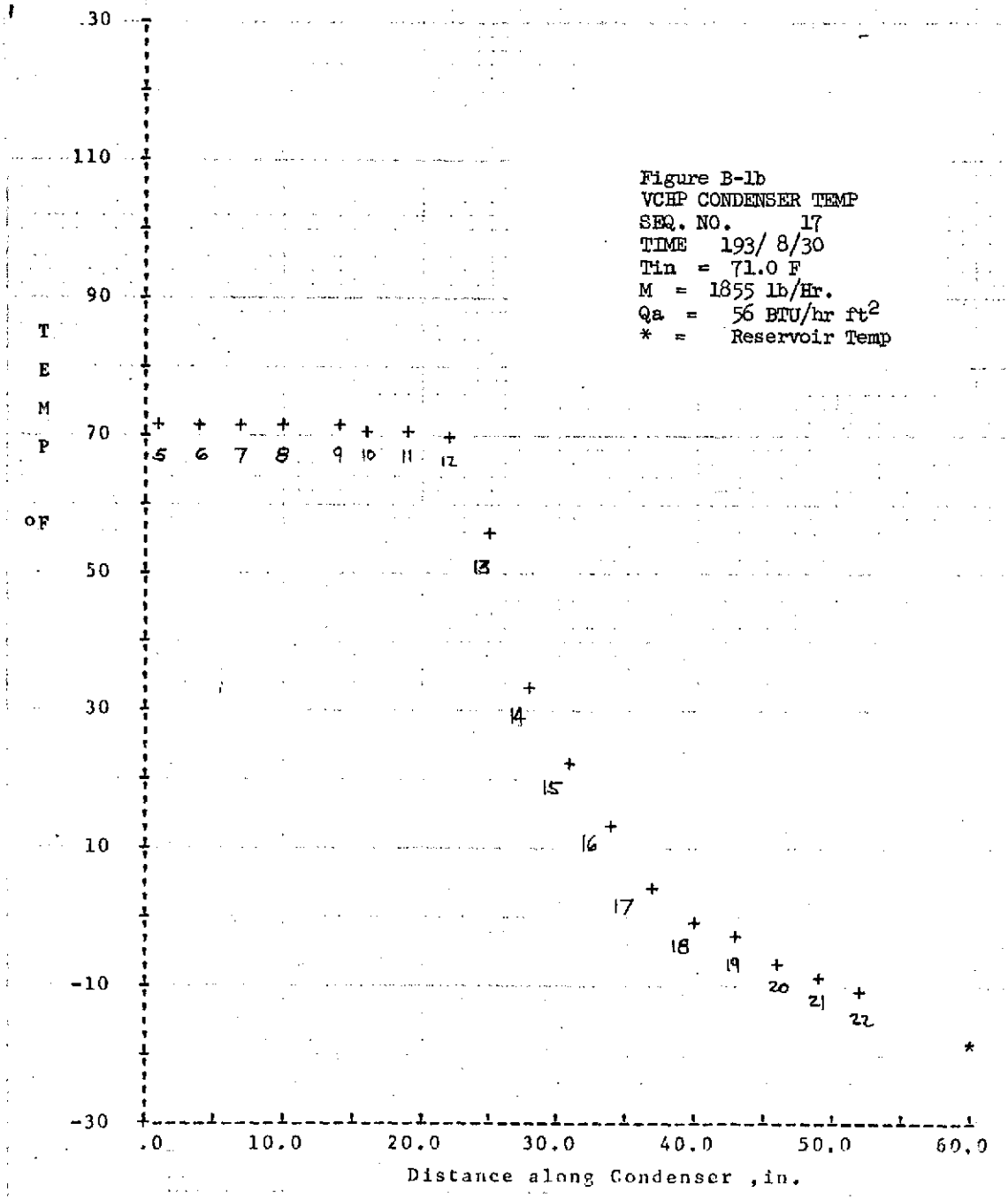
Figure B-1b
VCHP CONDENSER TEMP
SEQ. NO. 17
TIME 193/ 8/30
Tin = 71.0 F
M = 1855 lb/Hr.
Qa = 56 BTU/hr ft²
* = Reservoir Temp
TEMP °F
30
110
90
70
50
30
10
-10
-30
5
6
7
8
9
10
11
12
13
14
15
16
17
18
19
20
21
22
.0
10.0
20.0
30.0
40.0
50.0
60.0
Distance along Condenser , in.

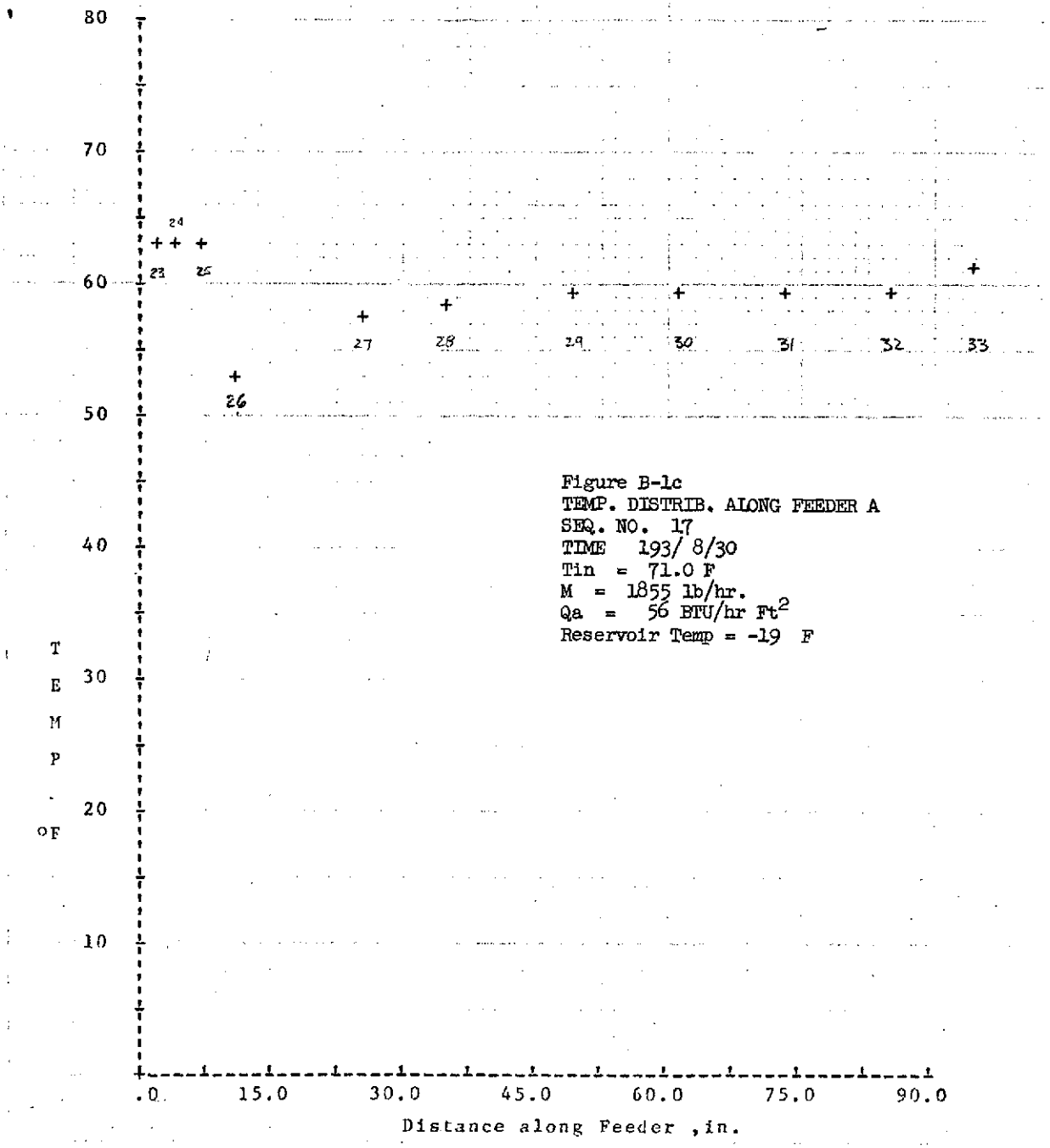

Figure B-1c
TEMP. DISTRIB. ALONG FEEDER A
SEQ. NO. 17
TIME 193/ 8/30
Tin = 71.0 F
M = 1855 lb/hr.
Qa = 56 BTU/hr Ft^2
Reservoir Temp = -19 F

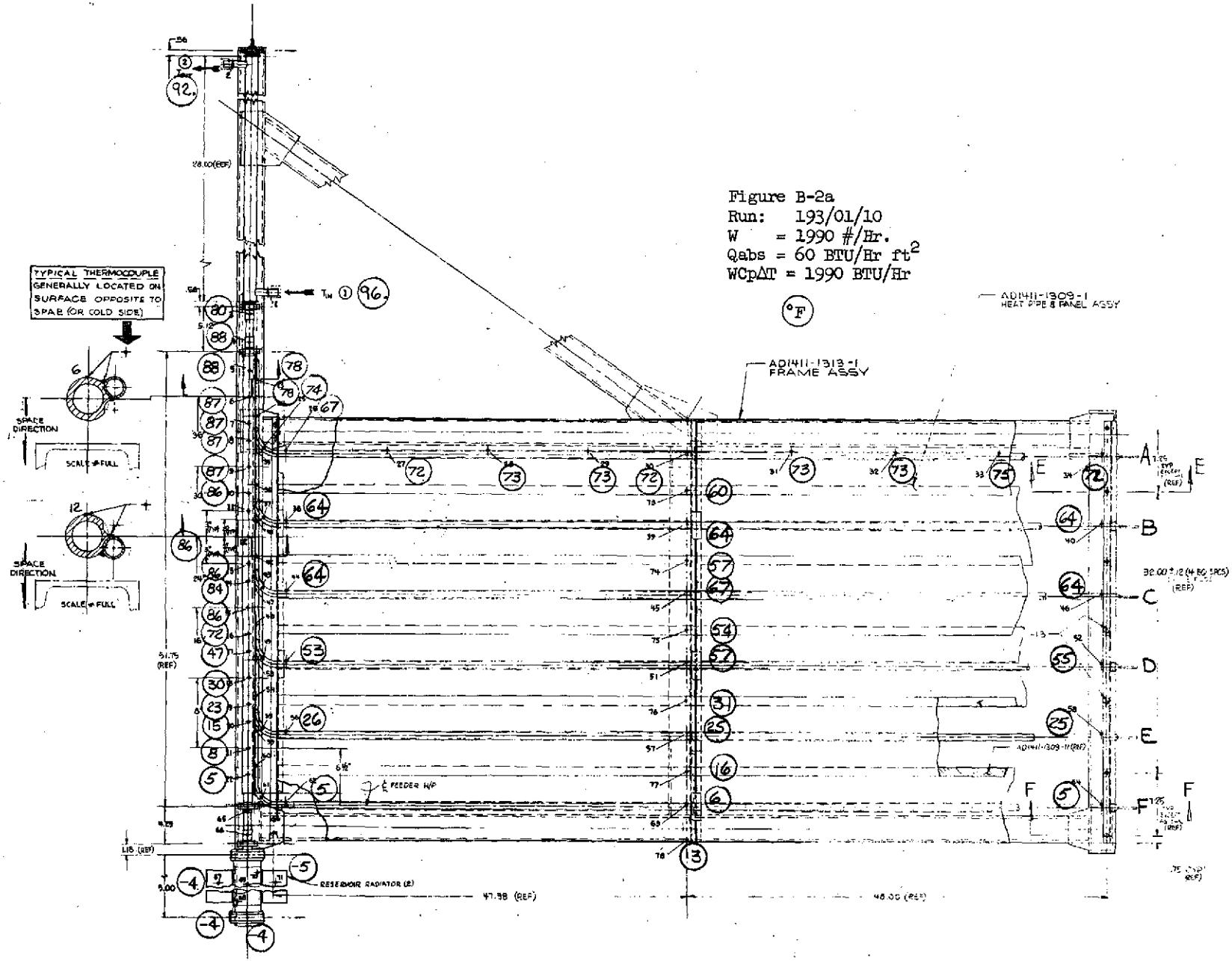

Figure B-2a
Run: 193/01/10
W = 1990 #/Hr.
Qabs = 60 BTU/Hr ft^2
WCpΔT = 1990 BTU/Hr

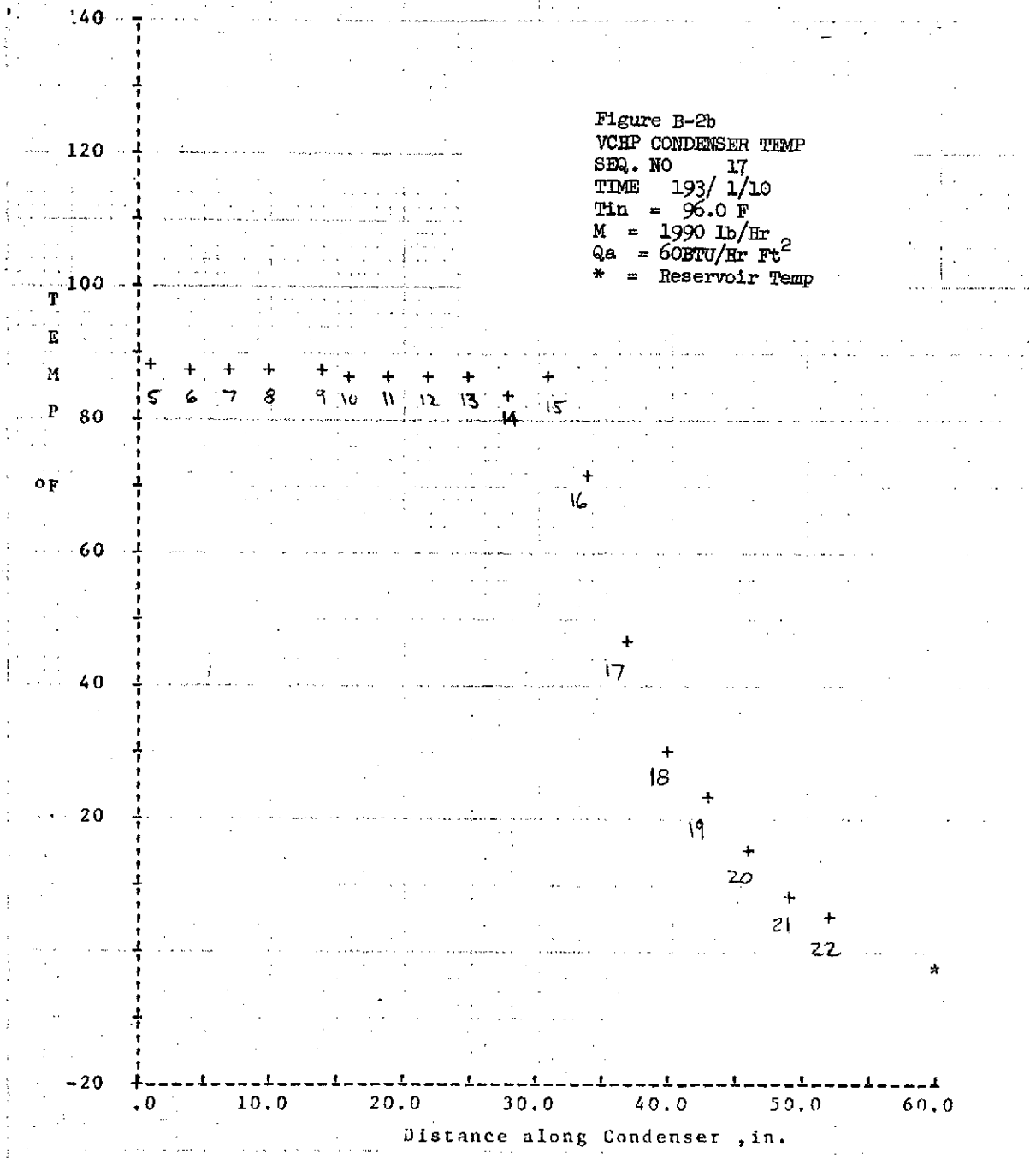
Figure B-2b
VCHP CONDENSER TEMP
SEQ. NO 17
TIME 193/ 1/10
Tin = 96.0 F
M = 1990 lb/Hr
Qa = 60BTU/Hr Ft2
* = Reservoir Temp
TEMP oF
140
120
100
80
60
40
20
-20
5
6
7
8
9
10
11
12
13
14
15
16
17
18
19
20
21
22
*
.0
10.0
20.0
30.0
40.0
50.0
60.0
Distance along Condenser ,in.

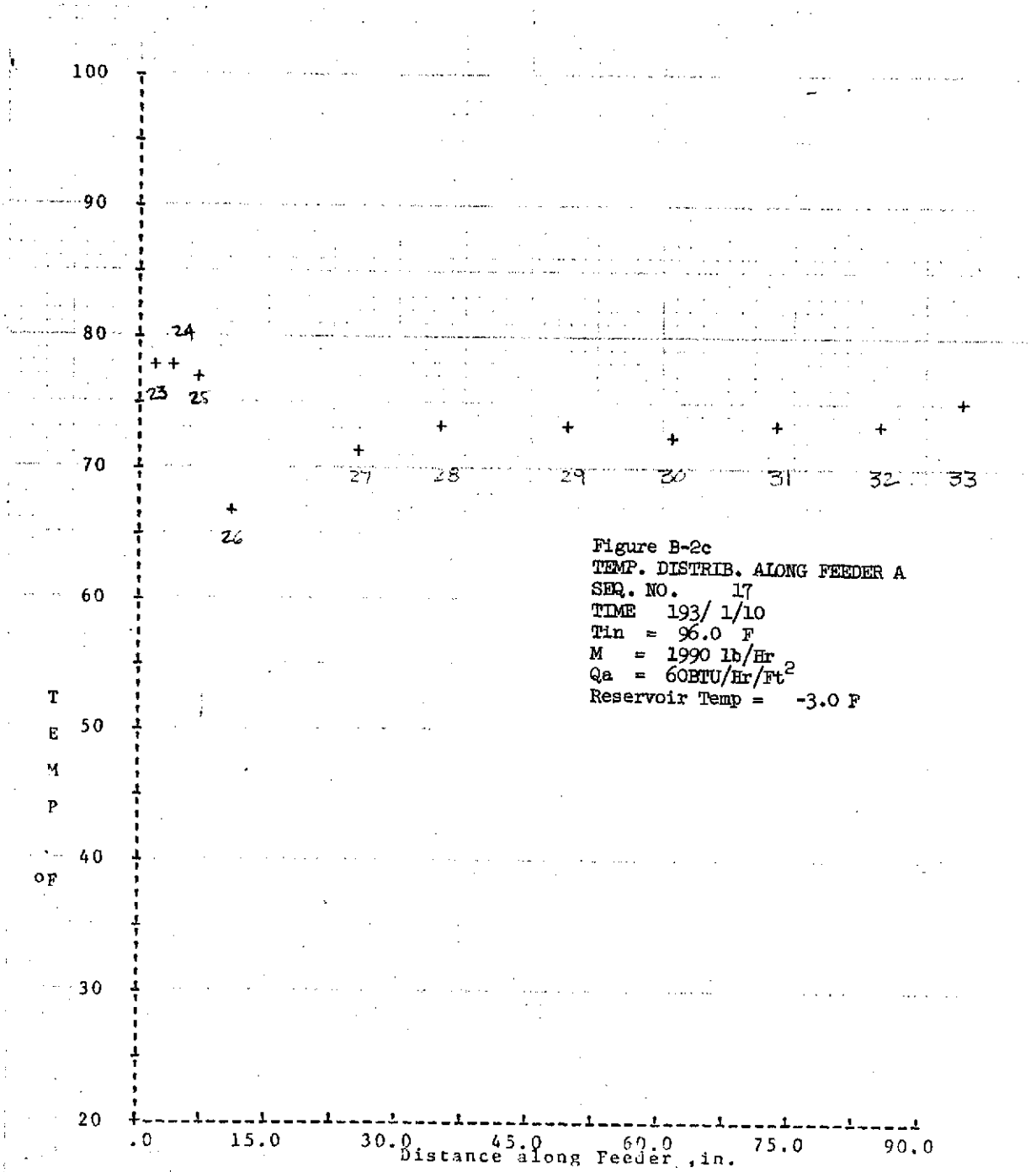

Figure B-2c
TEMP. DISTRIB. ALONG FEEDER A
SEQ. NO. 17
TIME 193/ 1/10
Tin = 96.0 F
M = 1990 lb/Hr
Qa = 60BTU/Hr/Ft^2
Reservoir Temp = -3.0 F

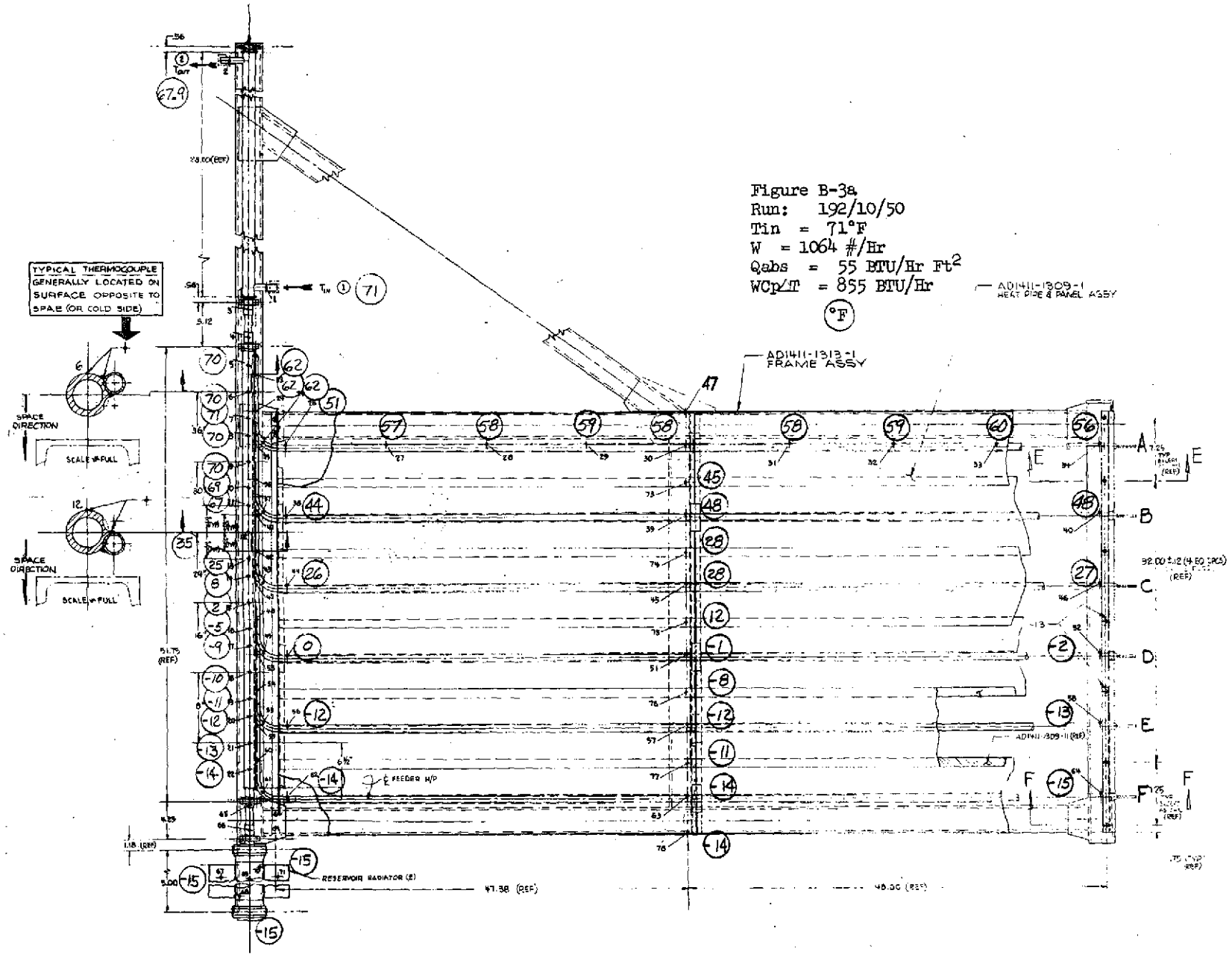

Figure B-3a
Run: 192/10/50
Tin = 71°F
W = 1064 #/Hr
Qabs = 55 BTU/Hr Ft^2
WCp/T = 855 BTU/Hr
°F

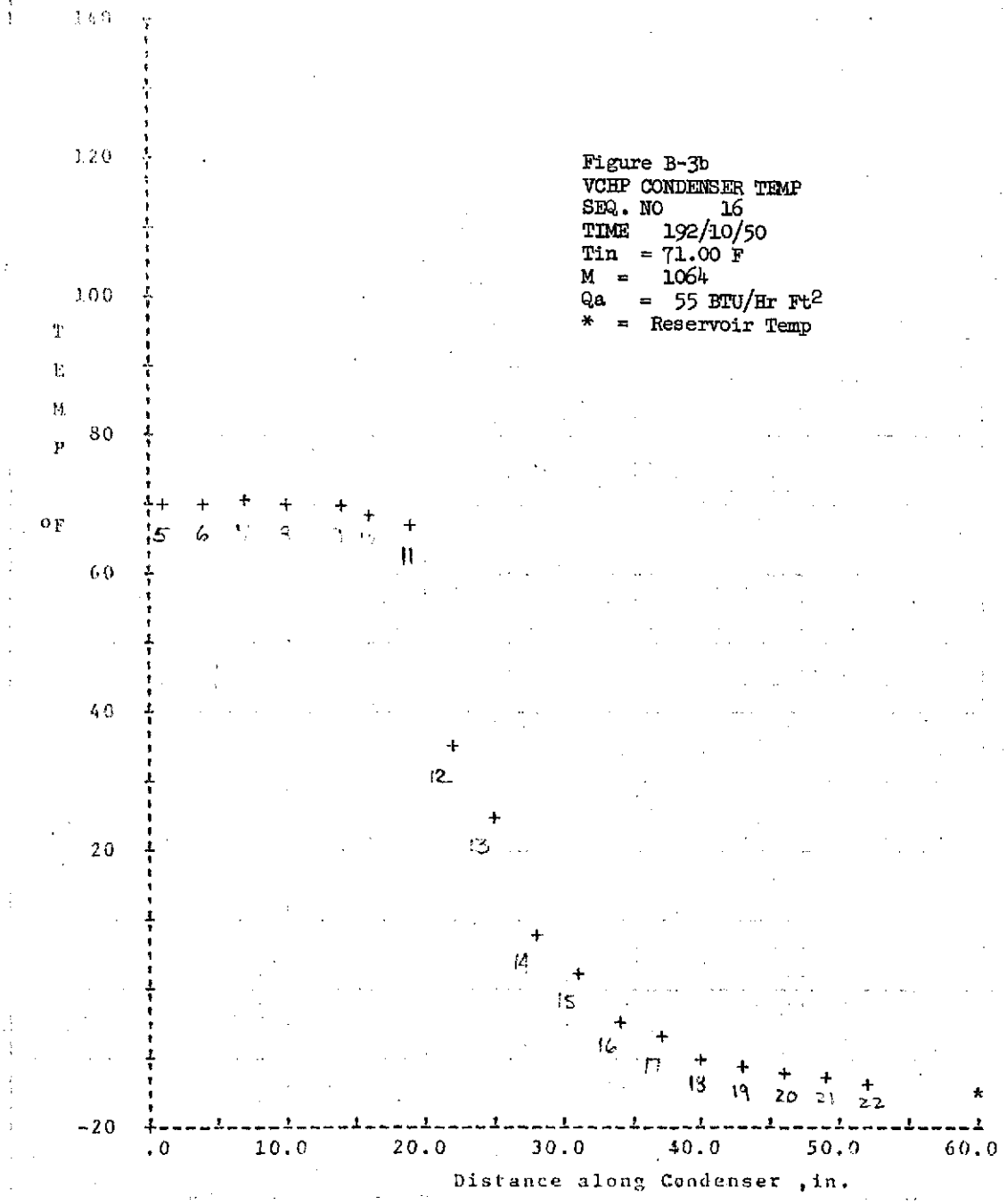
Figure B-3b
VCHP CONDENSER TEMP
SEQ. NO 16
TIME 192/10/50
Tin = 71.00 F
M = 1064
Qa = 55 BTU/Hr Ft2
* = Reservoir Temp
TEMP oF
140
120
100
80
60
40
20
-20
.0
10.0
20.0
30.0
40.0
50.0
60.0
Distance along Condenser ,in.

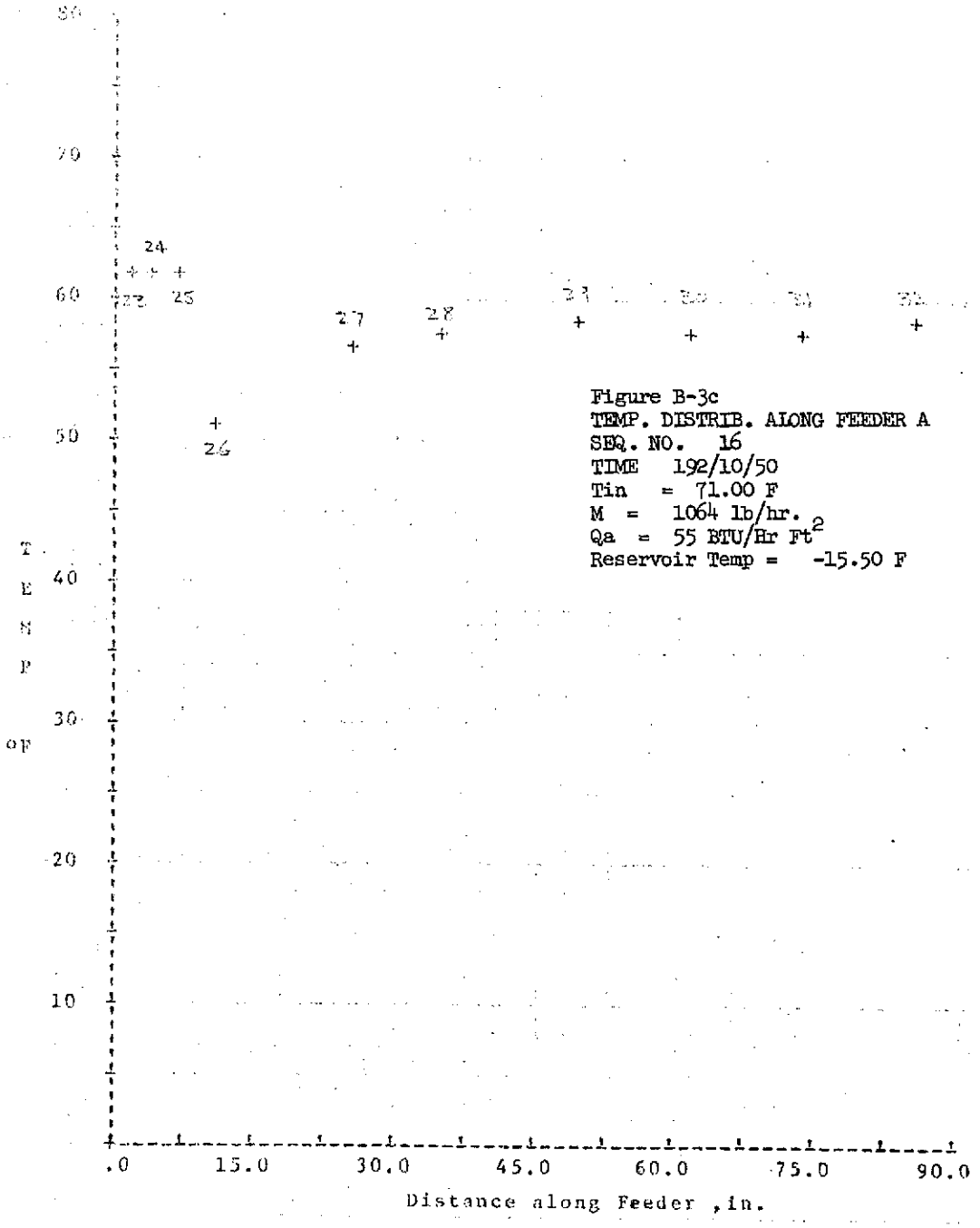

Figure B-3c
TEMP. DISTRIB. ALONG FEEDER A
SEQ. NO. 16
TIME 192/10/50
Tin = 71.00 F
M = 1064 lb/hr.
Qa = 55 BTU/Hr Ft^2
Reservoir Temp = -15.50 F

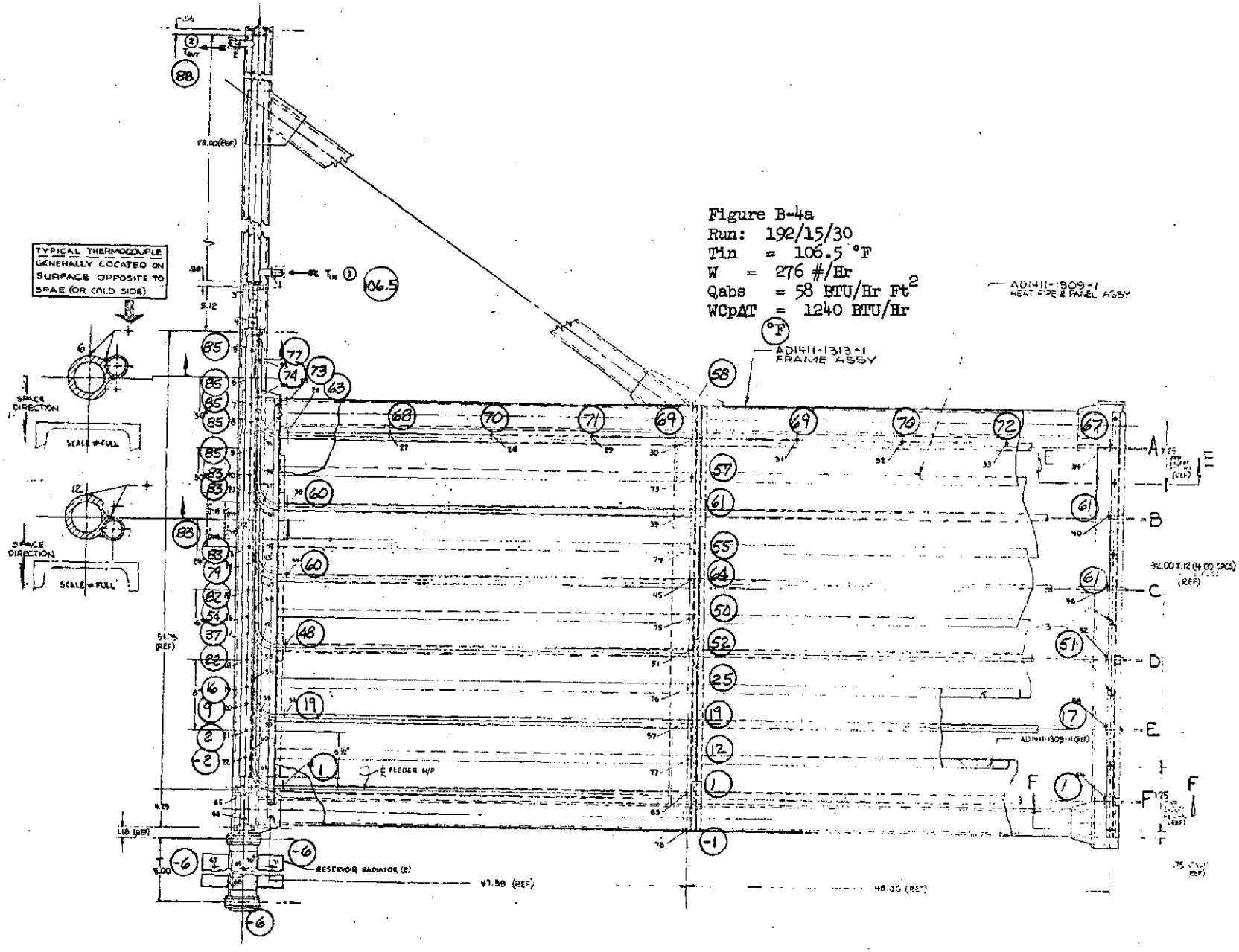

Figure B-4a
Run: 192/15/30
Tin = 106.5 °F
W = 276 #/Hr
Qabs = 58 BTU/Hr Ft^2
WCpΔT = 1240 BTU/Hr

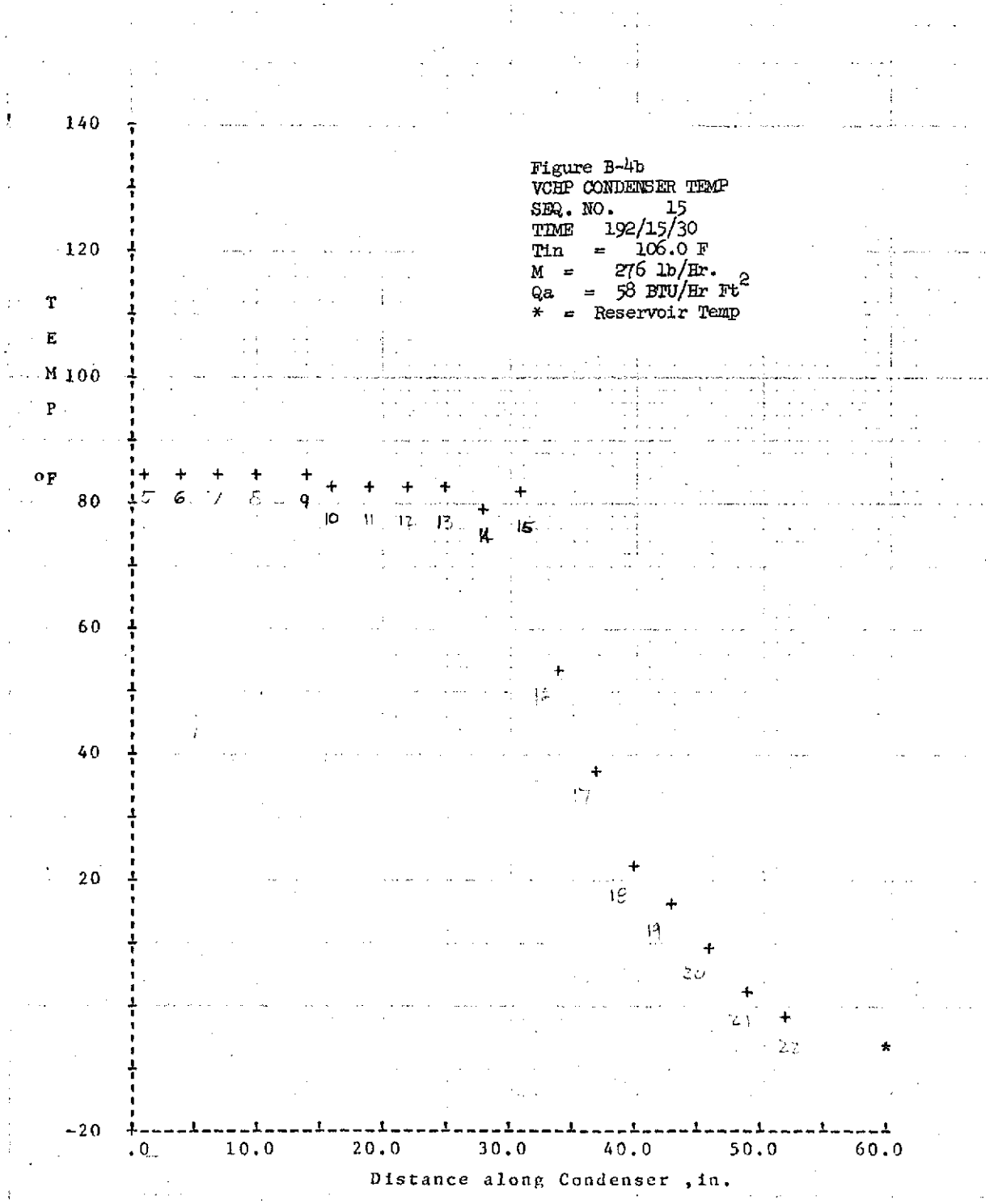
Figure B-4b
VCHP CONDENSER TEMP
SEQ. NO. 15
TIME 192/15/30
Tin = 106.0 F
M = 276 lb/Hr.
Qa = 58 BTU/Hr Ft2
* = Reservoir Temp
TEMP oF
140
120
100
80
60
40
20
-20
.0
10.0
20.0
30.0
40.0
50.0
60.0
Distance along Condenser ,in.

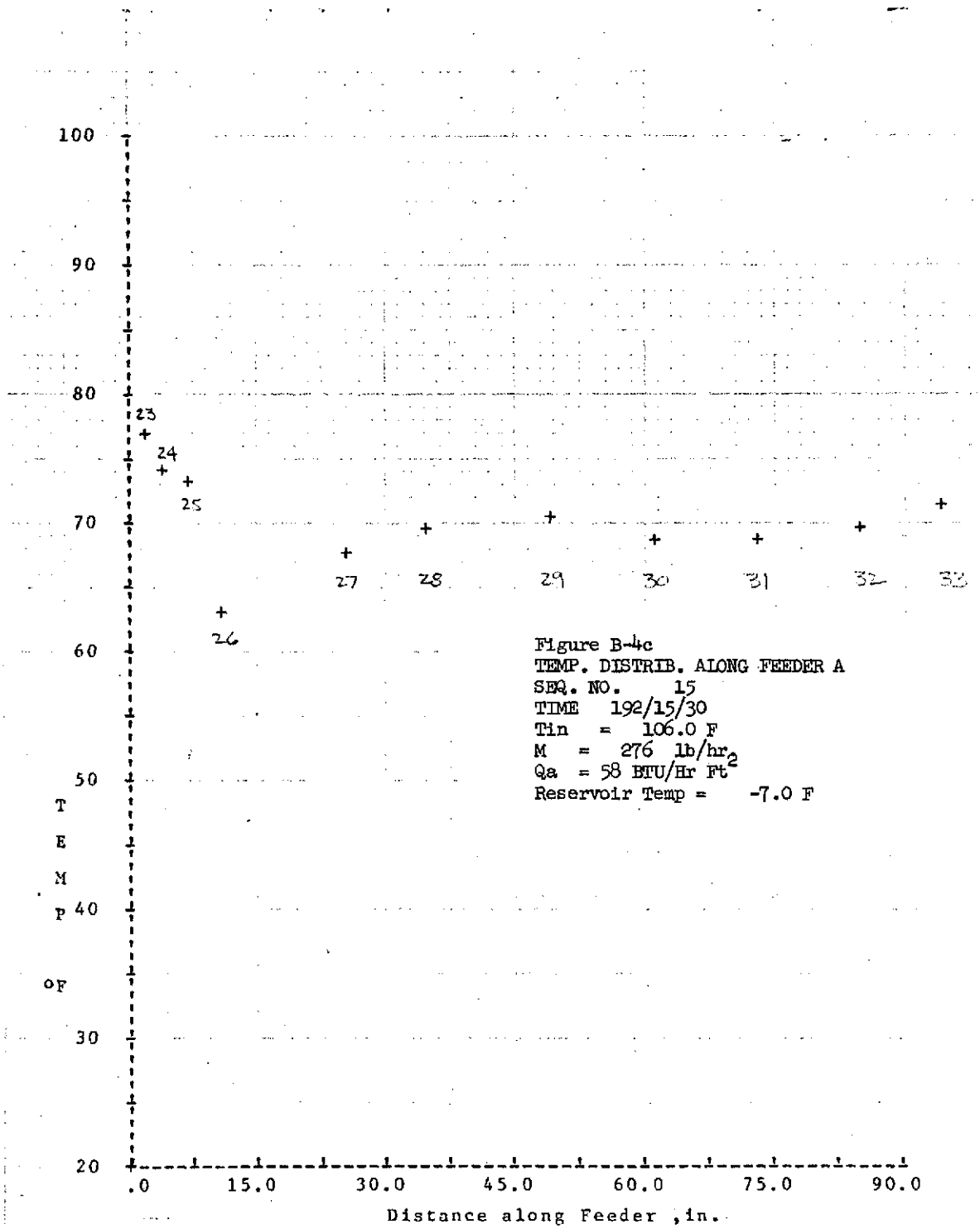

Figure B-4c
TEMP. DISTRIB. ALONG FEEDER A
SEQ. NO. 15
TIME 192/15/30
Tin = 106.0 F
M = 276 lb/hr
Qa = 58 BTU/Hr Ft^2
Reservoir Temp = -7.0 F

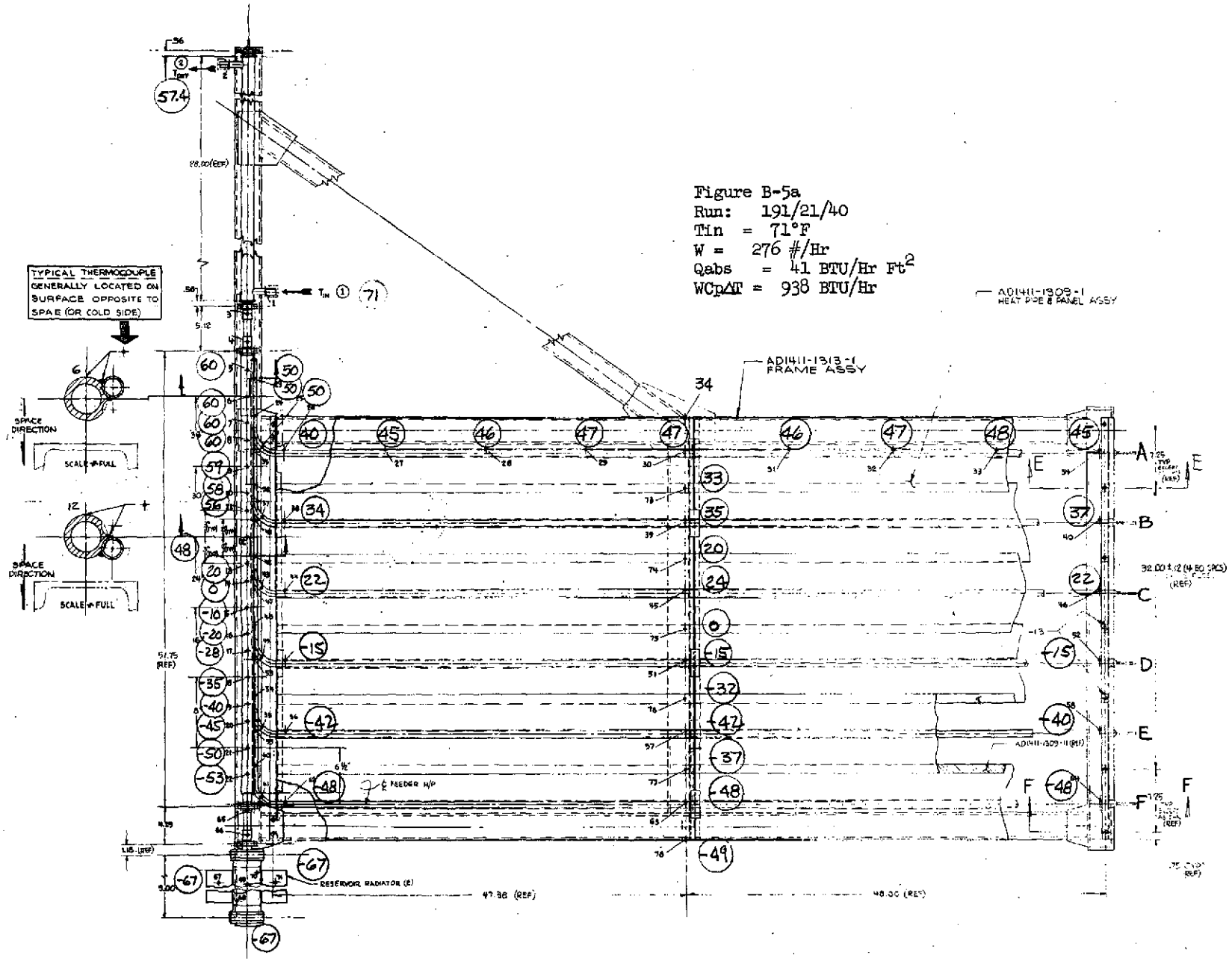

Figure B-5a
Run: 191/21/40
Tin = 71°F
W = 276 #/Hr
Qabs = 41 BTU/Hr Ft^2
WCpΔT = 938 BTU/Hr

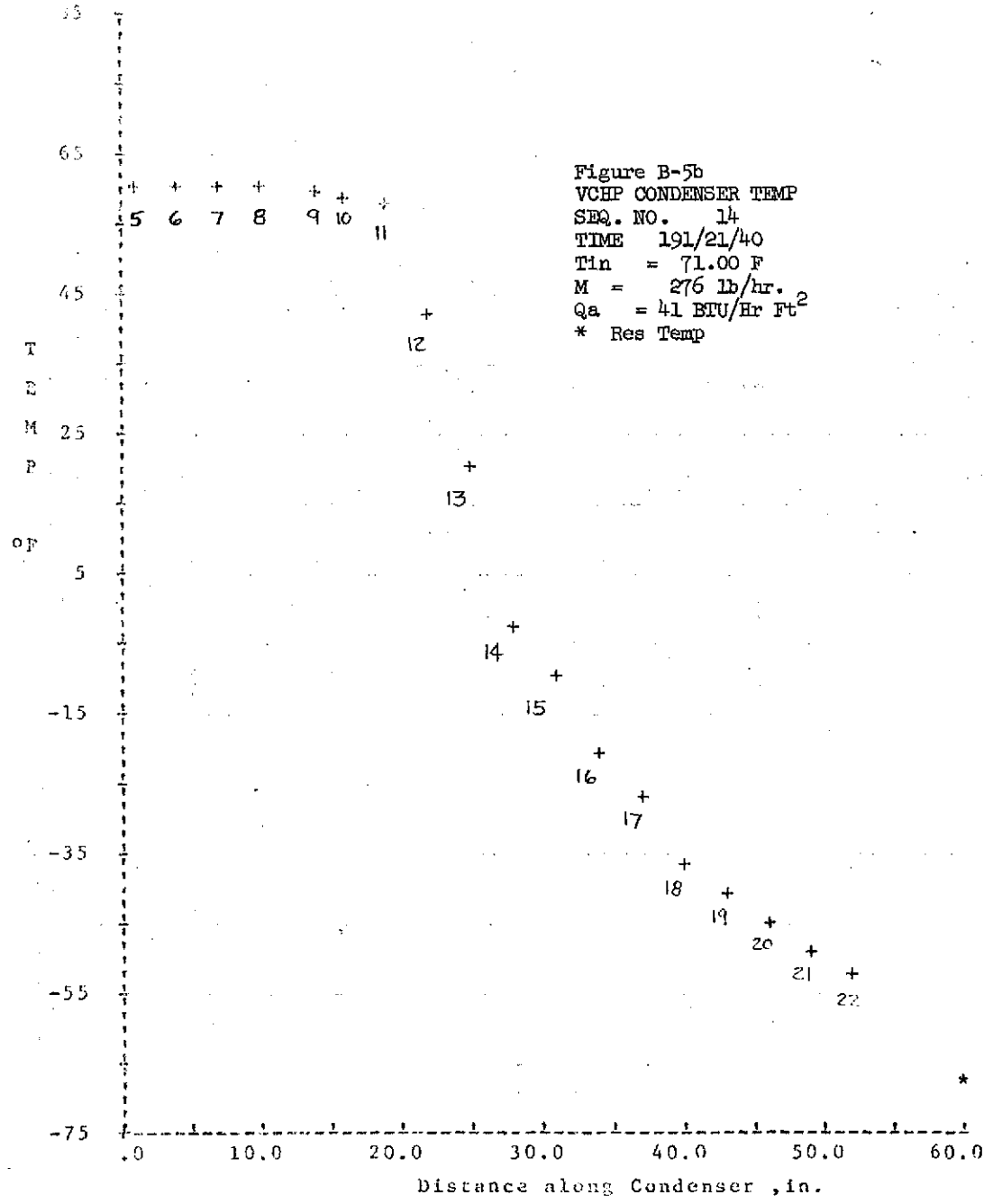
Figure B-5b
VCHP CONDENSER TEMP
SEQ. NO. 14
TIME 191/21/40
Tin = 71.00 F
M = 276 lb/hr.
Qa = 41 BTU/Hr Ft2
* Res Temp
TEMP oF
65
45
25
5
-15
-35
-55
-75
5
6
7
8
9
10
11
12
13
14
15
16
17
18
19
20
21
22
*
.0
10.0
20.0
30.0
40.0
50.0
60.0
Distance along Condenser ,in.

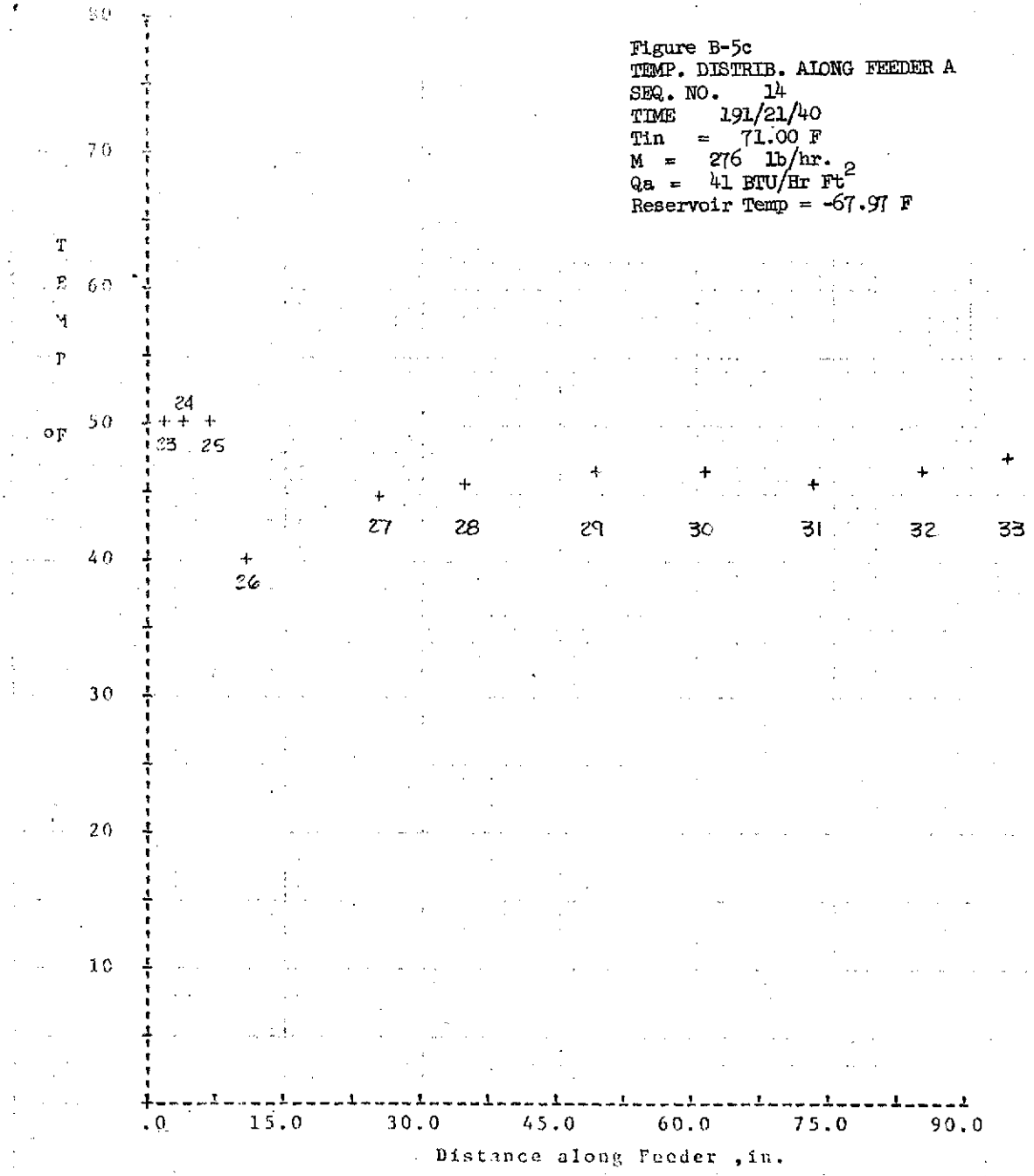
Figure B-5c
TEMP. DISTRIB. ALONG FEEDER A
SEQ. NO. 14
TIME 191/21/40
Tin = 71.00 F
M = 276 lb/hr.
Qa = 41 BTU/Hr Ft2
Reservoir Temp = -67.97 F
TEMP oF
70
60
50
40
30
20
10
24
23
25
26
27
28
29
30
31
32
33
.0
15.0
30.0
45.0
60.0
75.0
90.0
Distance along Feeder ,in.

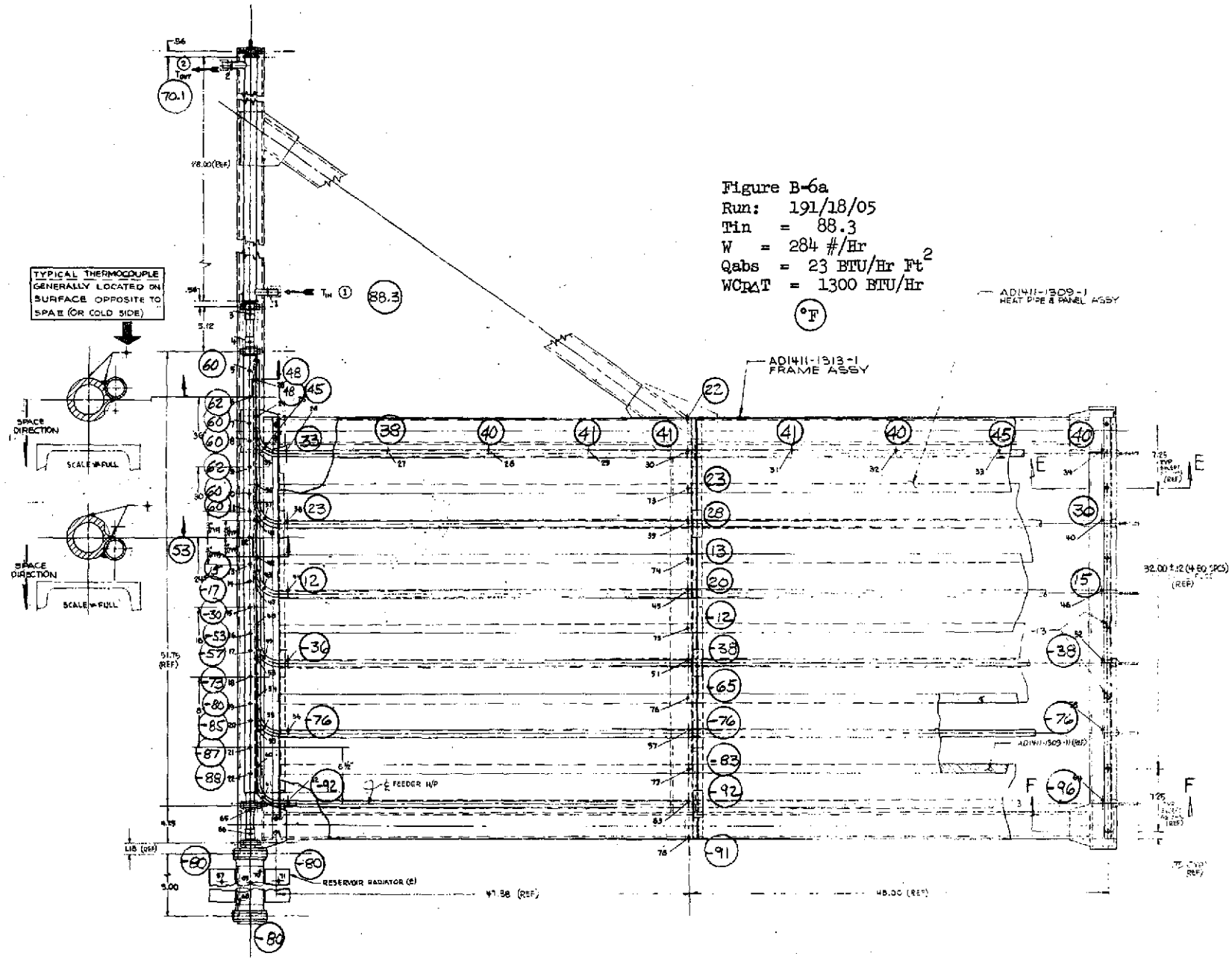

Figure B-6a
Run: 191/18/05
Tin = 88.3
W = 284 #/Hr
Qabs = 23 BTU/Hr Ft^2
WCpΔT = 1300 BTU/Hr
°F

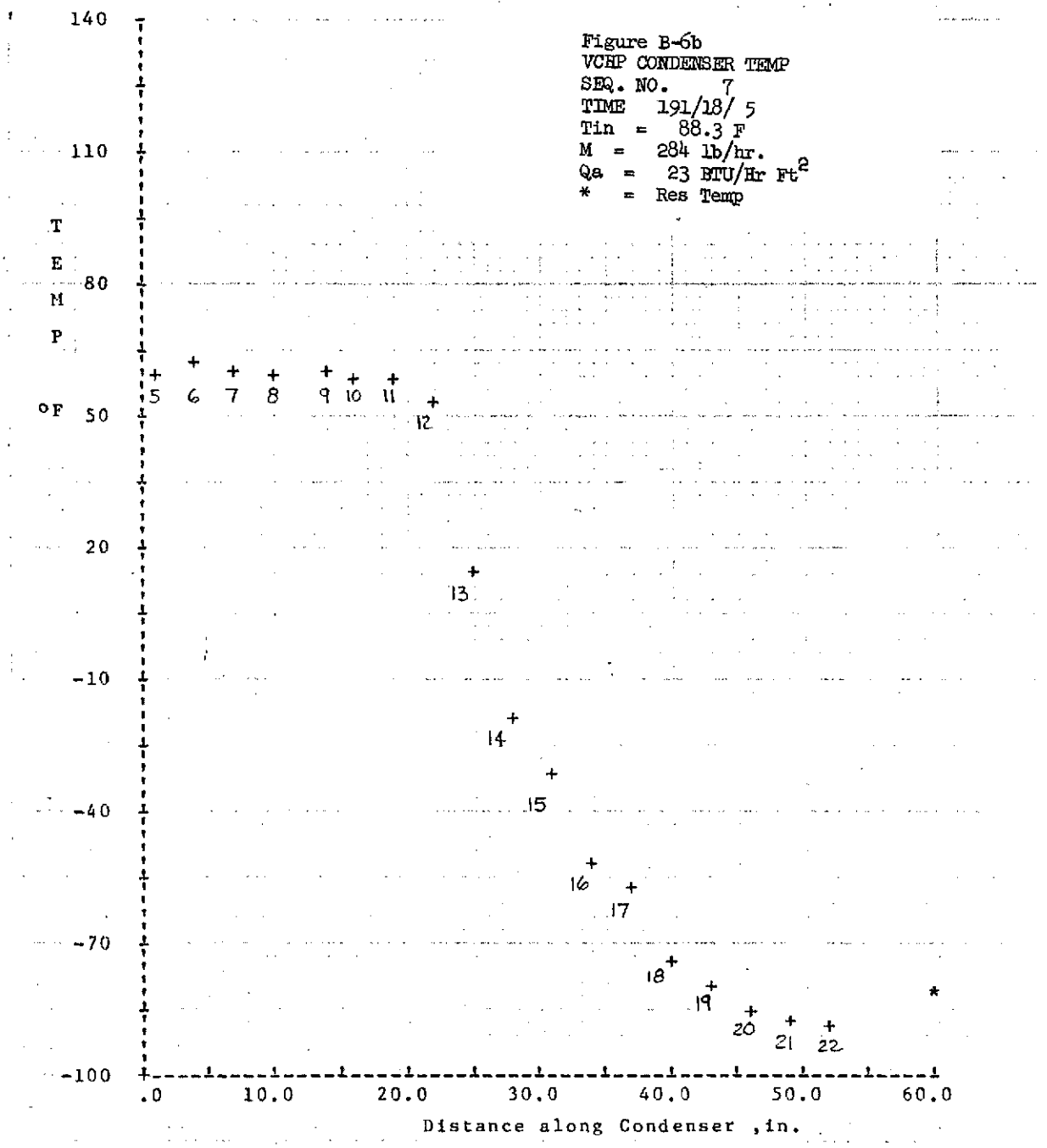
Figure B-6b
VCHP CONDENSER TEMP
SEQ. NO. 7
TIME 191/18/ 5
Tin = 88.3 F
M = 284 lb/hr.
Qa = 23 BTU/Hr Ft2
* = Res Temp
TEMP °F
140
110
80
50
20
-10
-40
-70
-100
5
6
7
8
9
10
11
12
13
14
15
16
17
18
19
20
21
22
.0
10.0
20.0
30.0
40.0
50.0
60.0
Distance along Condenser ,in.

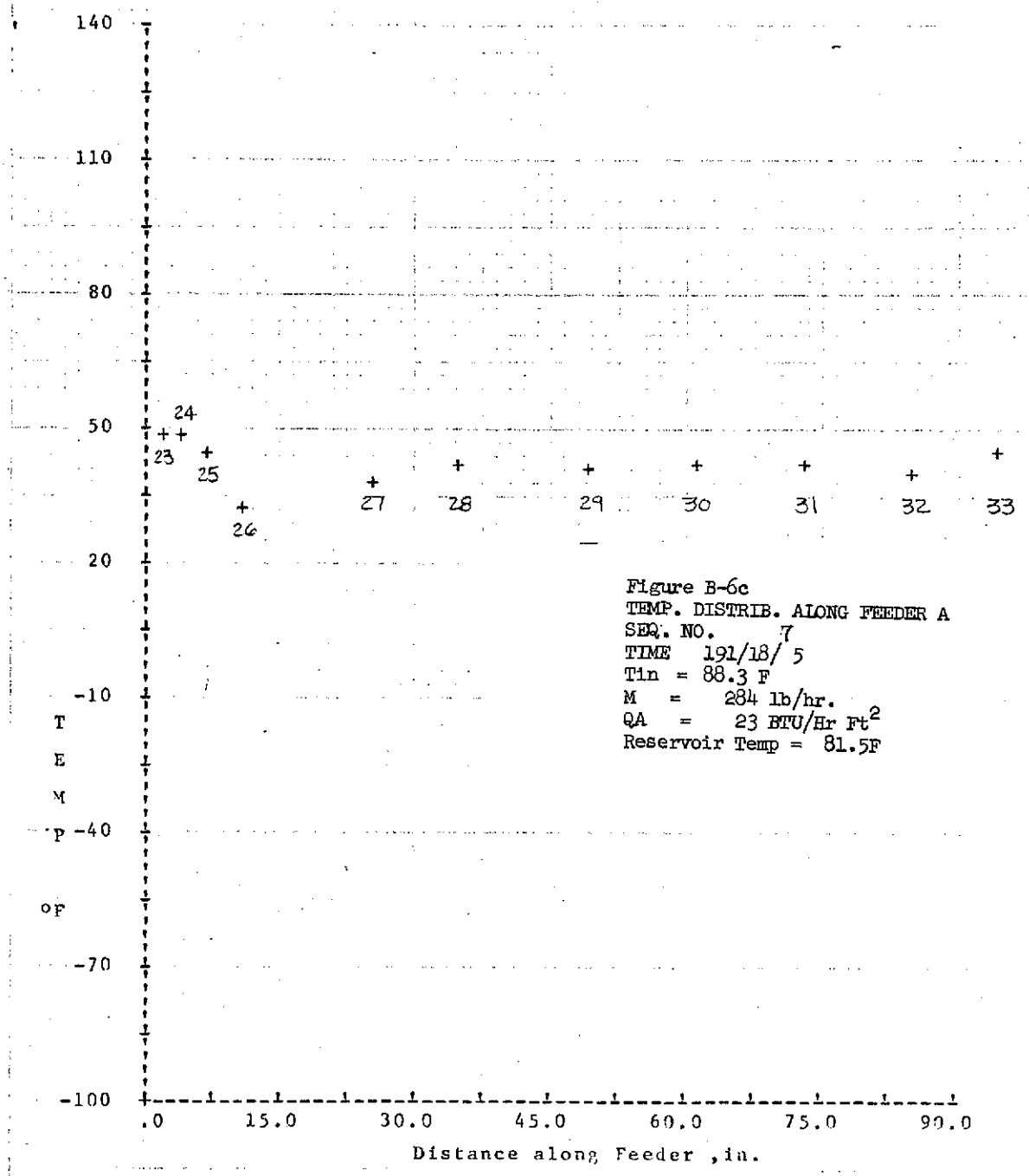

Figure B-6c
TEMP. DISTRIB. ALONG FEEDER A
SEQ. NO. 7
TIME 191/18/ 5
Tin = 88.3 F
M = 284 lb/hr.
QA = 23 BTU/Hr Ft^2
Reservoir Temp = 81.5F

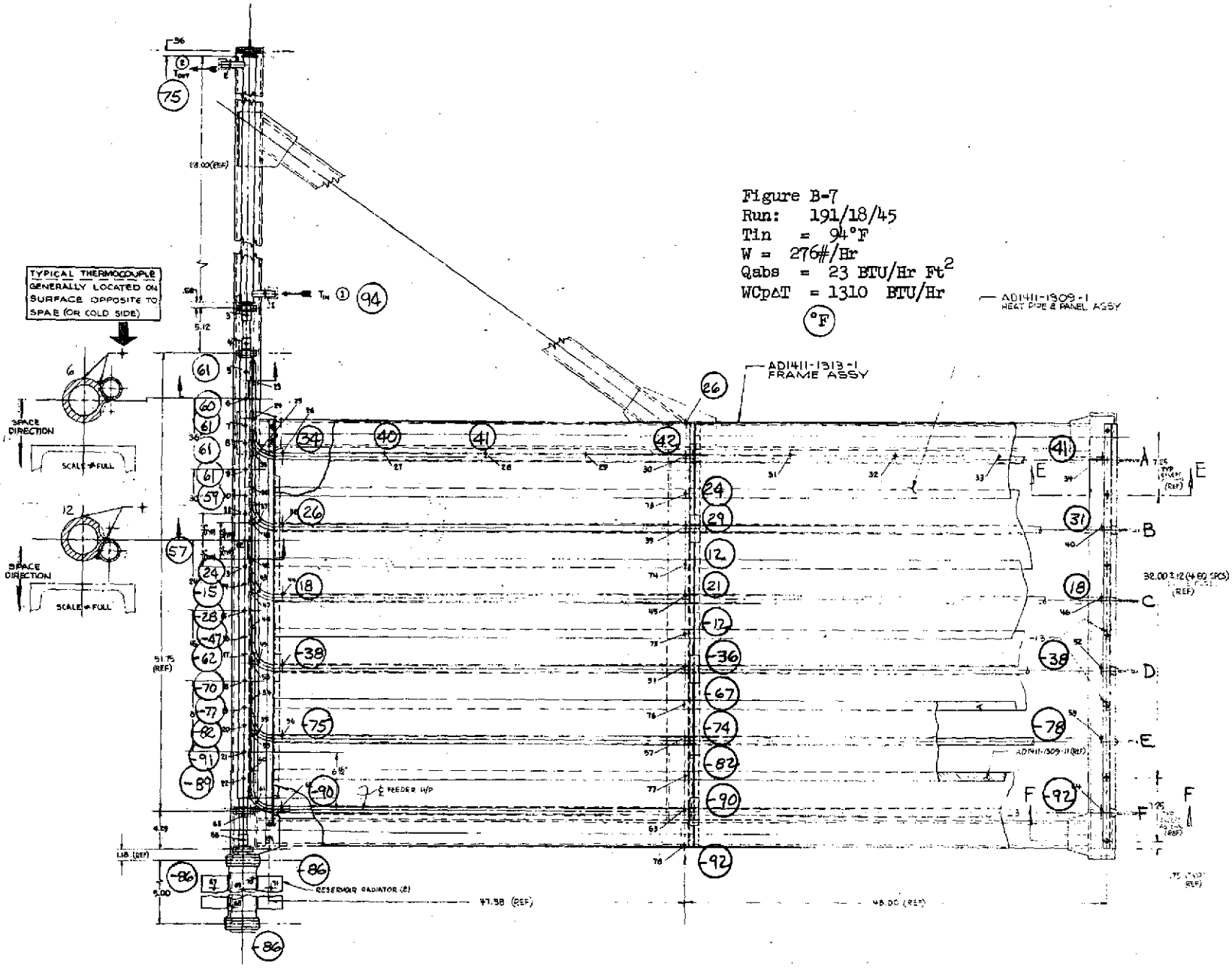

Figure B-7
Run: 191/18/45
Tin = 94°F
W = 276#/Hr
Qabs = 23 BTU/Hr Ft^2
WCpΔT = 1310 BTU/Hr
°F

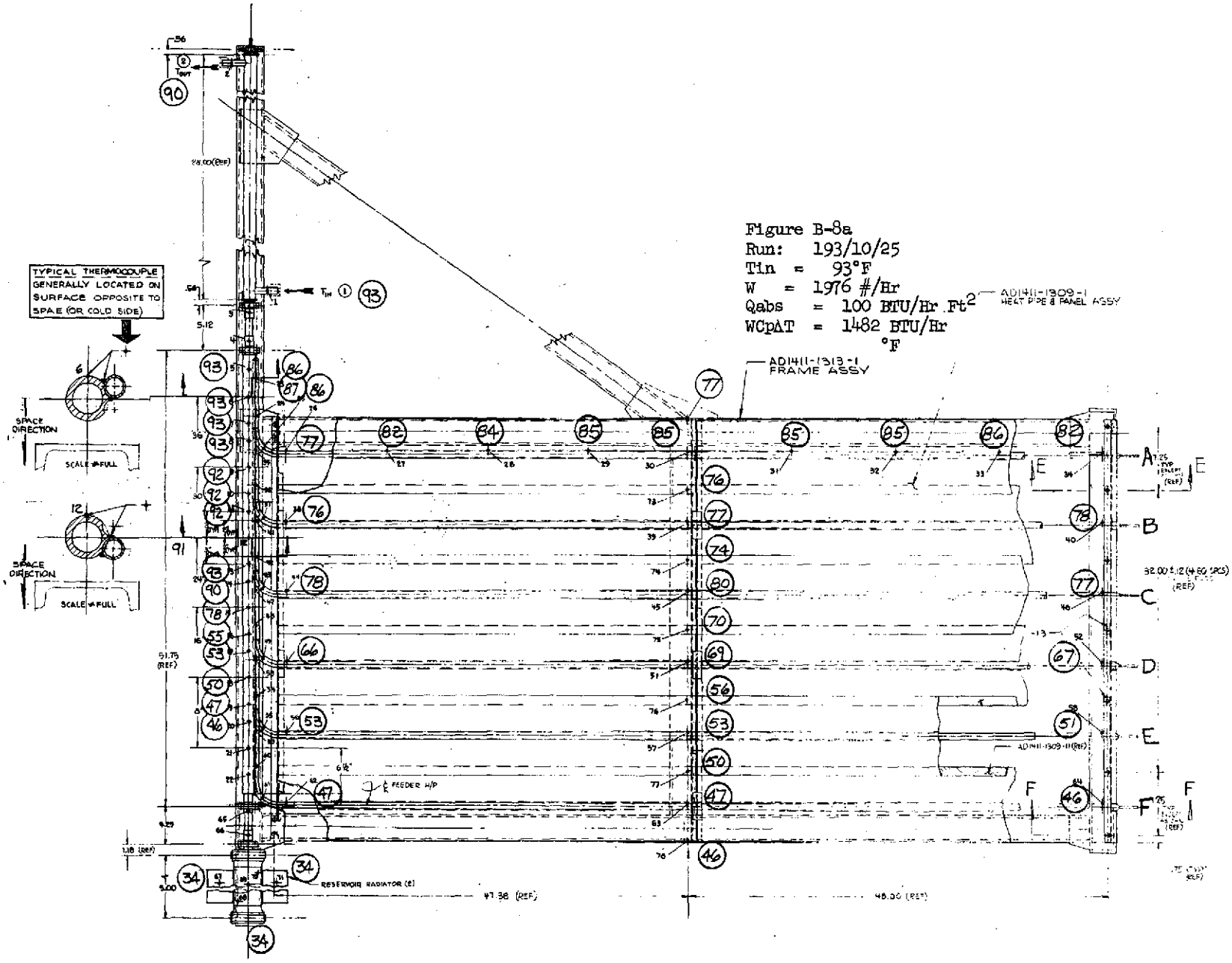

Figure B-8a
Run: 193/10/25
Tin = 93°F
W = 1976 #/Hr
Qabs = 100 BTU/Hr.Ft^2
WCpΔT = 1482 BTU/Hr
°F

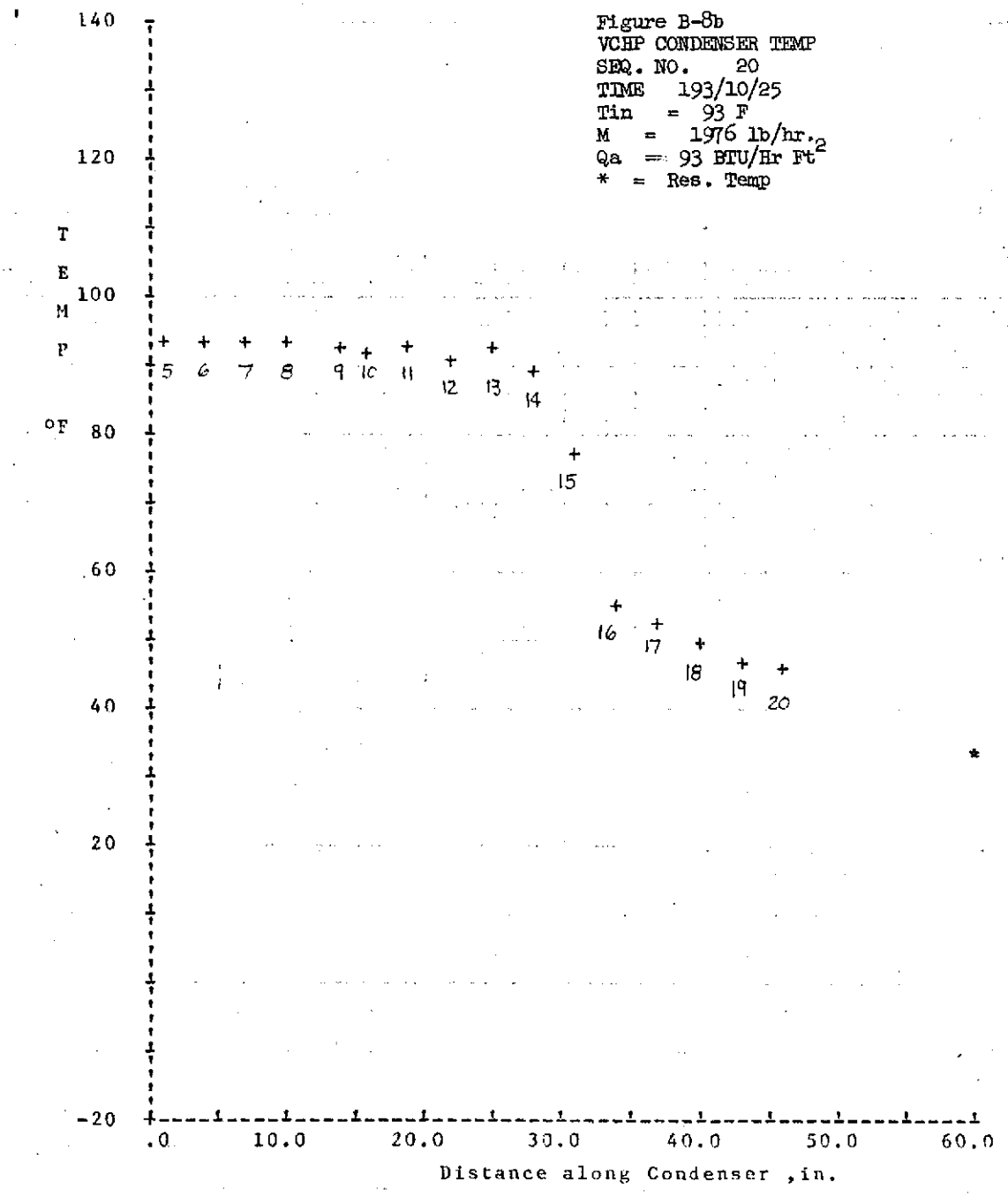
Figure B-8b
VCHP CONDENSER TEMP
SEQ. NO. 20
TIME 193/10/25
Tin = 93 F
M = 1976 lb/hr.
Qa = 93 BTU/Hr Ft2
* = Res. Temp
TEMP °F
140
120
100
80
60
40
20
-20
5
6
7
8
9
10
11
12
13
14
15
16
17
18
19
20
.0
10.0
20.0
30.0
40.0
50.0
60.0
Distance along Condenser ,in.

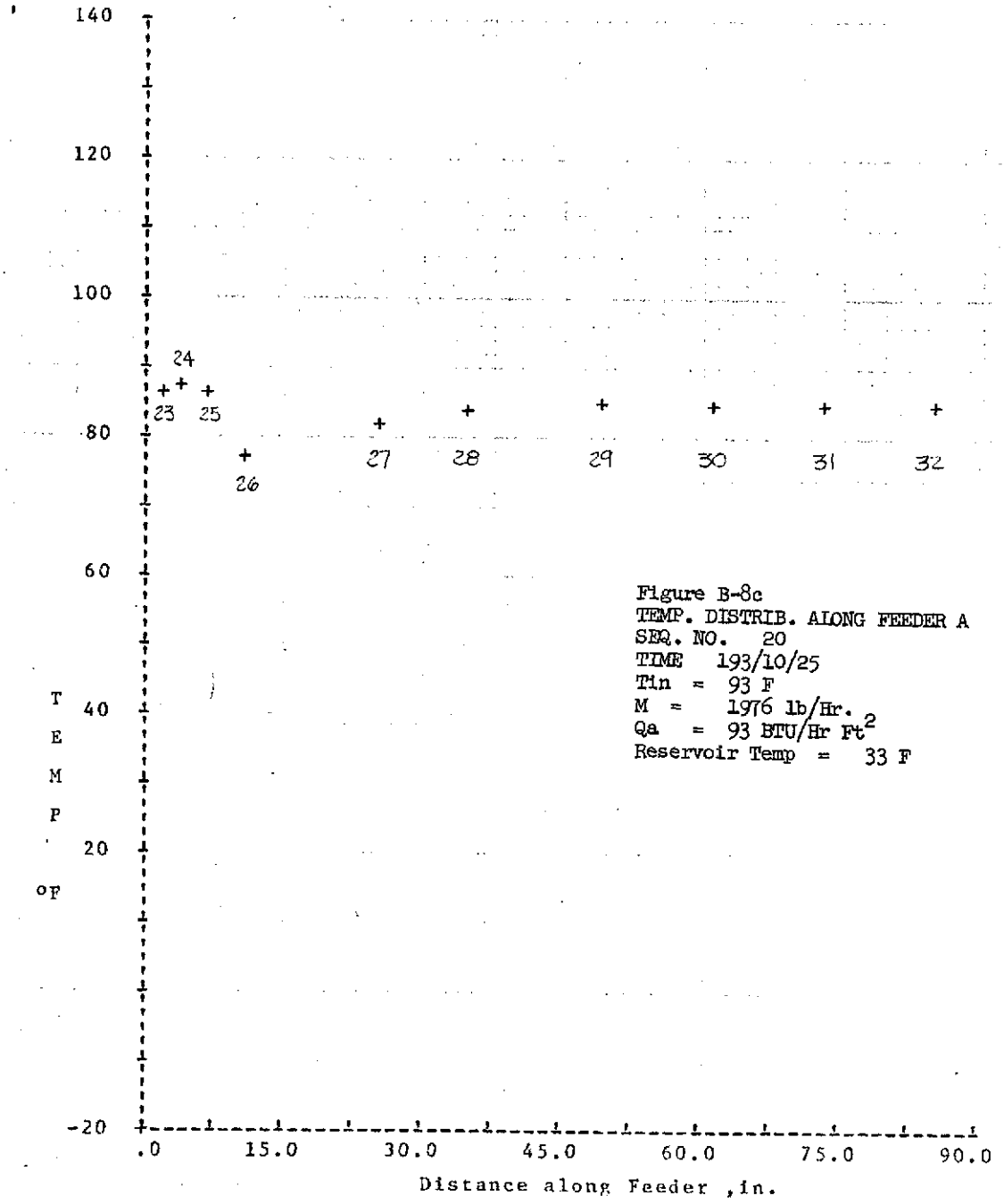

Figure B-8c
TEMP. DISTRIB. ALONG FEEDER A
SEQ. NO. 20
TIME 193/10/25
Tin = 93 F
M = 1976 lb/Hr.
Qa = 93 BTU/Hr Ft^2
Reservoir Temp = 33 F

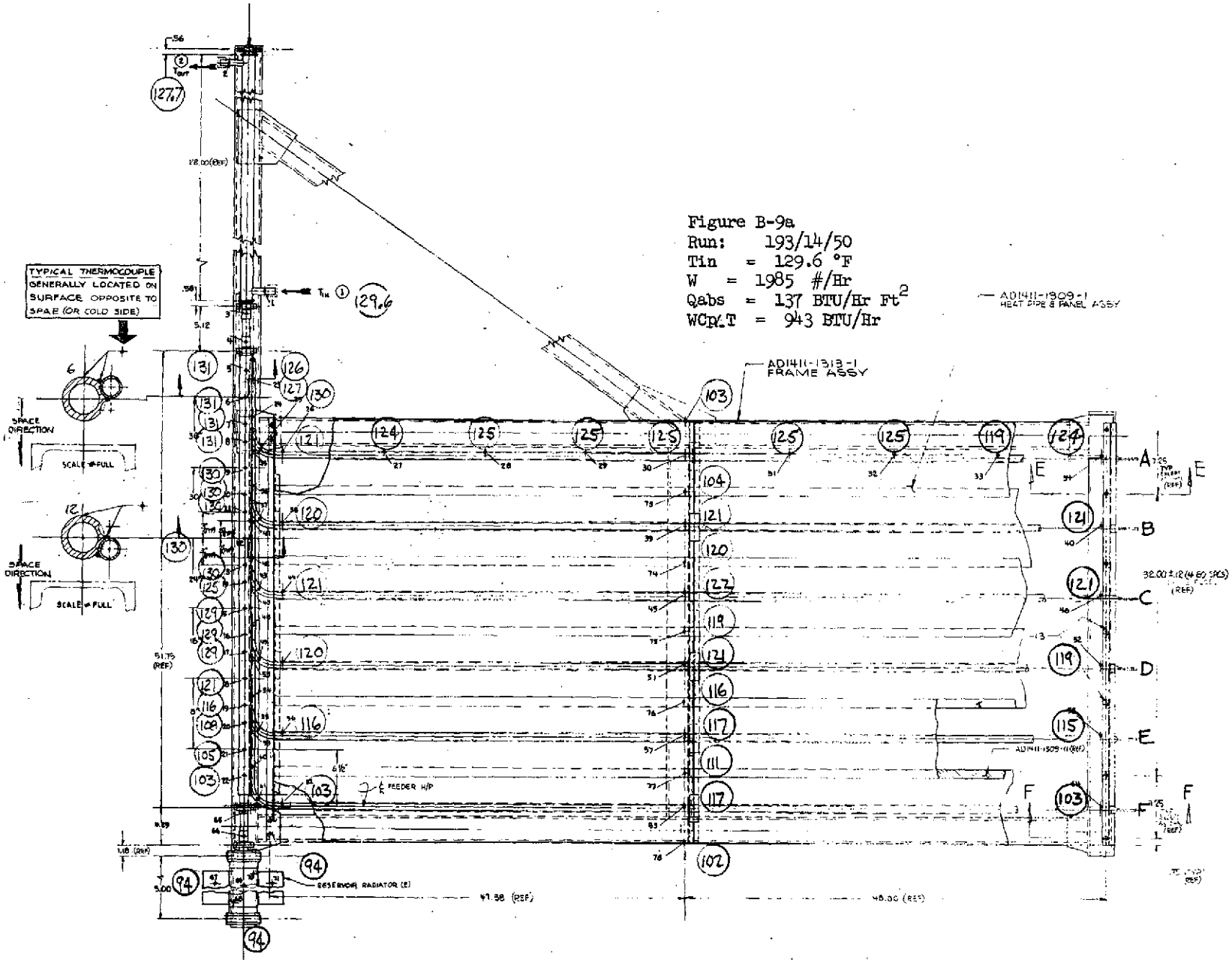

Figure B-9a
Run: 193/14/50
Tin = 129.6 °F
W = 1985 #/Hr
Qabs = 137 BTU/Hr Ft^2
WCp.T = 943 BTU/Hr

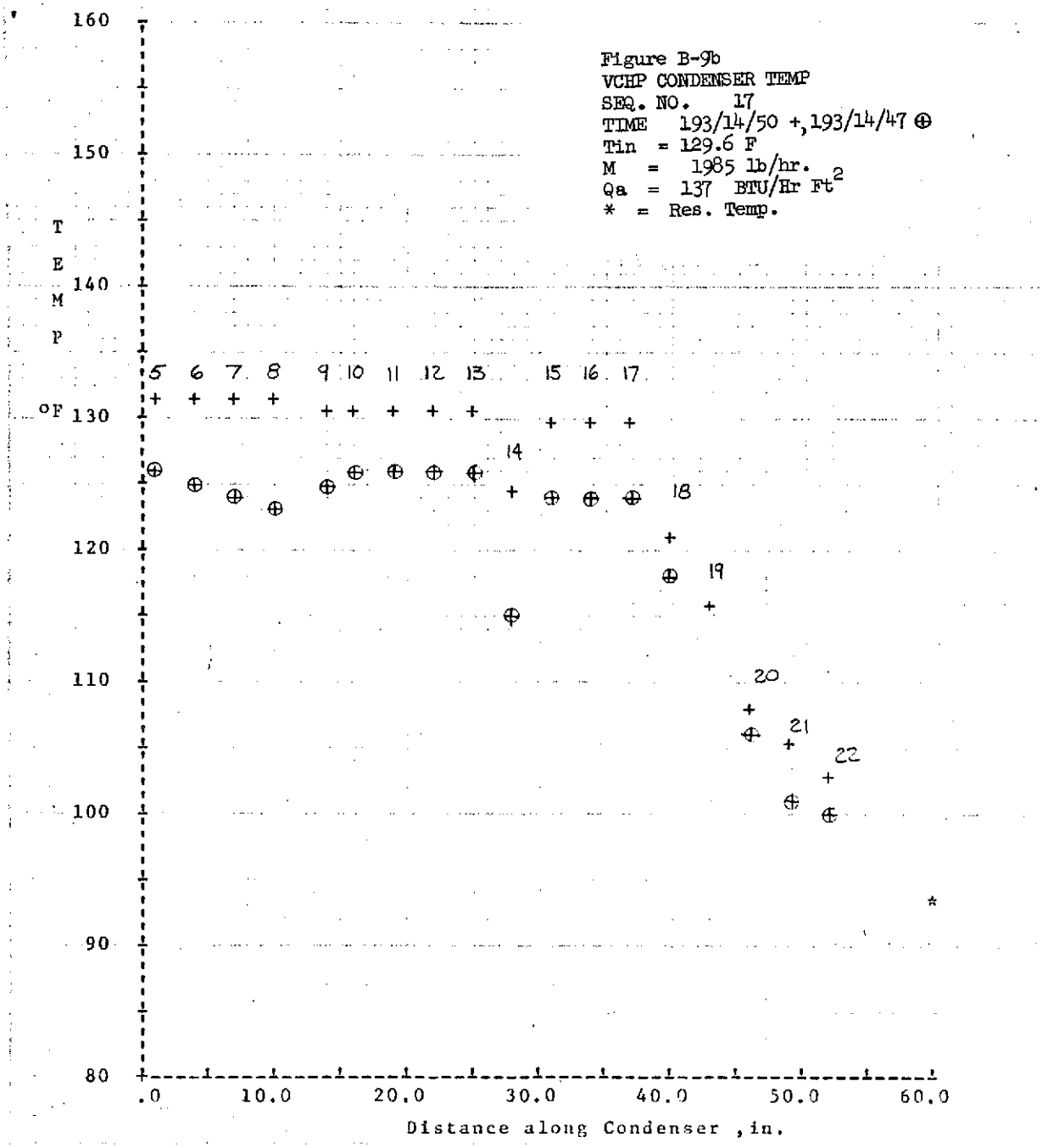
Figure B-9b
VCHP CONDENSER TEMP
SEQ. NO. 17
TIME 193/14/50 +, 193/14/47 ⊕
Tin = 129.6 F
M = 1985 lb/hr.
Qa = 137 BTU/Hr Ft²
* = Res. Temp.
TEMP °F
160
150
140
130
120
110
100
90
80
5 6 7 8 9 10 11 12 13 14 15 16 17 18 19 20 21 22
.0
10.0
20.0
30.0
40.0
50.0
60.0
Distance along Condenser , in.

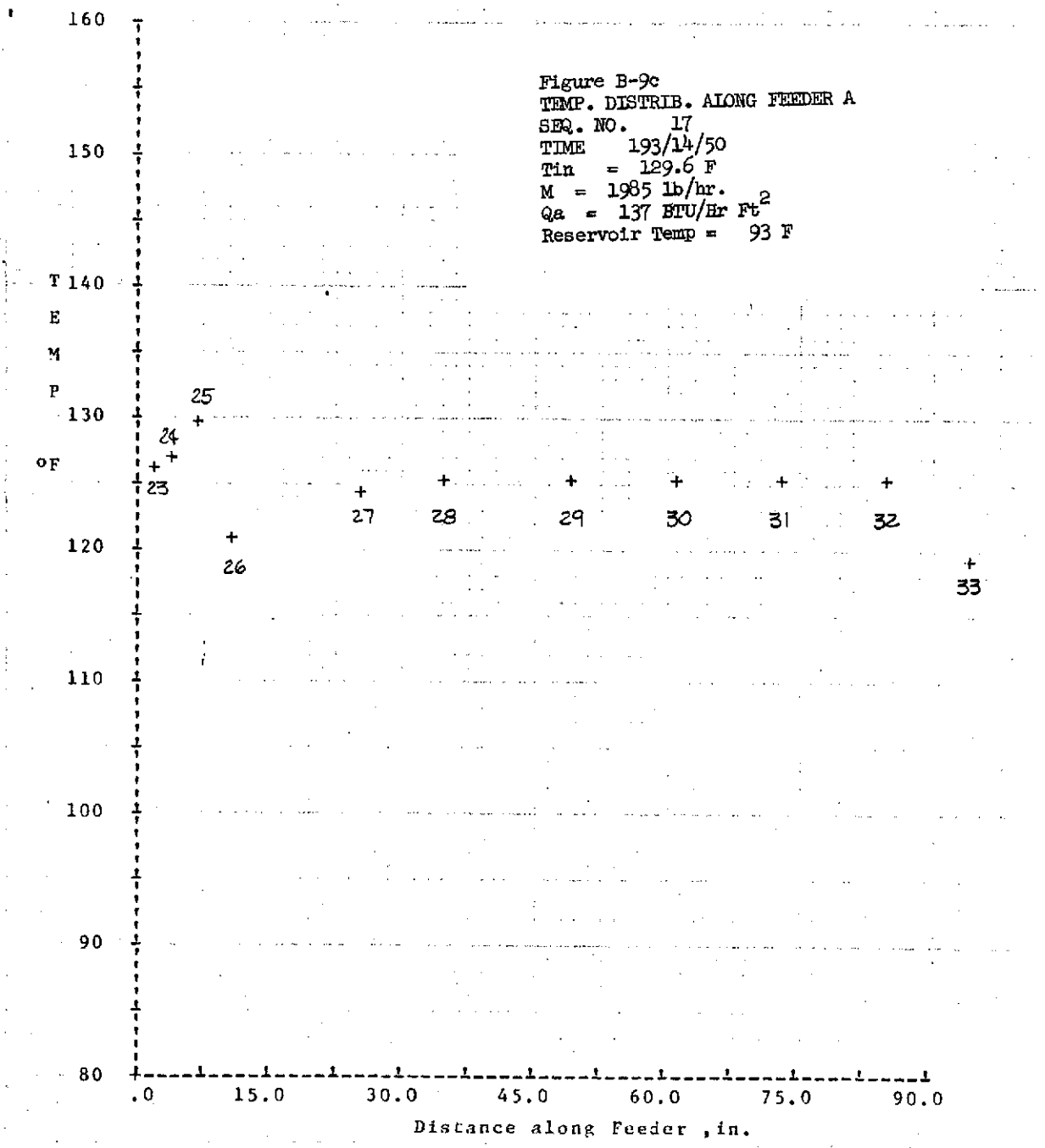
Figure B-9c
TEMP. DISTRIB. ALONG FEEDER A
SEQ. NO. 17
TIME 193/14/50
Tin = 129.6 F
M = 1985 lb/hr.
Qa = 137 BTU/Hr Ft2
Reservoir Temp = 93 F
TEMP oF
160
150
140
130
120
110
100
90
80
23
24
25
26
27
28
29
30
31
32
33
.0
15.0
30.0
45.0
60.0
75.0
90.0
Distance along Feeder , in.


GRUMMAN AEROSPACE CORPORATION
BETHPAGE, NEW YORK 11714